



TECHNISCHE
UNIVERSITÄT
WIEN



ICEBE
IMAGING
NATURE

Master Thesis

Separation of Lactic Acid from Grass Silage by Multistage Membrane Processes

Carried out for the purpose of obtaining the degree of Master of Science

Diplom-Ingenieur

Under the supervision of

Senior researcher. Dr. Amal El Gohary Ahmed

Ao. Univ.Prof. Dipl.-Ing. Dr.techn. Michael Harasek

Ph.D. researcher Mayuki Cabrera-González

Univ.Ass. Dipl.-Ing. Dr.techn. Christian Jordan

(E166 Institute of Chemical, Environmental and Bioscience Engineering)

Submitted at Technische Universität Wien

Faculty of Technical Chemistry

by

Timo Niklas Widmann



Vienna, April 2024

Timo Niklas Widmann, BSc



TECHNISCHE
UNIVERSITÄT
WIEN

Ich habe zur Kenntnis genommen, dass ich zur Drucklegung meiner Arbeit unter der Bezeichnung

Diplomarbeit

nur mit Bewilligung der Prüfungskommission berechtigt bin.

Ich erkläre weiters an Eides statt, dass ich meine Diplomarbeit nach den anerkannten Grundsätzen für wissenschaftliche Abhandlungen selbstständig ausgeführt habe und alle verwendeten Hilfsmittel, insbesondere die zugrunde gelegte Literatur, genannt habe.

Weiters erkläre ich, dass ich dieses Diplomarbeitsthema bisher weder im In- noch Ausland (einer Beurteilerin/einem Beurteiler zur Begutachtung) in irgendeiner Form als Prüfungsarbeit vorgelegt habe und dass diese Arbeit mit der vom Begutachter beurteilten Arbeit übereinstimmt.

Acknowledgements

I extend my gratitude to Ao. Univ.Prof. Dipl.-Ing. Dr.techn. Michael Harasek for his introduction to this intriguing field. His support has provided a foundational base for my thesis work. The moments of laughter and learning with his team have added a layer of enjoyment to this academic pursuit.

My deepest and most profound thanks are reserved for Dr. Amal El Gohary Ahmed, whose unwavering support and guidance have been the cornerstone of my thesis journey. Dr. Ahmed has been an extraordinary mentor, going above and beyond—far more than the extra mile—to assist, support, and encourage me at every turn. When faced with the most challenging obstacles, she stood by my side with unyielding support and innovative solutions. Her remarkable guidance, infused with humor and warmth, has been my beacon. Without her, this thesis would not have been possible.

Special thanks go to my high school teachers, Walter Kieweg and Robert Stania, for igniting my passion for higher education and chemistry, respectively. Their dedication and enthusiasm for teaching were the sparks that set me on this path.

I am grateful to my fellow students, especially Michael “..” and Joris Peter, for the shared experiences and the many moments of joy and camaraderie that made overcoming academic challenges possible.

My family deserves my wholehearted thanks for their endless support. My parents, Wolfgang, and Silvia, have been pillars of strength, providing financial and emotional backing that has been the bedrock of my academic journey. Their support has been invaluable, demonstrating that belief and encouragement transcend all barriers.

My sisters, Livia, and Leonie, have been a constant source of mental and emotional support.

Additional thanks to my extended family, Uncle Nik, and Aunt Marita, for their support during tough times and for always being there with open doors and hearts, ready to offer help in any form needed.

Lastly, to my partner, Noki, who has been by my side throughout my master’s journey, enduring the mood swings brought on by sleep deprivation and stress with incredible patience and love. Her unwavering support and ability to maintain composure, even in the most trying times, have been indispensable to me.

Abstract

The downstream process of grass silage to yield a highly valuable product like lactic acid is a challenging process. Lactic acid is produced from the fermentation of grass silage by Lactic acid bacteria (LAB). Lactic acid is in high demand worldwide, mostly due to its indispensable application in the production of polylactic acid (PLA) polymer and its applications in the food and pharmaceutical industries. However, producing lactic acid from grass silage can be complex and demanding. This lactic acid is then extracted and purified to obtain a high-quality final product.

Membrane processes are a cost-effective and eco-friendly solution for a variety of industrial applications and have promising potential for downstream grass silage applications.

Incorporating sustainable methods, the separation and concentration of Lactic Acid from grass silage through multistage membrane processes have been investigated in this research. Specifically, pressure-driven membrane processes have been studied.

This study aimed to identify the most effective multistage membrane processes at a laboratory scale, considering various factors, such as membrane type and pH, to enhance the recovery and purity of lactic acid.

The optimal multistage process was achieved through a three-stage membrane procedure, beginning with an adjustment of the real solution of grass silage to pH 2.5. At this pH, which is lower than the pKa of lactic acid, the lactic acid remained non-dissociated prior to pretreatment by microfiltration. The microfiltration membrane (first stage), with a pore size of 0.2 microns, provided excellent performance. Lactic acid purification was accomplished using a tight nanofiltration membrane (second stage) with a molecular weight cut-off (MWCO) of 300Da, which effectively fractionated the microfiltration permeate. During the nanofiltration process, glucose and fructose were completely rejected, while the NF permeate stream contained 60% lactic acid. The rejection rate for lactic acid was higher than for acetic acid. The concentration of lactic acid from the NF permeate was conducted using reverse osmosis; the RO 98pHt membrane was capable of achieving 100% rejection of lactic acid.

By identifying the most effective methods, this study could pave the way for improved Lactic acid purification and recovery from grass silage.

Zusammenfassung

Der nachgelagerte Prozess von Grassilage zur Gewinnung des hochwertigen Produkts Milchsäure ist ein anspruchsvoller Prozess. Milchsäure wird durch die Fermentation von Grassilage durch Milchsäurebakterien produziert. Milchsäure ist weltweit sehr gefragt, hauptsächlich aufgrund ihrer unverzichtbaren Anwendung in der Produktion von Polymilchsäure und ihrer Anwendungen in der Lebensmittel- und Pharmaindustrie. Die Herstellung von Milchsäure aus Grassilage kann jedoch komplex und anspruchsvoll sein. Um ein hochwertiges Endprodukt zu erhalten, wird die Milchsäure extrahiert und gereinigt.

Membranprozesse sind eine kostengünstige und umweltfreundliche Lösung für eine Vielzahl von industriellen Anwendungen und haben vielversprechendes Potenzial für nachgelagerte Grassilage-Anwendungen.

Unter Einbeziehung nachhaltiger Methoden wurden in dieser Forschung die Trennung und Konzentration von Milchsäure aus Grassilage durch mehrstufige Membranprozesse untersucht. Insbesondere wurden druckgetriebene Membranprozesse untersucht.

Ziel dieser Studie war es, die effektivsten mehrstufigen Membranprozesse im Labormaßstab zu identifizieren und dabei verschiedene Faktoren, wie Membrantyp und pH-Wert, zu berücksichtigen, um die Rückgewinnung und Reinheit von Milchsäure zu verbessern.

Der optimale mehrstufige Prozess wurde mit einem dreistufigen Membranprozess erreicht, indem die natürliche Lösung von Grassilage auf einen pH-Wert von 2,5 eingestellt wurde. Bei diesem pH-Wert, der niedriger als der pKa-Wert der Milchsäure war, war die Milchsäure vor der Vorbehandlung durch Mikrofiltration nicht dissoziiert. Die Mikrofiltrationsmembran (erste Stufe) mit einer Porengröße von 0,2 Mikrometern zeigte eine hervorragende Leistung. Die Reinigung der Milchsäure wurde durch Verwendung einer dichten Nanofiltrationsmembran (zweite Stufe) mit einer Molekulargewichtsschnittstelle (MWCO) von 300 Da erreicht, die das Mikrofiltrationspermeat fraktionierte. Im Nanofiltrationsprozess wurden Glukose und Fruktose vollständig zurückgehalten, während das Nanofiltrationspermeat 60% Milchsäure enthielt. Die Rückhalterate für Milchsäure war höher als für Essigsäure. Die Konzentration der Milchsäure aus dem Nanofiltrationspermeat durch Umkehrosmose durchgeführt wurde. Die RO98pHt-Membran war in der Lage, 100% der Milchsäure im Retentat zurückzuhalten.

Durch die Identifizierung der effektivsten Methoden könnte diese Studie den Weg für eine verbesserte Aufreinigung und Gewinnung von Milchsäure aus Grassilage ebnen.

Keywords

Acetic Acid, Gras Silage, Lactic Acid, Microfiltration, Nanofiltration, Reverse Osmosis

Table of Contents

Table of Contents

KEYWORDS.....	VI
ABSTRACT	III
ZUSAMMENFASSUNG	V
TABLE OF CONTENTS.....	VI
LIST OF FIGURES.....	IX
LIST OF TABLES	XII
LIST OF ABBREVIATIONS.....	XIII
STATEMENT OF ORIGINAL AUTHORSHIP	XIII
ACKNOWLEDGEMENTS	III
CHAPTER 1: INTRODUCTION	1
CHAPTER 2: LITERATURE REVIEW	3
2.1 GRASS SILAGE	3
2.1.1 Definition.....	3
2.1.2 Production	3
2.1.2.1 Pretreatment.....	4
2.1.3 Components in Grass Silage.....	6
2.1.3.1 Water-Soluble Carbohydrates (WSCs).....	6
2.1.3.2 Organic Acids.....	6
2.1.3.3 Nitrogenous Compounds.....	7
2.2 LACTIC ACID (LA).....	8
2.2.1 Chemical structure	8
2.2.2 Methods of Manufacturing.....	8
2.2.3 Application	9
2.2.4 Market Size.....	10
2.2.5 Extraction and Purification from Grass silage.....	11
2.3 MEMBRANE PROCESSES.....	12
2.3.1 Pressure-driven membrane processes	13
2.3.1.1 Membrane separation fundamental concepts and terminology.....	13
2.3.1.2 Microfiltration	15
2.3.1.3 Ultrafiltration.....	16
2.3.1.4 Nanofiltration	16
2.3.1.5 Reverse Osmosis	16
CHAPTER 3: MATERIAL AND METHODS	18
3.1 MATERIAL	18
3.1.1 Chemicals	18
3.1.1.1 Sulfuric Acid H ₂ SO ₄	18
3.1.1.2 MilliQ Water.....	18
3.1.1.3 Analyse Standards.....	18
3.1.2 Grass silage	19
3.1.3 Experiment Setup	19
3.1.4 Membrane.....	21
3.1.5 Analytical Equipment	22
3.1.5.1 Refractometer	22
3.1.5.2 Conductivity & pH meter	23
3.1.5.3 HPLC.....	25
3.2 METHOD.....	26
3.2.1 Feed Preparation.....	27
3.2.1.1 Filtration Preparation.....	28
3.2.1.2 Filtration Reset	31

3.2.1.3	HPLC.....	31
CHAPTER 4:	RESULTS AND DISCUSSION	33
4.1	SEPARATION AND CONCENTRATION OF LACTIC ACID BY MULTISTAGE MEMBRANE PROCESSES.....	33
4.1.1	<i>First arrangement of the multistage process</i>	34
4.1.2	<i>Second arrangement of the multistage process</i>	38
4.1.3	<i>Third arrangement of the multistage process</i>	42
4.1.3.1	<i>First Sub Arrangement</i>	43
4.1.3.2	<i>Second Sub Arrangement</i>	46
4.1.3.3	<i>Third Sub Arrangement</i>	49
4.1.4	<i>Fourth arrangement of the multistage process</i>	52
4.2	PERFORMANCE OF NANOFILTRATION	54
4.2.1	<i>Rejection</i>	54
CHAPTER 5:	CONCLUSION	57
	BIBLIOGRAPHY.....	60
	APPENDICES	63

List of Figures

Figure 1	Schematic of pretreatment of lignocellulosic biomass [8]	4
Figure 2	Chemical Structure of Lactic Acid [21]	8
Figure 3	A wide range of biotechnological applications of lactic acid [13]	9
Figure 4	Lactic acid market share, by application in 2021 [1]	10
Figure 5	Lactic acid market size 2022 -2023 [1]	10
Figure 6	Dead-End (A) vs. Cross-Flow (B) Filtration, the Two Main Types of Membrane Filtration [25]	12
Figure 7	Pressure-Driven Membrane Process [26]	13
Figure 8	Transmembrane pressure in a cross-flow membrane module. [28].....	15
Figure 9	arium® pro Ultrapure Water System.....	18
Figure 10	Experimental Equipment	20
Figure 11	Block Flow Diagram of Membrane Filtration Unit.....	21
Figure 12	Refractometer.	23
Figure 13	MU 6100H Unit, Conductivity Sensor, pH Electrode.....	24
Figure 14	ThermoScientific Vanquish HPLC System[52]	25
Figure 15	Original Experimental Design Flowchart.....	26
Figure 16	Final Experimental Design Flowchart.....	26
Figure 17	Sample ID Nomenclature	28
Figure 18	Experimental Design Flowchart: First Arrangement.....	34
Figure 19	Brix concentration Permeate and Retentate over time during MF (First Arrangement)	34
Figure 20	pH and Conductivity Measurement Points in MF Process Flow (First Arrangement)	35
Figure 21	pH, Conductivity and Brix Measurement Points in NF Process Flow (First Arrangement)	35
Figure 22	pH, Conductivity and Brix Measurement Points in RO Process Flow (First Arrangement)	36
Figure 23	Rejection Profiles of Lactic Acid, Acetic Acid, Fructose, and Glucose Across through the Stages of the First Arrangement	36
Figure 24	Experimental Design Flowchart: Second Arrangement	38
Figure 25	Brix concentration Permeate and Retentate over time during MF (Second Arrangement)	38
Figure 26	pH and Conductivity Measurement Points in MF Process Flow (Second Arrangement)	39

Figure 27 pH, Conductivity and Brix Measurement Points in NF Process Flow (Second Arrangement)	39
Figure 28 pH, Conductivity and Brix Measurement Points in RO Process Flow (First Arrangement)	40
Figure 29 Rejection Profiles of Lactic Acid, Acetic Acid, Fructose, and Glucose Across through the Stages of the Second Arrangement	41
Figure 30 Experimental Design Flowchart: Third Arrangement	42
Figure 31 pH and Conductivity Measurement Points in MF Process Flow (Third Arrangement)	42
Figure 32 Brix concentration Permeate and Retentate over time during MF (Third Arrangement)	43
Figure 33 Experimental Design Flowchart: First Sub Arrangement of First Sub Arrangement	43
Figure 34 pH, Conductivity and Brix Measurement Points in NF Process Flow (First Sub Arrangement).....	44
Figure 35 Rejection Profiles of Lactic Acid & Amino Acid through the NF Stage of the First Sub Arrangement.....	44
Figure 36 pH, Conductivity and Brix Measurement Points after Diafiltration (First Sub Arrangement)	45
Figure 37 Experimental Design Flowchart: Second Sub Arrangement of Second Sub Arrangement	46
Figure 38 pH, Conductivity and Brix Measurement Points in NF Process Flow (Second Sub Arrangement).....	46
Figure 39 Rejection Profiles of Lactic Acid & Acetic Acid through the NF Stage of the Second Sub Arrangement	47
Figure 40 pH, Conductivity and Brix Measurement Points after Diafiltration (Second Sub Arrangement).....	47
Figure 41 Rejection Profiles of Lactic Acid & Amino Acid after Diafiltration of the Second Sub Arrangement	48
Figure 42 Experimental Design Flowchart: Third Sub Arrangement of Third Sub Arrangement	49
Figure 43 pH [left], Conductivity and Brix Measurement Points in MF Process Flow (Third Sub Arrangement)	49
Figure 44 pH, Conductivity and Brix Measurement Points in NF Process Flow (Third Sub Arrangement).....	50
Figure 45 Rejection Profiles of Lactic Acid, Acetic Acid, Fructose, and Glucose Across through the Stages of the Third Arrangement	51
Figure 46 Experimental Design Flowchart: Fourth Arrangement	52
Figure 47 pH, Conductivity and Brix Measurement Points in MF Process Flow (Fourth Arrangement).....	53

Figure 48 Rejection Profiles of Lactic Acid & Acetic Acid through the NF Stage of the Fourth Arrangement.....53

Figure 49 Comparative Analysis of Feed Flux and Water Permeability Before and After NF Processes54

Figure 50 Efficacy of NF Stage in Rejecting Lactic and Acetic Acids: A Comparative View Across Different Arrangements55

Figure 51 Comparative Analysis of Feed Flux and Water Permeability Before and After RO Processes56

Figure 52 Efficacy of RO Stage in Rejecting Lactic and Acetic Acids: A Comparative View Across Different Arrangements56

List of Tables

Table 1 Silage and hay production in selected countries in 2000 [9]	3
Table 2 Overview of lignocellulosic biomass pretreatment processes [13].....	5
Table 3 Chemical properties of Lactic acid [2,21].....	8
Table 4 Overview of the major LA separation and purification technique [4]	11
Table 5 HPLC Standards [41]	19
Table 6 Grass Silage Composition [42]	19
Table 7 Membrane Characteristics.....	22
Table 8 Feed Acidification Parameters	27
Table 9 Operational Conditions of experimental Steps	29

List of Abbreviations

AA	Acetic Acid
ACN	Acetonitrile
CAGR	Compound Annual Growth Rate
GS	Grass Silage
GSJ	Grass Silage Juice
HPLC	High-Performance Liquid Chromatography
LA	Lactic Acid
LAB	Lactic Acid Bacteria
MF	Micro Filtration
MWCO	Molecular Weight Cut Off
NA	Not Available
NF	Nano Filtration
PLA	Polylactic Acid
RO	Reverse Osmosis
TFC	Thin-Film Composite Membranes
TMP	Transmembrane Pressure
UF	Ultra Filtration
USD	United States Dollar
WSC	Water-Soluble Carbohydrates



Die approbierte gedruckte Originalversion dieser Diplomarbeit ist an der TU Wien Bibliothek verfügbar
The approved original version of this thesis is available in print at TU Wien Bibliothek.

Chapter 1: Introduction

1.1 MOTIVATION

The demand for lactic acid worldwide is increasing due to its essential role in the production of polylactic acid (PLA) polymers. [1] PLA is viewed as an environmentally friendly alternative to traditional oil-based plastics because it is biodegradable and potentially less harmful to the environment. Lactic acid, its primary precursor, can be produced either synthetically or through biological fermentation. Currently, researchers are primarily focused on producing lactic acid through biological fermentation, raising questions about how to efficiently extract and purify it from the fermented feed mass.

This is where grass silage comes in. It's a feed for animals that's found all over the world and has a lot of lactic acid in it, which makes it seem like a good source for extraction. There have been attempts to get lactic acid out of grass silage before, but they all ran into different problems. These issues made those methods not practical, either because they were highly expensive or not completely sustainable. [2][3]

Membrane filtration technology has gained recognition for its range of selective properties, such as molecular weight and polarity, towards its feed material while offering scalability. This means that new processes can be optimized and made cost-effective on a small scale and then replicated on a larger scale. However, due to the significant setup costs and the lack of a fully optimized process, its use remains limited. This thesis presents a novel approach to efficiently extract lactic acid from grass silage. It aims to change the current landscape by demonstrating that the extraction can be cost-effective and eco-friendly, thereby making the initial investment more appealing to industries.[4]

We are at a turning point where innovative membrane technology could be used to make a significant difference in producing lactic acid more sustainably. By focusing on the utilization of grass silage, a resource that regrows, and by improving filtration techniques, this project could help in changing the way lactic acid is produced for the better. It's not just about making the process more efficient; it's about making it align with our goal of discovering resources for a better tomorrow.

1.2 AIM OF WORK

The primary objective of this thesis is to develop a reproducible and effective method for recovering lactic acid from grass silage using membrane filtration techniques. This endeavor is driven by the increasing industrial demand for sustainably produced lactic acid. A significant portion of this work will investigate the effects of pH adjustments—specifically, whether maintaining the original pH or lowering it to 2.5 and the selection of different membrane types on the yield and purity of the extracted lactic acid.

The methodology involves a multistage filtration process, initiating with microfiltration of the grass silage. This stage is crucial for the preliminary cleaning of the solution and concentration of lactic acid. The decision on when to adjust the pH either before or after microfiltration will be explored to determine its impact on the overall efficacy of the separation process. Following microfiltration, the solution undergoes nanofiltration, which further purifies and concentrates

the lactic acid. Only after this nanofiltration stage will the permeate be evaluated to ascertain if it meets the criteria for undergoing reverse osmosis for additional purification.

The effectiveness of the process will be quantitatively assessed by analyzing the lactic acid content in the filtered solutions. These analyses will be conducted with High-Performance Liquid Chromatography.

The goal is to establish a new, repeatable method for industrial-scale purification of lactic acid from grass silage. This method aims not only to be efficient but also to align with goals by utilizing grass silage as a sustainable resource for lactic acid for an industrial application. The focus on membrane selection and pH adjustment strategies underscores the innovative approach taken to optimize yield and purity, ensuring the method's viability for sustainable industrial application.

Chapter 2: Literature Review

2.1 GRASS SILAGE

2.1.1 Definition

Grass silage (GS) is a preserved form of grass or other plant materials, which is stored anaerobically to prevent spoilage, and mainly utilized as winter feed for ruminant livestock. GS advantage over hay stems from its reduced dependence on weather conditions and the capacity for multiple harvests annually. [5]

This traditional application of grasses for fodder is enriched by their extensive evolutionary history, with grasses being part of Earth's flora for about 55 to 70 million years. [6] In contemporary agriculture and industry, grasses have transcended their roles beyond grazing and animal feed. They are increasingly applied as a renewable carbon source for diverse industrial processes, and as a crucial feedstock for biorefineries, thanks to their widespread availability globally. [7]

The structural and chemical attributes of grasses, previously studied for biofuel production [8], underscore the untapped potential of this biomass. Although their primary use remains in agriculture for livestock feeding, especially as grass silage, the expanding applications of grasses in renewable energy and sustainable industrial practices are drawing attention. This pivot towards utilizing grasses as a biorefinery feedstock not only capitalizes on their renewable aspect, but also aligns with global sustainability objectives, underscoring the importance of continued research to fully exploit the advantages of grasses across various sectors beyond their conventional uses.

Table 1 Silage and hay production in selected countries in 2000 [9]

Country	Silage			
	1 million Tons dry matter			
	Hay	Grass	Corn	Other
Australia	4.5	0.9	0.3	0.04
Canada	45.0	NA	2.8	4.8
Chile	0.6	1.3	NA	NA
France	22.5	3.1	16.8	5.3
Italy	15.1	0.2	6.9	0.4
Japan	1.5	2.2	1.1	0.07
New Zealand	0.4	0.6	0.3	0.02
Spain	3.1	1.7	0.7	0.2
United Kingdom	2.5	9.4	1.1	0.4
United States	138	1.7	32.4	9.0

2.1.2 Production

Silage making, a practice likely over 4000 years old, finds mention in the Old Testament (Isaiah, 30:24), where it was noted that "the oxen and young asses ate salted, seasoned green fodder." This ancient method of preserving feed was also known to the Egyptians and Greeks, who stored grain and whole forage crops in silos.

Ensiling serves as an ideal storage system that preserves the organic contents of biomass and prepares it for subsequent use without adding excessive costs, process complexity, or safety and environmental concerns. To achieve this, grass is compressed to a density between 140 to 260 kg m⁻³ [10], and then wrapped or covered to prevent oxygen penetration. This process promotes lactic acid (LA) production by lactic acid bacteria (LAB, mainly *Lactobacillus* spp.), lowering the silage's pH to below 4. Such a low pH environment inhibits the growth of other microorganisms, ensuring the preservation of the grass silage. Alternative storage methods include the application of chemicals like sulfuric acid and calcium hydroxide to maintain the pH at levels either sufficiently high (> 11) or low (< 3) to prevent bacterial growth.

Extensive research has focused on optimizing grass storage to guarantee a consistent supply [11].

For grass utilization, it must be harvested, transported to a processing facility, and stored efficiently to ensure the feasibility of the entire process.

2.1.2.1 Pretreatment

Before utilizing grass for conversion, it is essential that the grass undergoes pretreatment due to the recalcitrant nature of lignocellulosic biomass. This process aims to dismantle the complex lignocellulosic structure, enhancing the efficiency of subsequent steps like hydrolysis and biological conversion. The challenge in degrading plant biomass primarily stems from the resilience of lignin and its structural carbohydrates. Lignin, along with phenolic compounds and ferulic acid, contributes to the robust polymeric organic structure of the biomass, acting as a barrier to biodegradation.

Within the plant, hemicellulose and cellulose serve as strong natural polymers providing structural support. These components are the primary targets for conversion processes but are shielded by lignin. Consequently, pretreatment technologies are crucial for either breaking down or removing lignin and hydrolyzing cellulose and hemicellulose into simpler monomer sugars, such as glucose and xylose (**Figure 1**). This step is vital for preventing the formation of inhibitory compounds (in the like of Hydroxymethylfurfural (HMF) and Furfural) that could hinder the growth of microorganisms during the biological conversion phase.

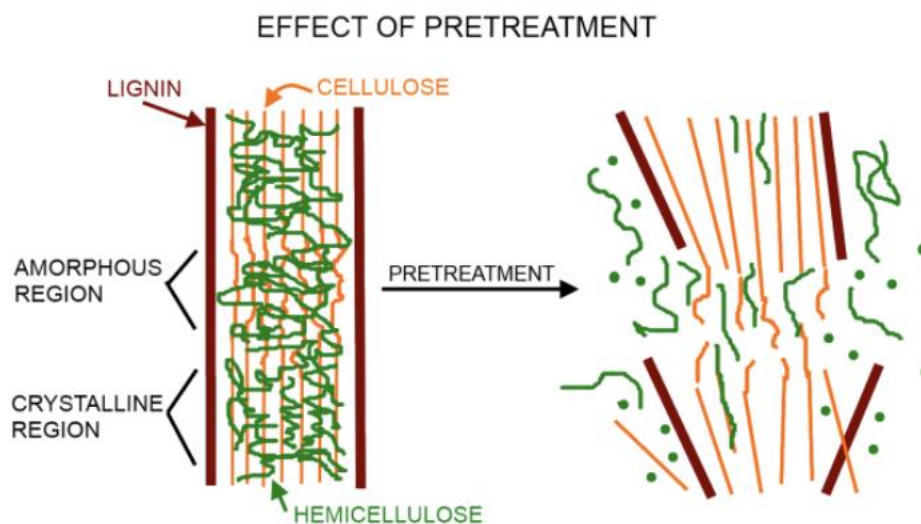


Figure 1 Schematic of pretreatment of lignocellulosic biomass [8]

Early pretreatment methods focused on biomass comminution to enhance biodegradability. Historical approaches, like using cutter machines for biomass size reduction, aimed to improve microbial activity. Nowadays, a variety of pretreatment methods have been developed, with cost being a primary consideration for large-scale operations. Biocompatibility and environmental sustainability are also critical factors in selecting pretreatment technologies, ensuring compatibility with biological processes. The choice of pretreatment method largely depends on the type of feedstock, with state-of-the-art technologies offering promising pathways. Common pretreatment categories include physical (grinding, milling), chemical (acid, alkali, solvent), and physio-chemical (steam explosion, wet oxidation, microwave, and ultrasound combined with chemical treatments). While physical methods are less expensive as well as less energy-intensive, they often result in lower sugar yields and delignification. Chemical treatments can improve cellulose accessibility but may leave toxic residues affecting enzyme activity and sugar yields. Milder acid and diluted alkali treatments have been explored to mitigate these issues. Microwave heating, a physio-chemical method, is typically used alongside physical or chemical processes to enhance effectiveness (**Table 2**).[12]

Table 2 Overview of lignocellulosic biomass pretreatment processes [13]

Techniques	Advantages	Disadvantages
Mechanical Comminution	<ul style="list-style-type: none"> • Reduced cellulose crystallinity 	<ul style="list-style-type: none"> • High power consumption
Pyrolysis	<ul style="list-style-type: none"> • Gas and liquid production 	<ul style="list-style-type: none"> • High temperature required. • Production of ash
Steam Explosion	<ul style="list-style-type: none"> • Cost-effective • Hemicellulose solubilization and lignin transformation • High yield of glucose and hemicellulose in a two-step process 	<ul style="list-style-type: none"> • Incomplete lignin degradation • Partial degradation of the xylan fraction • Not efficient for biomass with high lignin content • Toxic compounds such as acetic acid and a small amount of furan aldehydes generation
Ammonia Fiber Explosion	<ul style="list-style-type: none"> • Removes some lignin and hemicellulose • Low formation of inhibitors • Increased the accessible surface area; thus, cellulose becomes more accessible • Does not need a small particle size for efficacy 	<ul style="list-style-type: none"> • Not effective for high lignin content biomass • Recycling ammonia is needed • Alters lignin structure • High cost of ammonia
Carbon Dioxide Explosion	<ul style="list-style-type: none"> • Cost-effective • Increases the accessible surface area • No inhibitory compounds generated 	<ul style="list-style-type: none"> • No modification of lignin or hemicellulose can be made
Acid Hydrolysis	<ul style="list-style-type: none"> • High glucose yield • Solubilizes hemicellulose to xylose and other sugars • Alters lignin structure 	<ul style="list-style-type: none"> • High cost • High cost of corrosive-resistant equipment • Inhibitors such as aliphatic carboxylic acids (acetic acid, formic acid, levulinic acid) are generated
Alkaline hydrolysis	<ul style="list-style-type: none"> • Efficient removal of lignin and hemicellulose • Increases the accessible surface area 	<ul style="list-style-type: none"> • Long residence time required • Irrecoverable salts were incorporated into biomass • High cost of alkaline catalyst

	<ul style="list-style-type: none"> • Low inhibitor generation 	<ul style="list-style-type: none"> • Alteration of lignin structure
Ozonolysis	<ul style="list-style-type: none"> • Reduction of lignin content • No toxic compounds generation 	<ul style="list-style-type: none"> • Expensive process due to large amounts of ozone required
Oxidative delignification	<ul style="list-style-type: none"> • Degrades lignin • Low inhibitor generation 	<ul style="list-style-type: none"> • Not all oxidizing agents are effective for delignification
Organosolv process	<ul style="list-style-type: none"> • Hydrolyzes lignin and hemicellulose 	<ul style="list-style-type: none"> • Solvent to be drained from the reactor required, and it must be evaporated, condensed, and recycled • High cost
Biological Pretreatment	<ul style="list-style-type: none"> • Degrades lignin and hemicellulose • Requires low energy 	<ul style="list-style-type: none"> • Slow hydrolysis process

2.1.3 Components in Grass Silage

Grass silage is not only pivotal for livestock nutrition, but it is also a significant resource for biorefinery applications. The intrinsic value of grass silage is derived from its diverse chemical composition, which can be categorized into water-soluble carbohydrates, organic acids, and nitrogenous compounds.[10] Each of these groups plays a crucial role in the ensiling process, preservation quality, and utility of silage in both, feed and industrial applications.

2.1.3.1 Water-Soluble Carbohydrates (WSCs)

WSCs are the primary fermentable sugars in grass silage, serving as the fundamental substrates for lactic acid bacteria during the ensiling process. These carbohydrates include:

Fermentable Sugars,

such as glucose and fructose, which are directly utilized by microorganisms to produce lactic acid and thereby lowering the pH and preserving the silage.

In addition, these components also provide the basis for biofuel production and other bioproducts, leveraging the fermentative capacities of silage [14]

Polysaccharides,

which include cellulose and hemicellulose, which are not directly water-soluble but can be hydrolyzed into fermentable sugars. These complex carbohydrates contribute to the structural integrity of plants and, upon breakdown, add to the fermentable sugar pool available for microbial action.

Rich in carbohydrates, cellulose and hemicellulose are essential for biorefineries, serving as key ingredients for biofuel production, including bioethanol and biogas, derived from their conversion into fermentable sugars. They are also the basis for creating bioproducts such as bioplastics, chemicals like xylitol and furfural, and materials including biodegradable films and nanocellulose. [15]

2.1.3.2 Organic Acids

Organic acids are crucial for the preservation and stability of grass silage, contributing to its acidic pH, and inhibiting the growth of spoilage organisms. The main organic acids found in silage include:

Lactic Acid

As the dominant acid produced during the fermentation of WSCs, lactic acid effectively reduces silage pH, enhancing its preservation. Lactic acid is a versatile compound widely used

in food production, pharmaceuticals, and as a key component in biodegradable plastics like polylactic acid (PLA). [13]

Acetic Acid,

which acts as a secondary preservative acid, offering aerobic stability to the silage and preventing spoilage from yeasts and molds. Acetic acid can be used in manufacturing for the production synthetic fibers and adhesives, and as a solvent in the chemical industry. It is also utilized in agriculture as an effective herbicide. [16]

Butyric Acid

Typically associated with poor silage fermentation, butyric acid production indicates the presence of undesirable fermentation pathways. Butyric acid is utilized in biorefineries for biofuel production, particularly as a precursor for butanol, and in creating biodegradable plastics and bio-based chemicals. [17]

2.1.3.3 Nitrogenous Compounds

Nitrogenous compounds in grass silage arise from the protein content of the ensiled material and the microbial activity during ensiling. These compounds include:

Proteins,

which are essential for livestock nutrition, providing amino acids required for growth, milk production, and overall health. In biorefineries, proteins are utilized for enzyme production, bioplastics, and enhancing biofuel processes. [18]

Amides and Amines

Produced from the breakdown of proteins and amino acids during the ensiling process, amides and amines are key intermediates in biorefineries, used in making polymers, dyes, and pharmaceuticals, as well as supporting bio-based chemical production. [19]

2.2 LACTIC ACID (LA)

Lactic acid (2-hydroxypropanoic acid) is an organic acid that occurs naturally in fermented milk products. In 1780, the Swedish chemist Carl Wilhelm Scheele discovered lactic acid by isolating it from sour milk and naming it "acid of milk". Later, the French chemist Jean Baptiste André Dumas gave it the name lactic acid, which is derived from the Latin word "lac" meaning milk [20].

2.2.1 Chemical structure

Lactic acid is a type of carboxylic acid that has the chemical formula $C_3H_6O_3$. It contains a hydroxyl group that is situated next to the carboxyl group, which makes it an alpha-hydroxy acid (AHA). In a solution, lactic acid can easily lose a proton from the acidic group, which results in the formation of lactate ions.

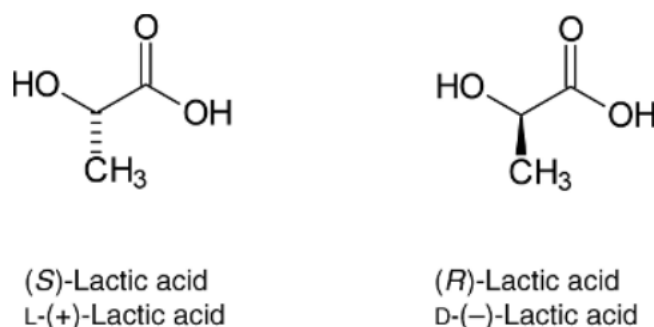


Figure 2 Chemical Structure of Lactic Acid [21]

Lactic acid has two optical isomers: L (+)-lactic acid and D (-)-lactic acid.

Table 3 Chemical properties of Lactic acid [2,21]

Chemical formula	$C_3H_6O_3$
Molecular Weight	90.08
pKa	3.86 at 25 °C
Melting Point	(52.7-52.8) °C for pure form and 16.4 °C
Solubility	Soluble in water and ethanol
Density at 20 °C (g/L)	1.249
Melting point (°C)	52.8 (D); 53.0 (L); 16.8 (DL)
Boiling point (°C)	82.0 (DL) at 0.5 mmHg; 122.0 (DL) at 15 mmHg; 103 (D) at 15 mmHg
Dissociation constant (pKa) at 25 °C	3.83 (D); 3.79 (L)
Heat capacity (J/mol·°C) at 20 °C	190 (DL)
Heat of solution (kJ/mol) at 25 °C	7.79 (L)
Heat of fusion (kJ/mol)	16.86 (L); 11.33 (DL)

2.2.2 Methods of Manufacturing

LA can be produced by two different methods: chemical synthesis or microbial fermentation. More than 90% of the lactic acid is produced by fermentation of carbon sources, especially sugars and alcohols. [22] The method of chemical synthesis involves reacting acetaldehyde with hydrogen cyanide to form acetonitrile, which thereafter is hydrolyzed to produce LA. The process of microbial fermentation involves using renewable resources, such as agricultural waste materials, as feedstock. Microorganisms, such as bacteria and fungi, are used to ferment the sugars present in the feedstock to produce LA. The chemical synthesis method is energy-

intensive and generates waste, while the microbial fermentation method is a more sustainable and eco-friendly option that reduces the carbon footprint, as well as offering a solution to manage agricultural waste by upcycling it into a valuable product. [23]

2.2.3 Application

Lactic acid is predominantly utilized in the food industry, which makes up about 70% of its use, especially in the production of yogurt and cheese due to its critical role in fermentation processes. In yogurt preparation, it is the main by-product of the co-fermentation of *Streptococcus thermophilus* and *Lactobacillus bulgaricus*. For cheese, the release of lactic acid decreases the pH, leading to the coagulation of casein micelles. [10] Beyond its culinary uses, lactic acid is a significant industrial product due to its versatile properties. It acts as a precursor for both, small molecules like propylene glycol and larger compounds, such as acrylic polymers. These polymers are biodegradable, making them suitable for packaging and labelling applications, and biocompatible, which is essential for creating prosthetic devices, sutures, and internal drug delivery systems. Polylactic acid is utilized in the textile, medical, and pharmaceutical industries, resulting in a wide range of applications.

In the cosmetic industry, lactic acid is a key component in the production of skincare and oral hygiene products, and is valued for its moisturizing, antimicrobial, and rejuvenating effects on the skin. Its derivatives, such as lactate esters, are widely used for their hygroscopic and emulsifying properties. The pharmaceutical industry employs lactic acid as a supplement in synthesizing dermatologic drugs and treatments for osteoporosis, highlighting its broad utility across various sectors. [13]

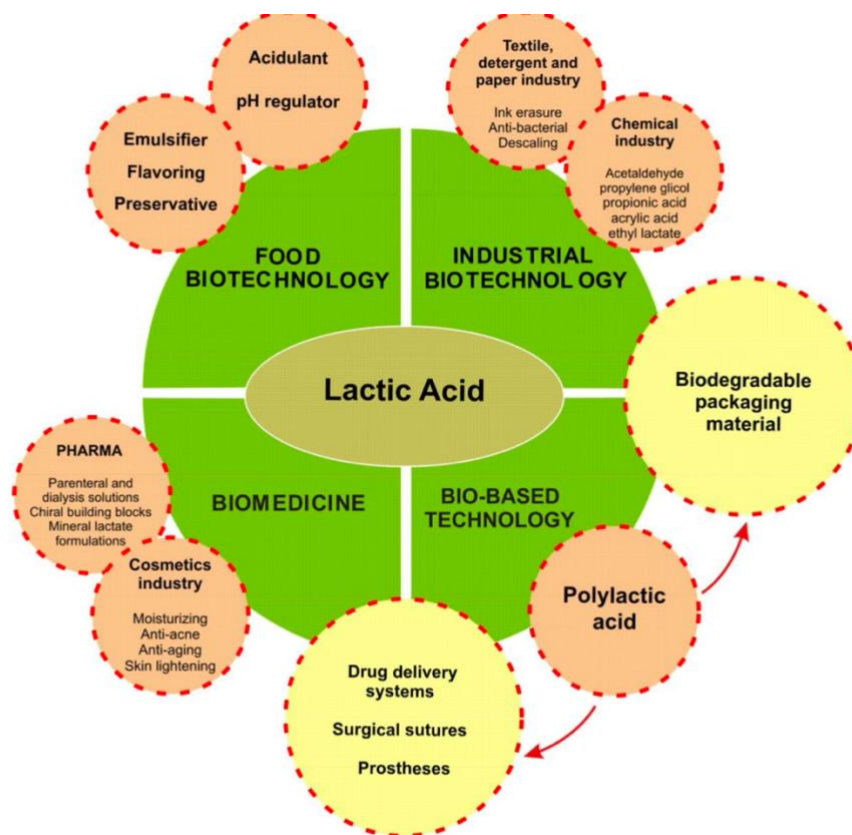


Figure 3 A wide range of biotechnological applications of lactic acid [13]

LACTIC ACID MARKET SHARE, BY APPLICATION, 2021 [%]

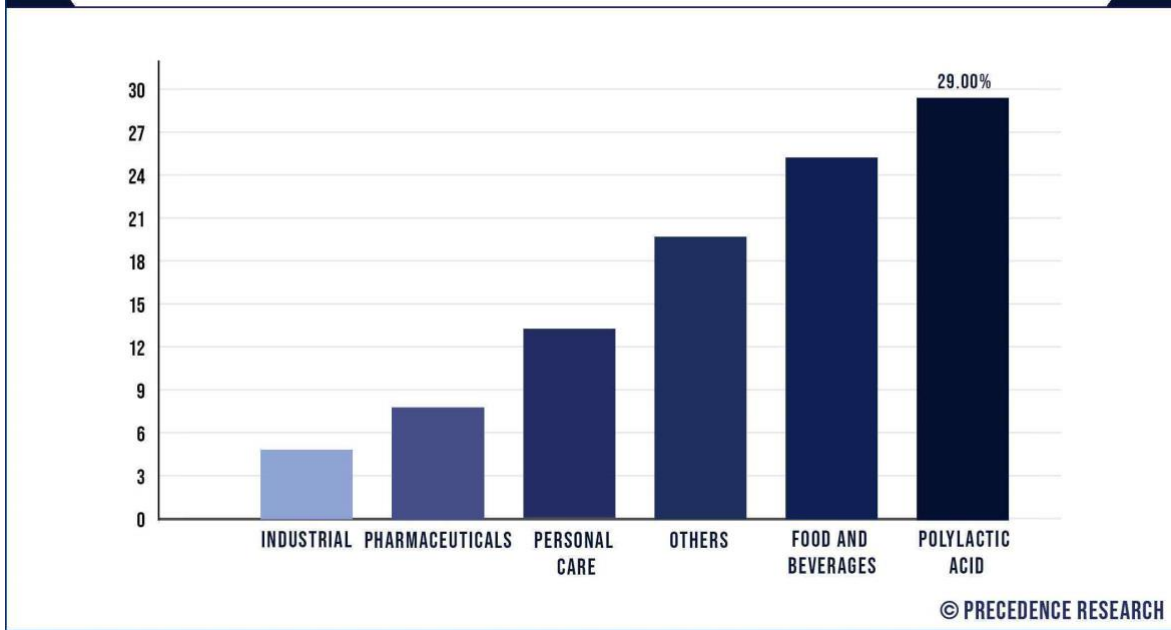


Figure 4 Lactic acid market share, by application in 2021 [1]

2.2.4 Market Size

The global lactic acid market was valued at USD 3.46 billion in 2022 and is projected to reach USD 7.93 billion by 2032, growing at a CAGR of 8.70%. This growth is attributed to the versatile usage of lactic acid across various industries, including food and beverages, pharmaceuticals, and biodegradable polymer production, with significant demand noted in developed and developing economies. [1]

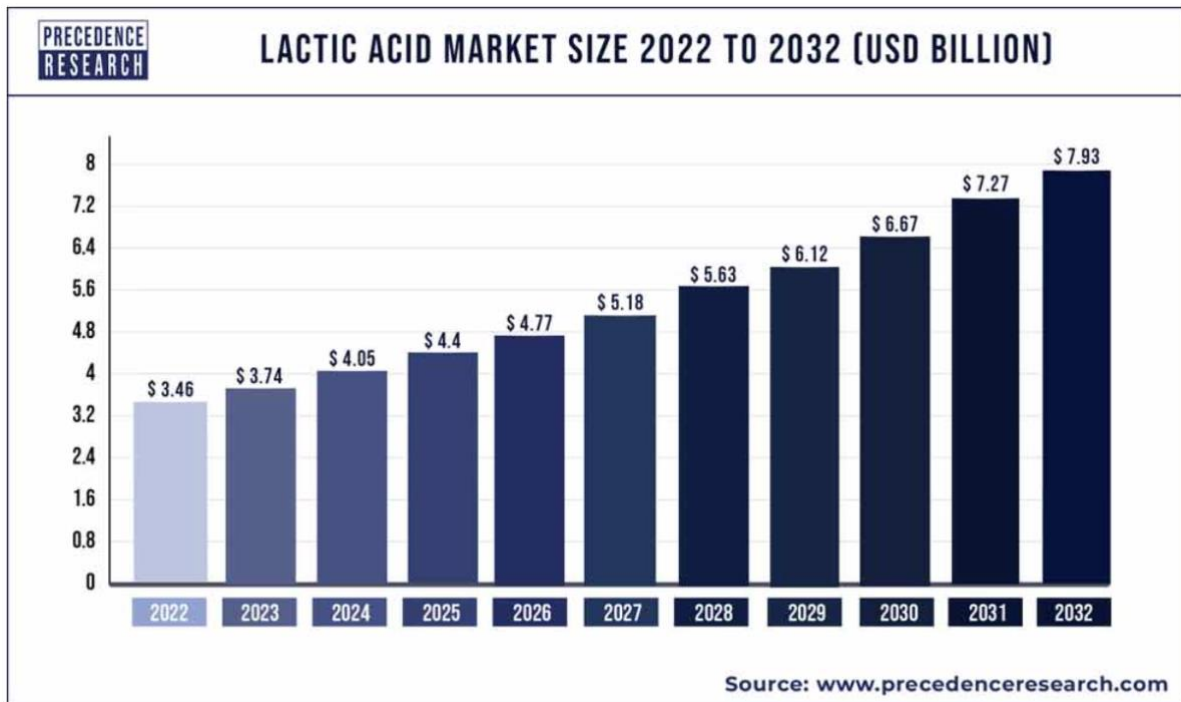


Figure 5 Lactic acid market size 2022 -2032 [1]

2.2.5 Extraction and Purification from Grass silage

Harnessing grass silage for lactic acid production aligns with eco-friendly principles, transforming agricultural waste into valuable chemicals and contributing to a circular economy. This approach does not only utilize a renewable biomass efficiently but also supports global efforts to reduce reliance on fossil fuels and decrease greenhouse gas emissions. [24]

Table 4, as taken from [4], contrasts different separation and purification methods as well as assessing their merits and demerits:

Table 4 Overview of the major LA separation and purification technique [4]

Techniques	Advantages	Disadvantages
Precipitation	<ul style="list-style-type: none"> • Ease in operation • Ease in process intensification (means from laboratory scale to plant scale) • Simple and reliable 	<ul style="list-style-type: none"> • Poor product purity • Have landfill problems due to huge generation of waste materials (such as gypsum) during process • Large sulfuric (H₂SO₄) requirements • Huge generation of wastewater • Time consuming
Adsorption	<ul style="list-style-type: none"> • Easy regeneration process • Minimum cost • Less environmental pollution 	<ul style="list-style-type: none"> • Minimum solvent lifetime • Limited adsorption capacity • Poor capacity • Time taking
Electrodialysis	<ul style="list-style-type: none"> • Minimum product inhibitory effect • High degree of separation • Large productivity 	<ul style="list-style-type: none"> • Huge generation of wastewater during process • Membrane fouling • Huge operational cost • Needs pre- treatments (such as ultrafiltration, decolorization, and removing of metals ions) of feed
Reactive distillation	<ul style="list-style-type: none"> • Minimum energy needs • High degree of purifications • Reduction in capital and operating costs • Both separation and reaction take place in single unit 	<ul style="list-style-type: none"> • Complex process • Energy intensive process • Used for reversible reactions in liquid phase • Forms high boiling esters and dimers in the case of homogeneous catalyst, the problems of separation and corrosion arise
Membrane methods	<ul style="list-style-type: none"> • High selectivity • No back mixing • Ease in scale of production • No direct exposure of microbes to toxic solvents • Ensuring biocompatibility • Easy to integrate with the fermenters which helps in 	<ul style="list-style-type: none"> • Large involvements of cost • Hindrances in process intensification • Problem of membrane fouling • Problems in polarization
Reactive extraction	<ul style="list-style-type: none"> • Simple and highly selective in nature • Economic and clean process • Provides high purity product • High product yield • Fast process • Low cost and environmentally benign 	<ul style="list-style-type: none"> • Product purity is not high • Needs stripping process to regain the solvents • Unfavorable distribution coefficients due to conventional solvents • Solvent toxicity
Emulsion liquid membrane	<ul style="list-style-type: none"> • High transfer rates due to the large interfacial surface area 40% less costly than solvent extraction 	<ul style="list-style-type: none"> • Poor ELM stability which creates further hindrances in its industrial scale applications

- Large-scale piloting availability
 - High mass transfer area to volume ratio ($1000\text{-}3000\text{ m}^2 / \text{m}^3$)
 - Low energy and chemical consumptions
 - Needs only small amount of organic solvents
 - Low volume ratio of organic to the aqueous phase
 - Simplicity of combination with other separation processes
 - Low capital investment
- Use of petroleum based organic solvents

2.3 MEMBRANE PROCESSES

The membrane separation technique is a physical process that involves using a membrane to filter and concentrate diverse materials and liquids selectively. It boasts many benefits, such as low energy consumption, small system volume, and ease of operation.

Membrane Technology involves separating multiple components using a membrane as the separating medium. The membrane is a permeable or semipermeable layer of organic or inorganic materials with typically different structures that often result in very selective separation of some particles in a fluid phase. The concept of a membrane separation process is represented in **Figure 6**

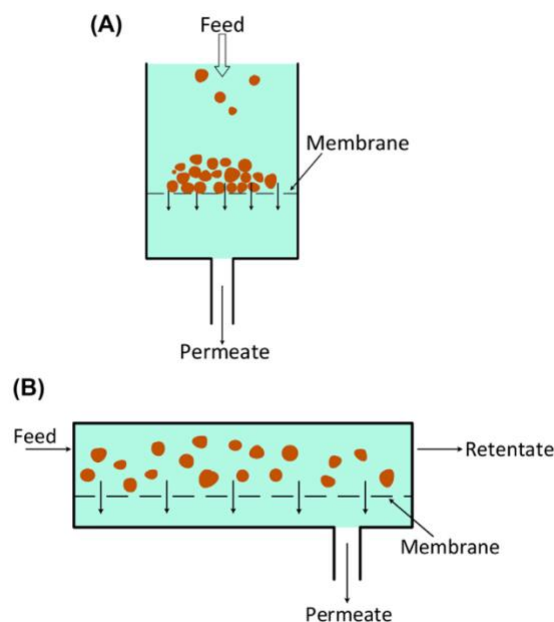


Figure 6 The Two Main Types of Membrane Filtration are Dead-End (A) & Cross-Flow (B) Filtration [25]

The membrane divides the feed into two streams, retentate, and permeate, by adjusting the relative transport rates of distinct species. The permeate, only contains the solvent and smaller molecules that can pass through the membrane; the retentate, consists of the molecules that cannot pass through the membrane; and finally, the membrane itself.

2.3.1 Pressure-driven membrane processes

Pressure-driven membrane-based processes can be categorized based on the size of membrane pores and solute particles. The four primary classes of these processes are microfiltration (MF), ultrafiltration (UF), nanofiltration (NF), and reverse osmosis (RO). Microfiltration employs larger pore and particle sizes to remove larger particles and suspended solids from a solution. In contrast, ultrafiltration is used to eliminate smaller particles such as bacteria and viruses. Nanofiltration removes dissolved ions and organic substances, while reverse osmosis is employed for desalination and the removal of salts and other dissolved solids (Figure 7).[26]

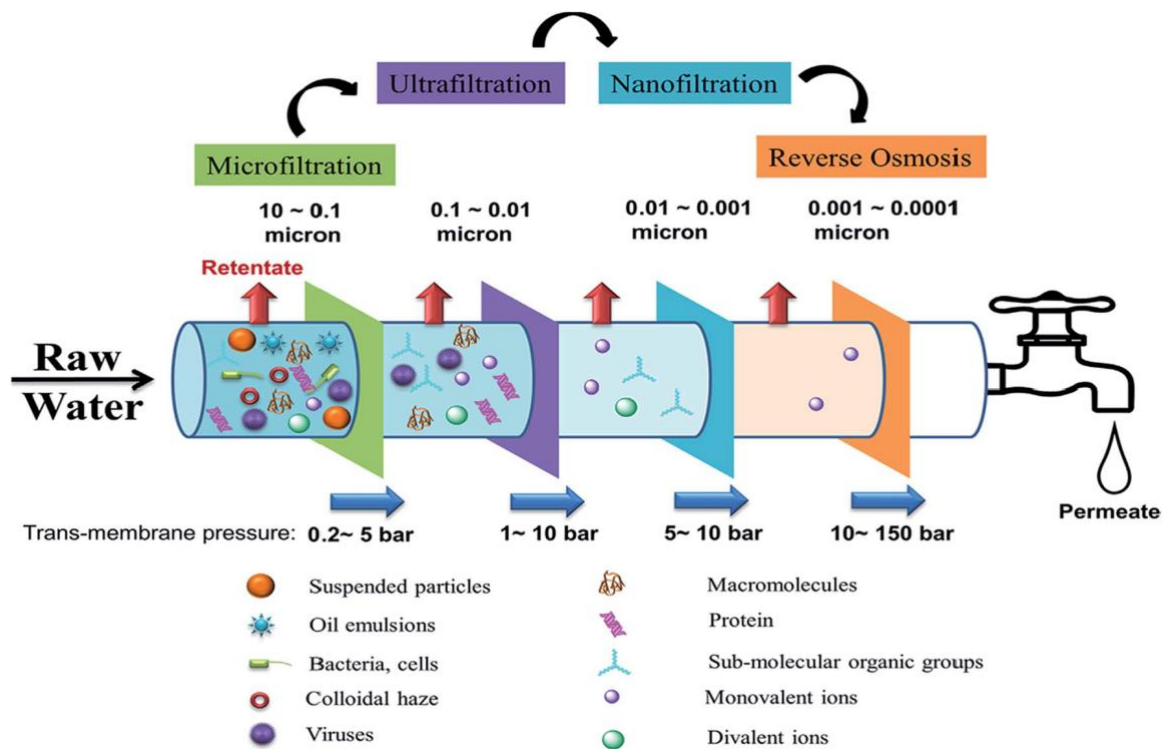


Figure 7 Pressure-Driven Membrane Process [26]

2.3.1.1 Membrane separation fundamental concepts and terminology

The performance characterization of membrane separation is determined by two crucial factors: permeate flux and membrane selectivity. These factors play a pivotal role in ensuring effective membrane separation. Permeate flux refers to the volume or mass of permeate that passes through a membrane in a certain amount of time per unit effective area of the membrane. As the driving force across the membrane is increased, the permeate flux is enhanced, meaning that the permeate flux is dependent on the driving force. The relation of flux and driving force is represented by the following equation [25]:

$$J = -L \frac{dX}{dx} \quad (2.1)$$

Where the variables are as follows:

J : permeation flux

L : phenomenological coefficient

dX/dx : the driving force, defined as the X gradient (pressure, temperature, concentration, etc.)

x : the coordinate (x).

The driving force could be a chemical potential gradient ($\Delta\mu$), an electrical potential gradient ($\Delta\varphi$), or the electrochemical potential, the transport equation of permeate flux when is the concentration gradient is the driving force is represented by Fick's law Eq. (2.2) [27]

$$J_A = -D_A \frac{dC_A}{dx} \quad (2.2)$$

Where the variables are as follows:

D_A : diffusion coefficient of component A across a membrane [$\text{m}^2 \cdot \text{s}^{-1}$]

Darcy's law (Eq. 2.3) can be used to describe pressure-driven convective flow, which is commonly observed in porous or capillary media. [25]

$$J_A = -K C_A \frac{dp}{dx} \quad (2.3)$$

Where the variables are as follows:

dp/dx : pressure gradient present in the porous medium,

C_A : concentration of component A in the medium

K : coefficient reflecting the nature of the medium.

The membrane's perm-selectivity toward a mixture is defined by Eq. (2.4) [25]:

$$a_{A/B} = \frac{y_A/y_B}{x_A/x_B} \quad (2.4)$$

Where the variables are as follows:

y_A, y_B, x_A and x_B : mole fractions of components A and B in the permeate and the retentate streams, respectively.

The rejection is defined as the fraction of solute in the feed, which is not permeate through the membrane, is expressed by Eq. (2.5) [25]:

$$R = \left(1 - \frac{c_p}{c_f}\right) \cdot 100\% \quad (2.5)$$

Where the variables are as follows:

C_f and C_p : feed and permeate solute concentrations, respectively.

The difference between the feed and permeate pressures is called transmembrane pressure (TMP), Eq. (2.6) [28] The transmembrane pressure is calculated for a cross-flow process as the mean of the pressures at the unit inlet and outlet **Figure 8**:

$$\text{TMP} = \frac{(P_{in} + P_{out})}{2} - P_f \quad (2.6)$$

Where the variables are as follows:

P_{in} and P_{out} : pressure of inlet and outlet, respectively

P_f : the pressure on the permeate side, is negligible.

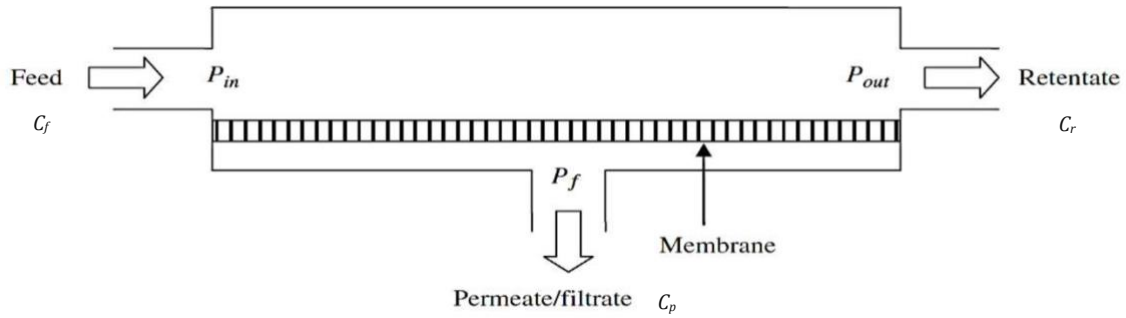


Figure 8 Transmembrane pressure in a cross-flow membrane module. [28]
 The permeate flux (J_A) across the membrane is proportional to the TMP. As in Eq. (2.7).

$$J_A = L_p TMP \quad (2.7)$$

Where the variable is as follows:

L_p : membrane's hydraulic permeability. (2.8) [28]:

$$L_p = \frac{J_A}{TMP} = \frac{\epsilon r^2}{8\mu\delta_m} \quad (2.8)$$

Where the variables are as follows:

ϵ : membrane porosity

r : pore radius

μ is the solvent viscosity

δ_m : membrane thickness

Equation (2.8) is only valid in the absence of osmotic pressure and/or solute rejection.

2.3.1.2 Microfiltration (MF)

Microfiltration membranes are a type of filtration technology that possess pores ranging from sub-micron to micron sizes, typically between 100 nm to 10 μ m, and fibers within the 100 μ m to 1 mm range. These membranes are designed to filter and separate particles based on their size, with larger particles being effectively captured through the process of sieving. One of the key benefits of microfiltration membranes is their ability to remove a wide range of particles, including bacteria, viruses, and other microorganisms, from fluids and liquids. Microfiltration membranes are commonly used as pre-filters for ultrafiltration processes, which are used to further purify fluids and liquids. By capturing larger particles before they reach the UF membrane, microfiltration membranes can help extend the lifespan of the UF membrane and improve the overall efficiency of the filtration process. Additionally, microfiltration membranes are used in a variety of industrial and commercial applications, including food and beverage processing, pharmaceutical manufacturing, and water treatment.

The initial stage in the downstream process of fermentation broth clarification is cross-flow microfiltration [29]. To recover lactic acid from dilute aqueous solutions, microfiltration using noisome of Span 80 modified by SDS was studied [30]. Microfiltration was utilized as a pre-purification step, with two downstream processes employed for the separation of lactic acid from a mixture of candy waste and digestate [31]. However, determining the optimal operating mode for cross-flow microfiltration remains a significant concern. Various operating modes of microfiltration were compared in terms of productivity and fouling rate to clarify the lactic acid fermentation broth [29]. H el ene Carr ere investigated the effects of the primary operating parameters involved in microfiltration (pore diameter, temperature, cross-flow velocity,

transmembrane pressure, permeate flux, and pH) on the permeate flux during fermentation broth clarification for lactic acid production [32].

2.3.1.3 Ultrafiltration (UF)

Ultrafiltration membranes have pore sizes in the 10–100 nm range. The pores of these membranes are small enough to allow water to pass through them under hydrostatic pressure while retaining particles and dissolved ions with high molecular weight.

UF membranes are widely used in various industries for the separation of small colloids such as water/oil microemulsions, bacteria, and viruses. In applications such as the paint and food industries, UF membranes are commonly used as pre-treatment membranes for NF and reverse osmosis.

UF can also be combined with other technologies and used as basic unit operations to concentrate lactic acid production. Brygida Wojtyniak [33] has demonstrated that a ZOSS UF membrane integrated into a fermentation process could separate the product of fermentation from fermentation broth.

2.3.1.4 Nanofiltration (NF)

Nanofiltration membranes have pore sizes in the 1–10 nm range (for 0.1–1 nm-sized particles). NF membranes are constructed as three-layer composite membranes, with a thin selective layer sandwiched between two porous support layers. The selective layer is responsible for the separation of the contaminants, while the support layers provide mechanical strength and stability to the membrane.

These membranes are capable of removing divalent ions and organic contaminants from water, while monovalent salts of smaller sizes, such as sodium chloride, pass through. NF membranes mainly retain divalent ions and multivalent salts such as sodium sulfate and calcium sulfate; consequently, taste, odor, and color are removed.

The mechanism of nanofiltration membranes is facilitated by steric or sieving hindrance, and electrostatic effects.

Nanofiltration is considered an important unit in the downstream processing of lactic acid and amino acids. NF of silage juice from a green biorefinery was investigated as a first step to purify lactic acid and amino acids by Werner Koschuh [34].

Also, the separation and purification of LA and AA in one-step nanofiltration have been investigated [35].

Further investigation was carried out on the downstream purification of lactic acid solution from its fermentation broth using three different NF membranes in a cross-flow membrane module. The results showed that properly selected nanofiltration membranes could effectively retain sugar for recycling while purifying lactic acid to a high degree [36].

However, when the clarified fermentation broth was treated by NF at the acidic pH required to convert lactate into undissociated lactic acid, LA rejection was low (35–58%) and like that of the inorganic salts present in the fermentation broth (45–76%). This is due to the electrostatic effect, which limits the recovery of lactic acid through NF [37].

2.3.1.5 Reverse Osmosis (RO)

During the process of reverse osmosis for membrane pore sizes of 0.1–1 nm, the feed is transported from a high concentration to a low concentration by applied pressures higher than the osmotic pressure of the solution; the water, therefore, flows from the concentrated salt water (feed solution) to the dilute water (draw solution). To overcome the osmotic pressure of the salt solution through the membrane, a hydraulic pressure of approximately 0.7 to 5.5 MPa is required. The advantages of using improved high-permeability membranes include efficiency

and reduced power consumption. Thin-film composite (TFC) polyamide RO membranes, with good flux and salt-rejection properties, are typical membranes used in desalination applications.

The membranes used for reverse osmosis have a thin-film composite structure that consists of several layers of material, including a thin layer of polyamide that is responsible for the membrane's excellent salt-rejection properties. The material used in TFC membranes is highly resistant to fouling and scaling.

During downstream processes, a polyamide composite membrane was used for the separation of lactic acid through RO. The membrane swelled at a feed solution pH of 2.2, and no solute-membrane affinity was detected. [38]

To enhance the separation of lactic acid through reverse osmosis, J.M.K. Timmer conducted model studies. [39]

Chapter 3: Material and Methods

3.1 MATERIAL

3.1.1 Chemicals

3.1.1.1 Sulfuric Acid H₂SO₄

For precise pH adjustment of the samples, concentrated sulfuric acid (Merk, CAS number: 7664-93-9), with a concentration of up to 96 %, was utilized. The selection of this particular acid was not solely based on its efficacy in pH modulation but also on the ease of detection and removal of its cations/anions in subsequent production stages. Additionally, the pK_a value of sulfuric acid facilitated effective pH control using relatively minimal quantities of the acid, thereby rendering the process both efficient and focused.

3.1.1.2 MilliQ Water



Figure 9 arium® pro Ultrapure Water System

Dilution and purification processes in all experiments were consistently performed using ultrapure water. To obtain this high-purity water, the arium® pro Ultrapure Water System was employed (**Figure 9**), which efficiently deionizes tap water.

The arium® pro system can produce water with a conductivity of $0.055 \mu\text{S}\cdot\text{cm}^{-1}$, equivalent to a resistivity of $18.2 \text{ M}\Omega\cdot\text{cm}^{-1}$ at 25 °C. [40]

3.1.1.3 Analysis Standards

For the High-Performance Liquid Chromatography (HPLC) analysis, the following standards were employed:

Table 5 HPLC Standards [41]

Standard	Standard Substance	CAS-Nr.
Acetate	Sodiumacetate	127-09-3
Formate	Sodiumformate	141-53-7
Fructose	D- (-)-Fructose	57-48-7
Glucose	D (+)-Glucose-Monohydrate	77938-63-7
Lactate	Calciumlactate-Pentahydrate	5743-47-5

3.1.2 Grass silage

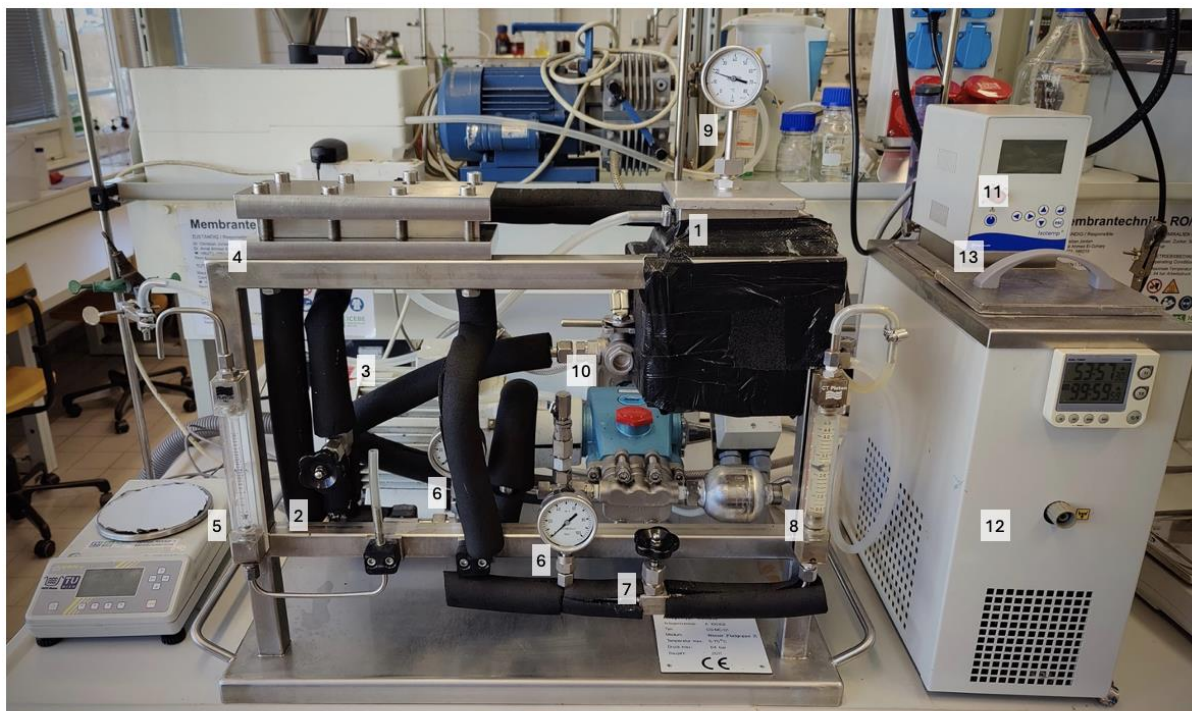
Grass silage, provided by local farmers, was processed through a screw press to extract grass silage juice (GSJ). This GSJ was subjected to pre-filtration via a bag filter before being transported to TU Wien, where it was stored at -20°C pending utilization in membrane processing experiments. The compositional details of the Grass Silage are outlined in **Table 6** [42]

Table 6 Grass Silage Composition [42]

Material	Concentration [g.L ⁻¹]
Lactic Acid	20.4
Acetic Acid	3.31
Amino Acid	19.3
Arginine	1.91
Aspartic Acid	2.04
Leucine	1.84
Glucose	4.27
Fructose	6.53
Ca ²⁺ , Mg ²⁺ (sum)	1.09
Cl ⁻	1.01
SO ₄ ²⁻	0.23
Na ⁺ , K ⁺ , NH ₄ ⁺	4.2
Dry Matter	102

3.1.3 Experiment Setup

The experimental setup is divided up into three stages, each employing a specific membrane type while keeping the experimental apparatus setup the same. At the heart of this configuration lies the OS-MC-01 membrane filtration unit, manufactured by Osmo in 2011. This unit is equipped with a feed tank capable of holding up to 2 L and features a membrane module with an active surface area of 0.008 m², capable of working under a maximum operational pressure of 64 bar. [43]



Osmo MemCell (Membrane Filtration Unit):

1. Dual-Walled Temperature-Controlled Feed Tank
2. Feed Recirculation Valve
3. High Pressure Piston Pump
4. Membrane Module
5. Permeate Flow Meter
6. Pressure Gauges
7. Pressure Regulating Valve

8. Retentate Flow Meter
9. Thermometer
10. Three-Way Ball Valve

Thermal Bath Circulator Unit

11. System Monitor
12. Temperature Control Unit (TCU)
13. Thermostat Control Panel

Figure 10 Experimental Equipment

A piston pump from CAT Pumps, model 231, is utilized to feed the solution into the recirculation loop. This pump, characterized by its oscillating high-pressure piston and triplex design, enables the introduction of the feed at pressures up to 60 bar and flow rates reaching $3.7 \text{ L} \cdot \text{min}^{-1}$. [44]

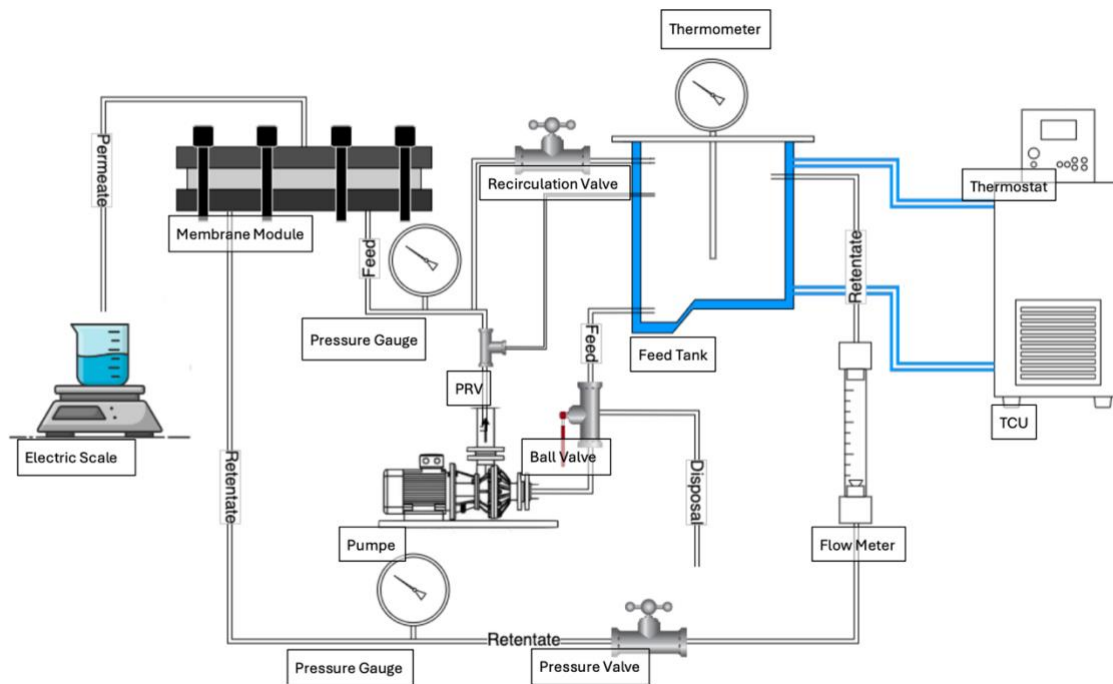


Figure 11 Block Flow Diagram of Membrane Filtration Unit

The recirculation speed is modulated through a gate valve situated in the feed recirculation line, where closing the valve reduces the bypass to the feed tank and enhances the circuit's flow rate. The flow of permeate and retentate is quantified by rotameters, with the permeates mass flow rate being carefully documented at set intervals via a digital precision scale during the experiments.

Pressure within the loop is monitored by two barometers, placed before and after the membrane module, to facilitate the identification of both the pressure put on the system and any potential membrane clogging.

The temperature of the feed solution or retentate is gauged with an analog thermometer mounted on the feed tank's lid. Temperature regulation is achieved by the addition of cold or hot water to the double-jacketed feed tank, which is linked to a Fisherbrand™ Isotemp™ R20 Refrigerated and Heated Bath Circulator unit. This arrangement guarantees the preservation of a stable temperature throughout the experiment, controlled by a thermostat. [45]

3.1.4 Membrane

In the experimental component of the study, five different membranes were deployed throughout the various experimental steps: two microfiltration membranes, MFG-1- Alfa Laval and MFG-2-Alfa Laval; two nanofiltration membranes, NF- Alfa Laval and NP010- Nadir; and a reverse osmosis membrane, RO98pHt- Alfa Laval. These membranes were chosen based on their unique properties and efficacy, pivotal for the intended filtration processes. It is noteworthy that the membranes were supplied as rolled sheets, with dimensions ranging from 0.5 to 1 m², and required precise cutting to fit the experimental setup before use. The comprehensive attributes of these membranes, as delineated by their respective manufacturers, are concisely compiled in **Table 7**. This compilation includes crucial technical specifications and performance metrics, which are key to choosing the right membrane for specific filtration tasks.

Table 7 Membrane Characteristics

Membrane	Filtration Type	Chemical Composition	Pore Size/ MWCO	pH	P [bar]	T [°C]
MFG-1 Alfa Laval [46]	Micro Filtration	Polypropylene Polysulfone	1 µm	1.5-12	1-3	5-75
MFG-2 Alfa Laval [46]	Micro Filtration	Polypropylene Polysulfone	2 µm	1.5-12	1-3	5-75
NF Alfa Laval [47]	Nano Filtration	Polyester Thin-Film Composite	0.3 – 10 kDa	3-10	15-42	5-50
NP010 Nadir [48]	Nano Filtration	Polypropylene Polyethersulfone	1-1.2 kDa	0-14	15-40	5-95
RO98pHt Alfa Laval [47]	Reverse Osmosis	Polypropylene Thin-Film Composite	<0.2 kDa	2-11	15-42	5-60

3.1.5 Analytical Equipment

3.1.5.1 Refractometer

To analyze the glucose and fructose content in samples of feed, retentate, and permeate, a digital refractometer from A.KRÜSS Optronic, model DR6100-T, was utilized. This instrument can perform measurements within the ranges of nD 1.3200 to 1.7000 and 0 to 95 °Bx, enabling precise determination of both the Brix value and the refractive index, nD. The sugar concentrations were measured in °Bx, and the refractive index nD was also recorded. [49]



Figure 12 Refractometer.

$^{\circ}\text{Bx}$ is a metric used to assess the total amount of solid substance, typically sugars, dissolved in a liquid, as demonstrated by the equation:

$$\rho[x^{\circ}\text{Brix}] = \rho \left[\frac{x g_{\text{Suc}}}{100 g_{\text{Sol}}} \right] \quad (3.1)$$

Where:

g_{Suc} = Sucrose in gram

g_{Sol} = Solvent in gram

The refractive index (n_D) of a substance is calculated by the ratio of the speed of light in a vacuum (c) to its speed in that substance (v). This measure is essential for determining the degree to which the speed of light is reduced within the substance.

$$n = \frac{c}{v} \quad (3.2)$$

3.1.5.2 Conductivity & pH meter

The VWR MU 6100 H, a highly precise pH and conductivity meter, was utilized for the analysis of feed, retentate, and permeate samples. Equipped with an advanced Epoxy pH gel electrode 111, featuring an integrated temperature sensor (cable length of 1 m), and a conductivity sensor CO 11, also with an integrated temperature sensor (cable length of 1.5 m),

the device covers a pH measurement range from -2 to 20 with an accuracy of ± 0.005 and a conductivity range from 0 to 2500 $\mu\text{S/cm}$ with an accuracy of ± 1 $\mu\text{S/cm}$. The device's automatic conversion of measurement values eliminates the need for manual calculations. Conductivity, influenced by ion concentration and mobility as well as solution temperature, serves as an indicator of a solution's electrical conductivity. Typically, inorganic compounds are strong electrical conductors, whereas organic polar molecules exhibit lower conductivity in solution. [50]



Figure 13 MU 6100H Unit, Conductivity Sensor, pH Electrode

3.1.5.3 High Performance Liquid Chromatography (HPLC)

The quantification of organic solutes such as lactic acid, acetic acid, formic acid, glucose, and fructose was performed using the ThermoScientific Vanquish HPLC System, comprising:

Quaternary Pump C: Supports multi-solvent blending with flow rates of 0.001 to 10 mL/min and pressures up to 700 bar, featuring a 400 μ L mixer and integrated vacuum degasser.[51]

Split Sampler CT: Offers high precision and accuracy for sample handling up to 700 bar, with temperature control from 4 to 40 $^{\circ}$ C and injection volumes ranging from 0.010 to 100 μ L. [51]

Column Compartment C: Provides temperature control from 5 to 85 $^{\circ}$ C, accommodating two columns up to 300 mm in length with options for air temperature regulation. [51]

Variable Wavelength Detector C: Delivers low peak dispersion and a high dynamic range, supporting fast wavelength switching across a range of 190 to 750 nm. [51]

Aminex HPX-87H Column: Specialized for separating organic acids and sugars with high sensitivity and resolution, operating at ambient to 60 $^{\circ}$ C, and designed for complex mixtures. [51]



Figure 14 ThermoScientific Vanquish HPLC System[52]

3.2 METHOD

The experimental protocol was initially designed to commence with microfiltration, followed by a pH adjustment to either 2.5 or maintaining it at 4.5, before proceeding to nanofiltration and reverse osmosis as shown in **Figure 15**

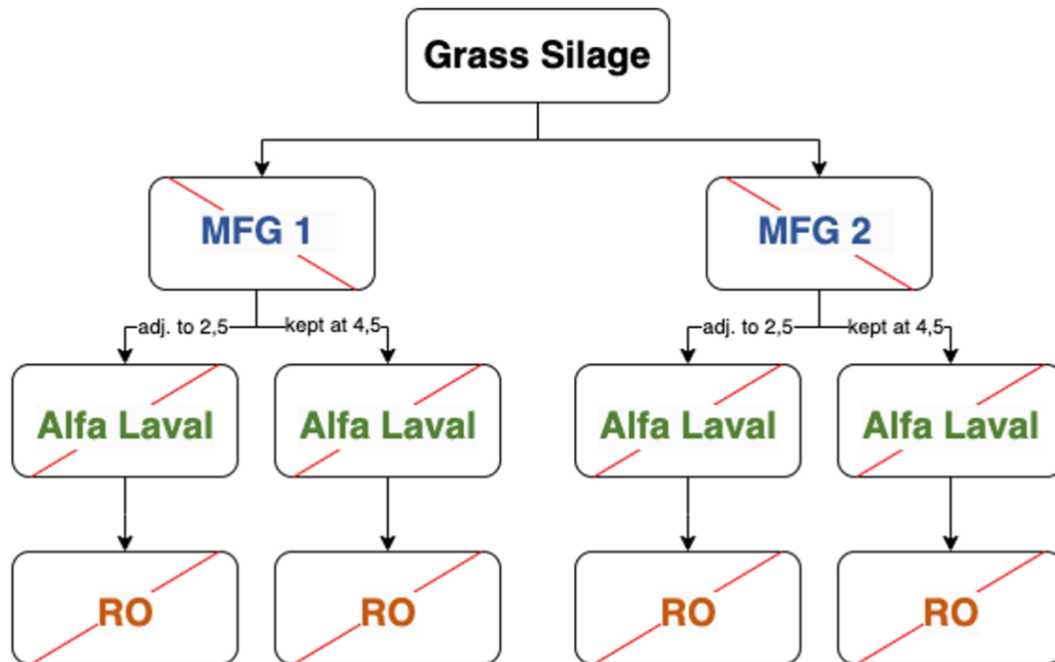


Figure 15 Original Experimental Design Flowchart

However, during the initial attempt to adjust the pH, turbidity was observed in the solution, leading to the formation of a precipitate. This resulted in the blocking of the first membrane, necessitating a revision of the experimental procedure, pictures in the flow chart in **Figure 16**

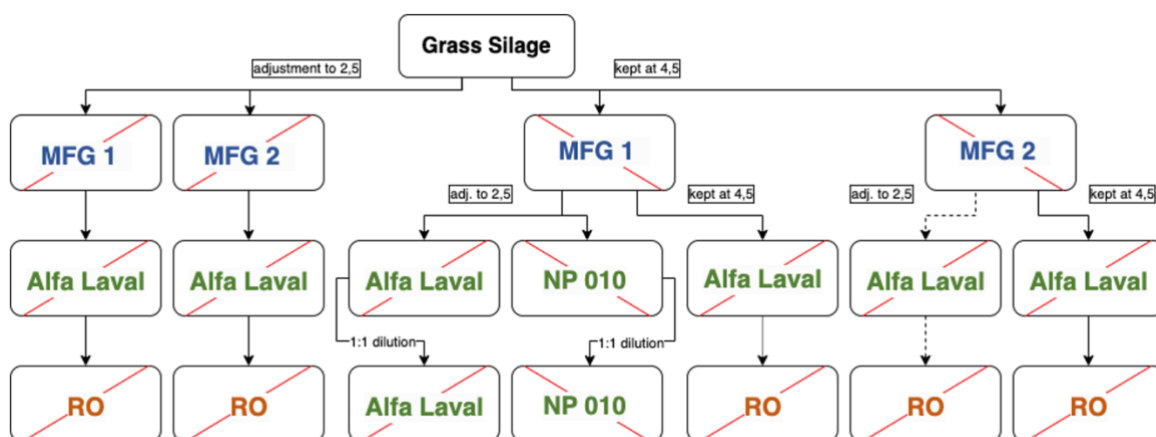


Figure 16 Final Experimental Design Flowchart

The modification aimed to remove the precipitate and to assess its impact on the final product. Accordingly, the pH was first adjusted and then followed by microfiltration. The acidified,

microfiltered permeate was subsequently diluted 1:1 with water and filtered through two different nanofiltration membranes for comparative analysis.

3.2.1 Feed Preparation

For the microfiltration process, the feed originated from one of our 20 L grass silage containers, typically kept frozen for more than seven days to ensure preservation. For nanofiltration experiments, the feed comprised the combined permeate from a preceding microfiltration trial, while for reverse osmosis experiments, it was sourced from the collective permeate of prior NF experiments.

Thawing

Due to the presence of proteins and organic compounds in grass silage, a meticulous thawing process was essential to prevent denaturation. The standard protocol entailed moving the silage containers from the freezer to the cooling cell the Friday before the experiment, allowing a gradual thaw by Monday. Alternatively, a lukewarm water bath could be used, but this method, taking over 12 h, was feasible only for smaller permeate containers of 1.2 – 1.3 L, not the larger 20 L storage containers.

Withdrawal from Storage Container

Withdrawal from the grass silage storage container involved simple decanting, paying close attention to the presence of solids in the feed. Consequently, the canister was disturbed as minimally as possible, leaving about one liter of liquid behind to prevent sediment contamination. The filtration machine's feed container, although rated for 2 L, actually has a fill volume of 2.2 L, a factor consistently accounted for during feed withdrawal. The amount of feed removed was carefully controlled to match the day's experimental needs and was determined by weight rather than volume.

pH Adjustment

Initially, pH adjustment was planned to occur post-microfiltration and pre-nanofiltration but was revised to precede microfiltration to address precipitation observed in all but two experiments. pH adjustments were made at the outset for experiments designated for a pH of 2.5, without further adjustments during subsequent filtration stages. The natural pH of the solution, typically around 4.5, was carefully monitored and maintained. Adjustments were made under continuous stirring, monitored with a VWR pH meter, with sulfuric acid added dropwise until the target pH was achieved. For a 2200 g feed batch, the required sulfuric acid ranged from 30-40 g, equating to 1.3- 1.85 % by weight.

Table 8 Feed Acidification Parameters

Date	Membrane	pH [-]	Total Feed [g]	Added Acid [g]	Final pH [-]	Acid Mass Fraction [%]
Microfiltration-Feed						
19.07.23	MFG-2 Alfa Laval	2.5	2464.99	42.50	2.478	1.72
20.07.23	MFG-2 Alfa Laval	2.5	2420.00	40.50	2.620	1.67
26.07.23	MFG-1 Alfa Laval	2.5	2034.54	26.62	2.622	1.31
26.07.23	MFG-1 Alfa Laval	2.5	2062.16	36.24	2.243	1.76
31.07.23	MFG-1 Alfa Laval	2.5	2096.73	30.20	2.779	1.44

05.02.24	MFG-2 Alfa Laval	2.5	2663.48	45.00	2.555	1.69
06.02.24	MFG-2 Alfa Laval	2.5	2172.07	31.50	2.730	1.45
07.02.24	MFG-2 Alfa Laval	2.5	2116.48	30.00	2.740	1.42
08.02.24	MFG-2 Alfa Laval	2.5	2028.30	32.00	2.650	1.58
07.02.24	MFG-1 Alfa Laval	2.5	2095.12	30.50	2.813	1.46
08.02.24	MFG-1 Alfa Laval	2.5	2130.34	36.00	2.600	1.69
09.02.24	MFG-1 Alfa Laval	2.5	2047.12	30.00	2.831	1.47
09.02.24	MFG-1 Alfa Laval	2.5	2095.97	30.00	2.820	1.43
Nanofiltration-Feed						
13.07.23	NF Alfa Laval	2.5	1941.95	36.00	2.464	1.85
17.07.23	NP010 Nadir	2.5	2077.80	36.00	1.965	1.73

Feed Analysis

Prior to entering the filtration system, key parameters of the feed were assessed and recorded: pH, conductivity, Brix, and nD.

Sampling

The preparatory step involved taking a 50 mL sample, assigning an experiment and sample ID, dating, and then freezing it for quality assurance and subsequent analysis.

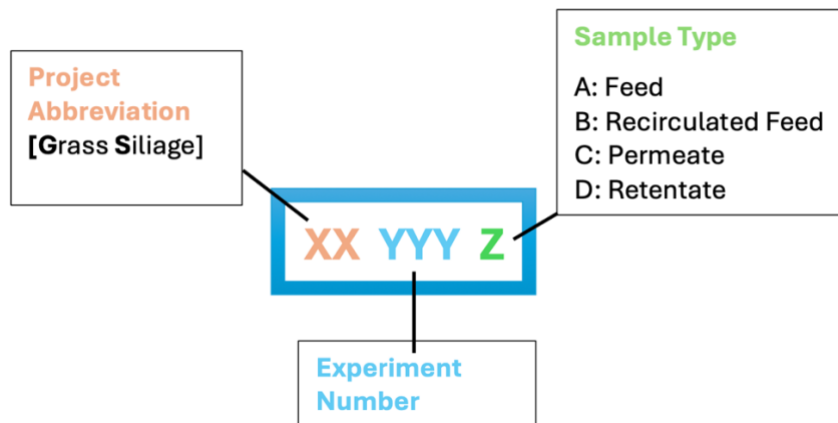


Figure 17 Sample ID Nomenclature

3.2.1.1 Filtration Preparation

Membrane preparation

The membrane area was 0.008 m², necessitating the precise cutting of the appropriate piece from the membrane sheets for each experiment. Each membrane sheet was inspected for potential damage before cutting a piece measuring 20 cm in length and 4 cm in width. Subsequently, the membrane piece had to be soaked in water for 30 min to swell before it could

be installed in the membrane module. The membrane, with its coated side facing downwards, was placed on the moistened membrane holder, and secured by placing the top part of the holder. The membrane was then checked for any wrinkles on the sides before being secured with eight screws.

Compaction

Once secured in the module, the membrane needed to be compacted. This was achieved by filling the system with water and circulating it at the temperature planned for the subsequent experiments (25 °C), without applying pressure to prevent feed water from permeating the membrane and to keep the membrane's surface moist and clean. Care was taken to slowly increase the circulation speed only after completely removing air from the system. After reaching the maximum flow rate, water was circulated for 15 min.

Parameters

The parameters for the experiments were predefined, primarily differing in the applied pressure and are shown in **Table 9**.

Table 9 Operational Conditions of experimental Steps

Filtration Type	Membrane	Membrane Area [m ²]	pH	P [bar]	T [°C]
Micro Filtration	MFG-1	0.008	2.5/	2	25
	MFG-2		4.5		
Nano Filtration	NF NP010	0.008	2.5/4.5	30	25
Reverse Osmosis	RO98pHt	0.008	2.5/4.5	40	25

Water permeability

To determine water permeability, a specific approach was adopted both before and after each filtration experiment. Initially, the setup was filled with deionized water. With the system operational and the pressure set to zero, the environment was kept at room temperature for 20 min.

After this compacting phase, the temperature within the system was regulated to a consistent 25 °C, aligning with the experimental requirements. The flow rate was carefully adjusted to 3.6 L·min⁻¹. Pressure adjustments were made according to the specific needs of each filtration type, as detailed in the previously mentioned parameters table. This customized approach was vital for preventing any damage to the membranes and for accurately evaluating their performance.

Once the system had stabilized under these conditions, the next step was to measure the mass flow rate of the permeate, which was done at intervals of five minutes.

After completing the permeability test, the procedure for shutting down the system was carried out. Initially, the pressure within the system was carefully reduced back to zero, ensuring a gradual transition to avoid any stress on the membranes. Following this, the flow rate was also decreased to zero, signaling the end of active testing. With these conditions met, the machine was then turned off and all the water was thoroughly drained from the system.

Feed Recirculation

The feed was introduced into the system and circulated for approximately 10 min or until it reached the target temperature of 25 °C. This circulation step was conducted without applying pressure to prevent the feed from prematurely permeating through the membrane. The purpose of this procedure was twofold: firstly, to ensure the fluid reached the desired temperature, and secondly, to thoroughly mix it with the water already present in the system. This mixing action was aimed at creating a homogenous solution. A gradual increase in circulation speed to its maximum was carefully executed after confirming the complete removal of air from the system, ensuring optimal preparation for filtration.

Sampling

The recirculated feed was sampled and labelled with its designated sample ID, as outlined in **Sampling**, then stored in a freezer for quality assurance and further analysis.

Recirculated Feed Analysis

Before commencing filtration, critical parameters of the recirculated feed were evaluated and documented.

Inline: The electrodes of the pH meter and the conductivity meter were rinsed with Milli-Q water, inserted into the feed tank, and the readings were recorded.

Atline: Concurrently, a sample was taken using a single-use pipette and analyzed with a refractometer to determine the Brix and nD values.

Filtration

To initiate filtration, the pressure of the already recirculating system was carefully increased to the level specified for the experiment. This adjustment was made cautiously, monitoring the barometer closely due to potential initial fluctuations and unexpected surges in pressure. The tare weight of the permeate container was noted. The first 10 – 80 g of permeate were collected, and the start weight was timed using a stopwatch. Subsequently, the permeate weight was periodically measured to deduce the mass flow rate of the permeate, along with performing atline and inline measurements of the permeate and retentate.

Attention was paid to first note the permeate weight, then to promptly take samples for atline analysis, and immediately thereafter, conduct inline measurements. For inline measurements, care was taken to first measure the permeate, wash the electrode, then measure the retentate to minimize the risk of contamination.

The experiment typically concluded when the feed tank level dropped below 45% of its capacity, indicated by the exposure of the PRV return pipe.

Other termination criteria included:

- Experiment duration exceeding 5 h
- Excessively high flow rate (indicative of membrane damage)
- Very low flux early in the experiment

Sampling

Permeate and retentate were sampled, labelled with their assigned sample IDs as described in **Sampling**, and then frozen for quality assurance and subsequent analysis.

Permeate & Retentate

The permeate was decanted into an appropriate sample container, sealed airtight, and stored either for long-term in the deep freeze or for mid-term in the cooling cell if further use was anticipated.

Retentate

The retentate was drained through the disposal line into a tared sample container, and then the remaining feed tank contents were transferred into the sample container using a pipette to determine the mass of the permeate. This process allowed for the calculation of loss in comparison to the original feed mass. With two exceptions, the permeate was directly moved to long-term storage.

3.2.1.2 Filtration Reset

Resetting

The system was flushed repeatedly with water to ensure cleanliness. This involved filling the system with Milli-Q water, circulating the water for 1 minute as described in **Compaction**, then sequentially opening the pressure valve, followed by the recirculation valve, and finally turning off the pump. Subsequently, the system was drained via the disposal line and the process was initiated again. This cycle was repeated until the conductivity electrode could no longer detect any impurities.

Water permeability

At the experiment's conclusion, the system was once again filled with Milli-Q water and circulated until the operational temperature of 25 °C was reached. Following the procedure outlined in **Water permeability**, the membrane's permeability was tested to assess its condition. Depending on the state of the membrane, the water was then drained, and the membrane removed, or a new filtration process was initiated if the membrane's condition permitted.

3.2.1.3 HPLC

Sample Preparation

Selected samples from each filtration stage were thawed and diluted with Milli-Q water at a 1:9 ratio, following standard laboratory procedures. The diluted samples were then passed through a nylon filter into autosampler vials via syringe, readying them for HPLC analysis. This straightforward preparation ensures samples are clear of particulates and at a suitable concentration for accurate detection of solutes.

HPLC preparation

Membrane Preparation and Analysis Setup

The Aminex HPLC column was preconditioned by heating initially at $0.2 \text{ mL} \cdot \text{min}^{-1}$ to $40 \text{ }^\circ\text{C}$, after which the temperature was raised to $60 \text{ }^\circ\text{C}$ once the pressure stabilized. The flow rate was then increased to $0.6 \text{ mL} \cdot \text{min}^{-1}$, ensuring the pressure did not exceed 50 bar. The system was prepared for sample introduction by circulating 2-3 MilliQ-Water once a stable pressure was achieved.

HPLC System Preparation

Running mediums were attached (ensuring correct line allocation for A, B, C) and purged at 33 % for each. The column was installed, checking for secure attachment. The running medium formulation was set according to the start point method (A = 81 %, B = 15 %, C = 4 %), and the column was equilibrated by gradually increasing the flow to $1 \text{ mL} \cdot \text{min}^{-1}$. The UV lamp was activated only when the medium was flowing, and the sequence was queued for analysis once the pressure and UV signal stabilized, typically within 30-40 min.

Sample Analysis

Upon stabilization of the system, the sequence was initiated. A timer was set to track the sequence completion. Following the analysis, the running medium was replaced with acetonitrile (ACN) for purging all lines. The column was exclusively rinsed with ACN at a flow of $0.8 \text{ mL} \cdot \text{min}^{-1}$

for 15-20 min, then removed from the system. The acetonitrile line was switched to isopropanol for another purging session, followed by a system-wide isopropanol flush at $1 \text{ mL} \cdot \text{min}^{-1}$ for 30 min before shutting down the flow.

Chapter 4: Results and Discussion

Two distinct and highly effective microfiltration membranes were conducted to treat grass silage solution for the subsequent concentration and purification of lactic acid by Nanofiltration and reverse osmosis. Each MF membrane was specifically chosen to feature a pore size range of 0.1 μm -0.2 μm , as this range was ideal for permeating the desired lactic acid molecules while retaining any unwanted impurities.

Evaluation of the microfiltration procedures at different pH levels was investigated, considering the pKa of lactic acid to determine the optimal pH ranges (2.5-4.5). This ensured that the lactic acid molecules were effectively filtered and purified without being compromised or damaged by the pH levels.

This preliminary MF stage was essential and crucial for removing cell biomass without major lactic acid losses before proceeding to nanofiltration and reverse osmosis.

The grass silage treated with MF was separated into different components using Nanofiltration. During the NF process, Glucose and Fructose were retained in the retentate stream, whereas lactic acid was collected in the permeate stream. Tight NF membranes from Alfa Laval and Loose NF membranes were tested to determine their effectiveness.

Lactic acid concentration was achieved using the Reverse Osmosis process. The RO 98pHt membrane from Alfa Laval was conducted for Lactic acid concentration. Different multistage membrane processes were examined to obtain highly purified and concentrated Lactic acid.

4.1 SEPARATION AND CONCENTRATION OF LACTIC ACID BY MULTISTAGE MEMBRANE PROCESSES

The study was conducted on four distinct configurations of multistage membrane processes [as seen in **Figure 16**] each of which involved three different types of membrane filtration techniques: microfiltration, nanofiltration, and reverse osmosis. The purpose of this study was to determine the efficacy of each multistage arrangement in purifying and concentrating LA from grass silage.

4.1.1 First arrangement of the multistage process

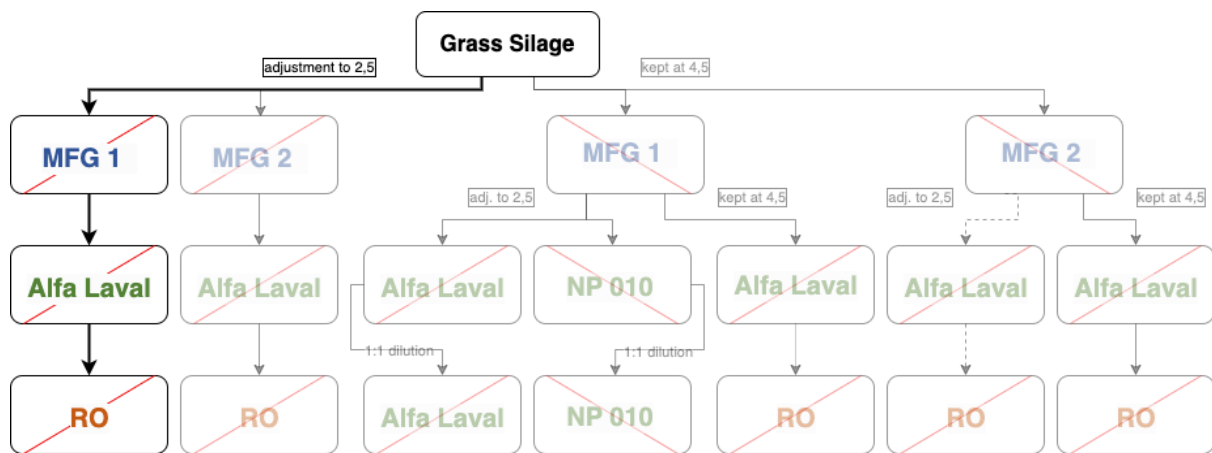


Figure 18 Experimental Design Flowchart: First Arrangement

The pH of the grass silage was modified to 2.5 by adding H_2SO_4 . Next, the silage underwent filtration using the $0.1 \mu m$ MF membrane, MFG-1, manufactured by Alfa Laval. At the start of the filtration, the MFG1 flux was $31 \text{ Kg}\cdot\text{m}^{-2}\cdot\text{h}^{-1}$. The recovery rate reached 55% as the filtration process ended, reducing flux to $27 \text{ Kg}\cdot\text{m}^{-2}\cdot\text{h}^{-1}$. During the filtration process, the MFG-1 flux experienced a decrease due to blocking some of the membrane porosity. The drop in permeate flux during microfiltration could be attributed to the concentration polarization and the formation of a cake layer from the microbial cells [53]. Despite this, the retentate and permeate maintained a consistent Bx measurement throughout the entire filtration period. Specifically, the Brix measurement for the retentate remained steady at 12° Bx , while the Permeate maintained a constant 11° Bx reading **Figure 19**

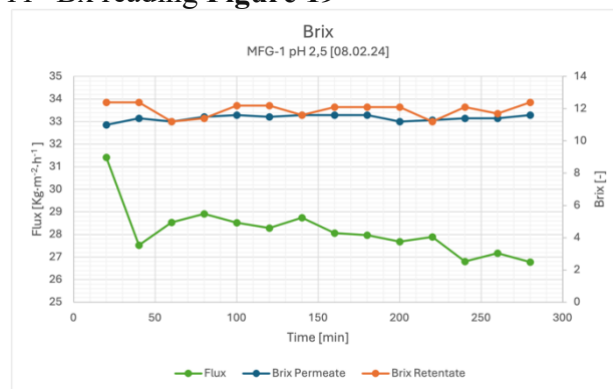


Figure 19 Brix concentration Permeate and Retentate over time during MF (First Arrangement)

After conducting the MF process no significant difference in the conductivity levels of the retentate and permeate was observed. Both the retentate and permeate had an approximate conductivity of $21.8 \text{ mS}\cdot\text{cm}^{-1}$ at the end of the filtration process **Figure 20** This indicates that the MF process effectively separated the particles without altering the conductivity levels of the liquid. This behavior can be attributed to the sieving effect of the MF membrane, which is directly related to its pore size. Furthermore, the conductivity change can be attributed to the absence of Lactic acid dissociation at a lower pH of 2.5. [54] The pH of both the retentate and permeate stream was at 2.7 during the whole microfiltration process **Figure 20**

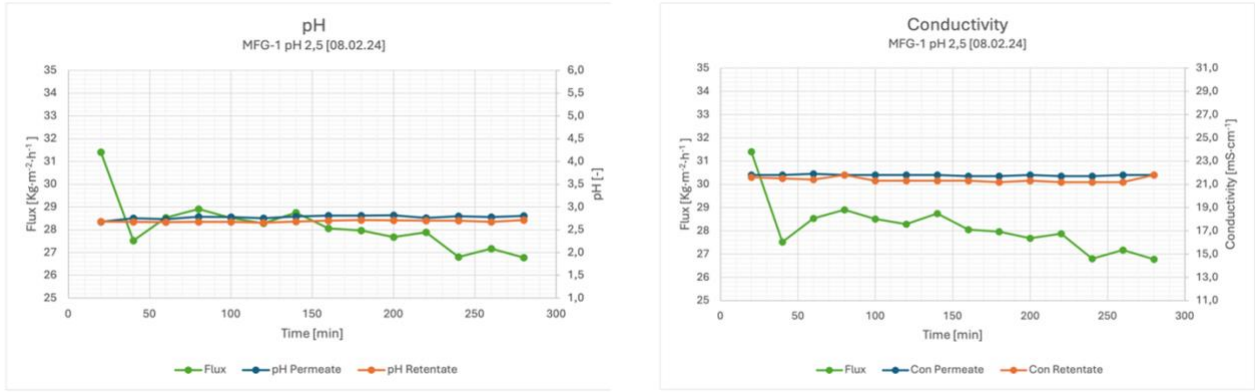


Figure 20 pH and Conductivity Measurement Points in MF Process Flow (First Arrangement)

The MF Permeate stream underwent fractionation through a Nanofiltration membrane (Alfa Laval NF) at operating conditions 30 bar and 25°C, resulting in an average flux of approximately $45 \text{ Kg}\cdot\text{m}^{-2}\cdot\text{h}^{-1}$. The accompanying figure illustrates that the retentate's sugar concentration increased from 10.8 to 15.6°Brix . It is worth noting that there was a 15% sugar loss on the permeate side during the process. The conductivity of the Permeate was increased from 2.97 to $4.69 \text{ mS}\cdot\text{cm}^{-1}$ due to the NF-Process, indicating an increase in mineral content.

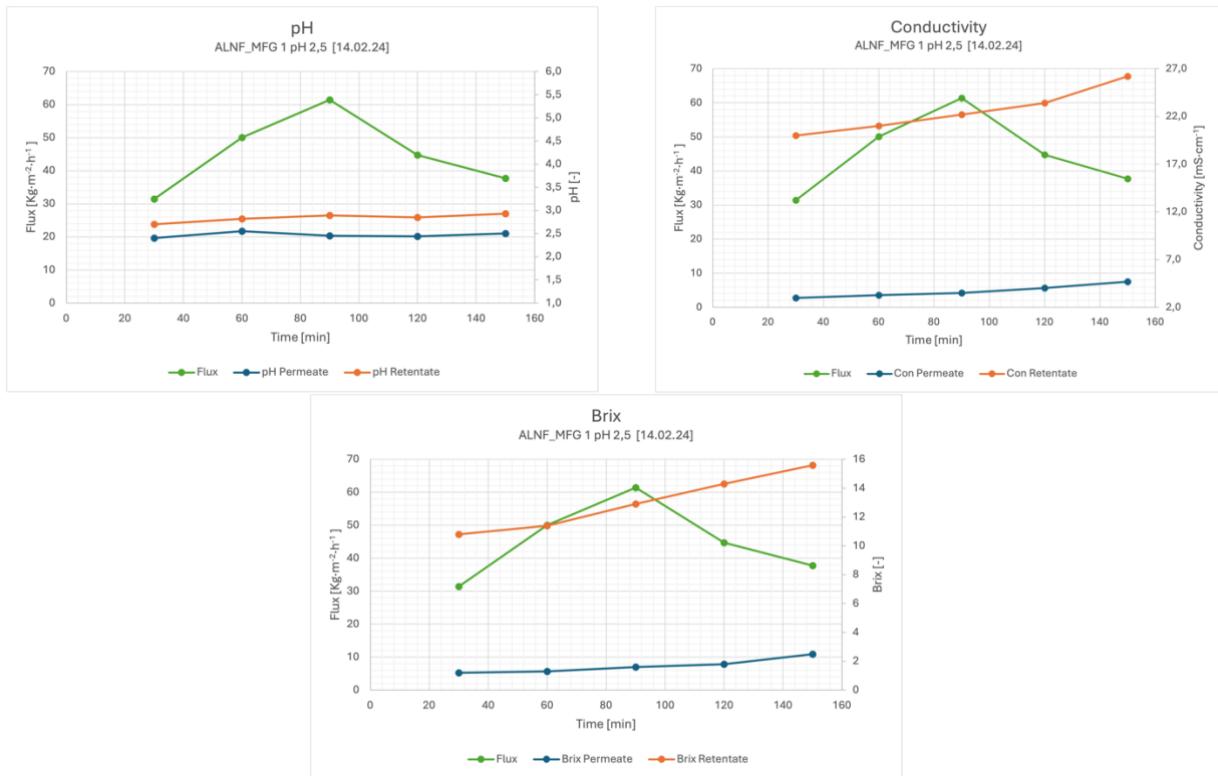


Figure 21 pH, Conductivity and Brix Measurement Points in NF Process Flow (First Arrangement)

The permeate obtained from the nanofiltration process was further processed using a reverse osmosis membrane (RO98pHt) manufactured by Alfa Laval. The process was carried out at a pressure of 40 bar and room temperature. The retentate stream was used to collect the concentrated lactic acid.

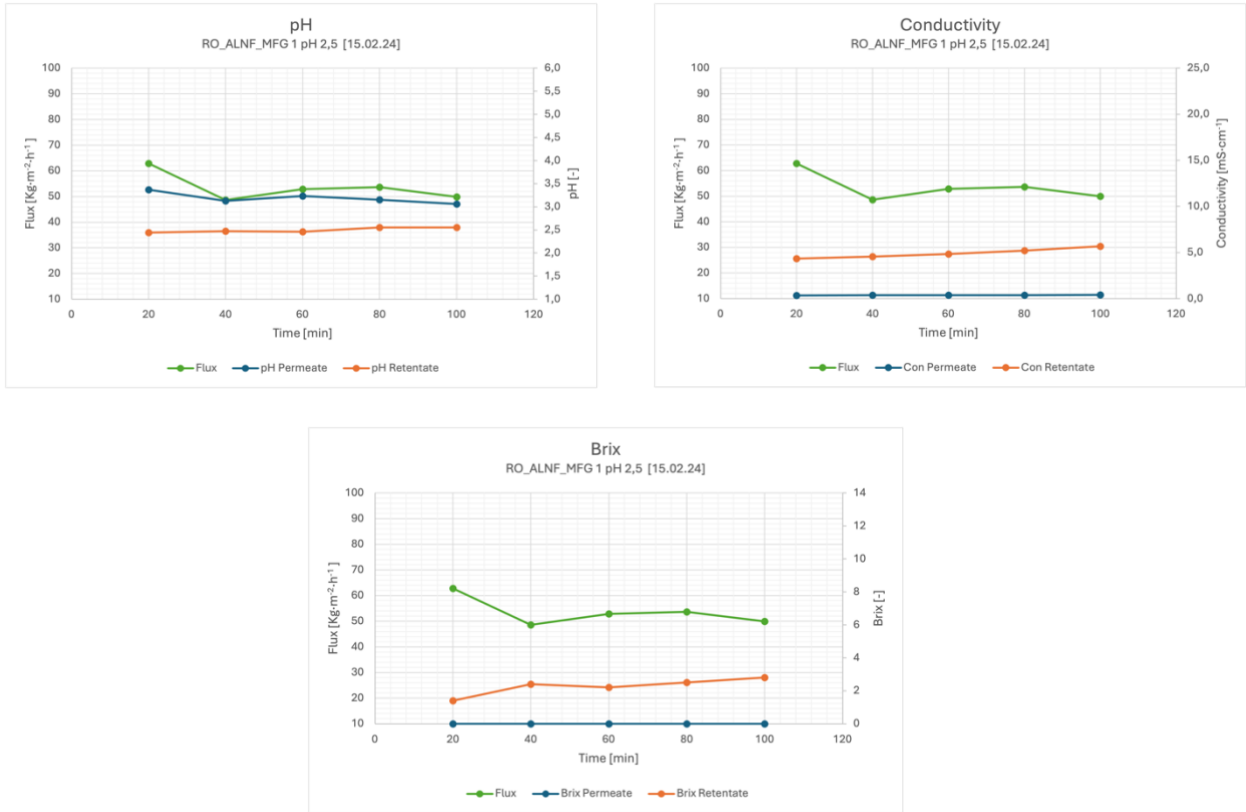


Figure 22 pH, Conductivity and Brix Measurement Points in RO Process Flow (First Arrangement)

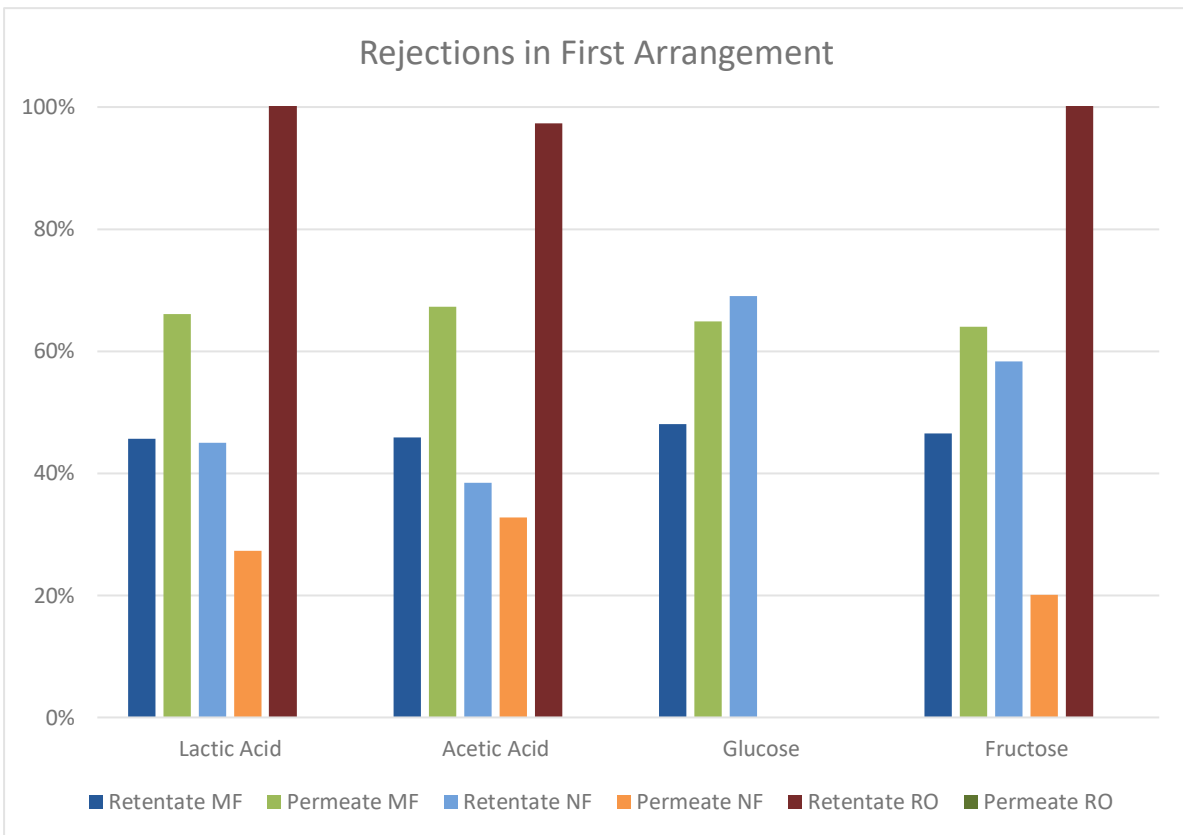


Figure 23 Rejection Profiles of Lactic Acid, Acetic Acid, Fructose, and Glucose Across through the Stages of the First Arrangement

The loss of Lactic Acid through the Microfiltration process was approximately 21.2% [Rejection], and the fractionation of lactic acid achieved was 41.2%, which aligns with the findings presented [42]. The Reverse Osmosis membrane successfully concentrated the lactic acid, with all the lactic acid remaining, in the retentate. This retentate is our product, containing pure lactic acid.

The second most abundant organic acid in grass silage juice is acetic acid. The Microfiltration membrane retained 16.45% of acetic acid, whereas the negatively charged nanofiltration membrane allowed all acetic acid to pass to the permeate side. It can be inferred that there is an inverse correlation between the order of diffusion coefficients and the rejection sequence. It appears that ions with the highest diffusion coefficient are more likely to pass through the membrane. Specifically, the charged acid ions, acetate, and lactate have diffusion coefficients of $1.06 \cdot 10^{-9}$ and $1.38 \cdot 10^{-9}$, respectively. Nanofiltration removed 99% of glucose and left it on the retentate side. For neutral solutes like glucose, nanofiltration retains based on size exclusion, with negligible electrostatic interactions.

The reverse osmosis membrane could not separate the acid from the feed, so it was directed to the retentate side instead. This suggests acetic acid might be separable from lactic acid after the concentration through another type of membrane.

4.1.2 Second arrangement of the multistage process

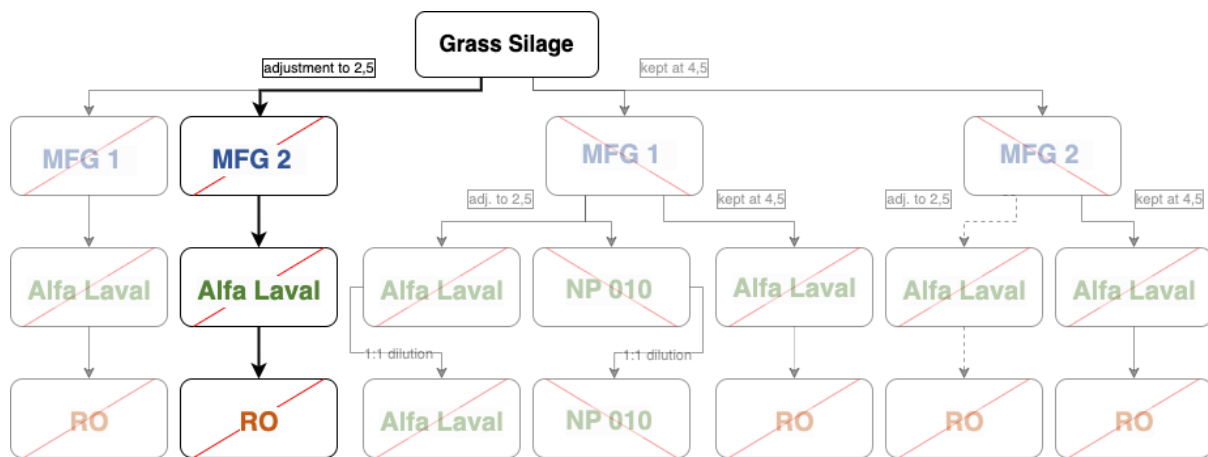


Figure 24 Experimental Design Flowchart: Second Arrangement

The pH of the grass silage was adjusted to 2.5 using H_2SO_4 , setting the stage for its treatment through Microfiltration (MF). Utilizing the MFG-2 membrane from Alfa Laval, characterized by pore size of $0.2 \mu m$ and an operational pressure of 2 bar, the process was conducted at a steady temperature of $25^\circ C$.

Initially, the flux of MFG-2 was recorded at $36.7 \text{ Kg}\cdot\text{m}^{-2}\cdot\text{h}^{-1}$, which gradually decreased throughout the filtration, eventually stabilizing the recovery rate at 70%. This led to a flux reduction to $30.1 \text{ Kg}\cdot\text{m}^{-2}\cdot\text{h}^{-1}$, resulting in an average flux of $32.6 \text{ Kg}\cdot\text{m}^{-2}\cdot\text{h}^{-1}$. Despite the flux reduction, both the retentate and permeate exhibited stable Brix measurements throughout the filtration, with the permeate Brix value remaining constant and the retentate Brix slightly increasing, as illustrated in **Figure 25**

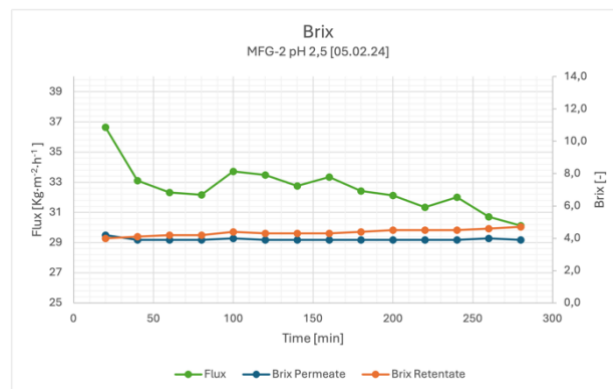


Figure 25 Brix concentration Permeate and Retentate over time during MF (Second Arrangement)

MF filtration analysis revealed no significant difference in conductivity levels between the retentate and permeate, with MFG-2 showing a mineral rejection rate of 3.3%. This indicates that minerals predominantly migrated towards the permeate side, as **Figure 26** depicts. This outcome suggests that the MF process effectively separated particles without altering the conductivity levels of the grass silage solution. Throughout the microfiltration process, the pH levels of both the retentate and permeate streams were maintained at 2.7, as shown in **Figure 26**.

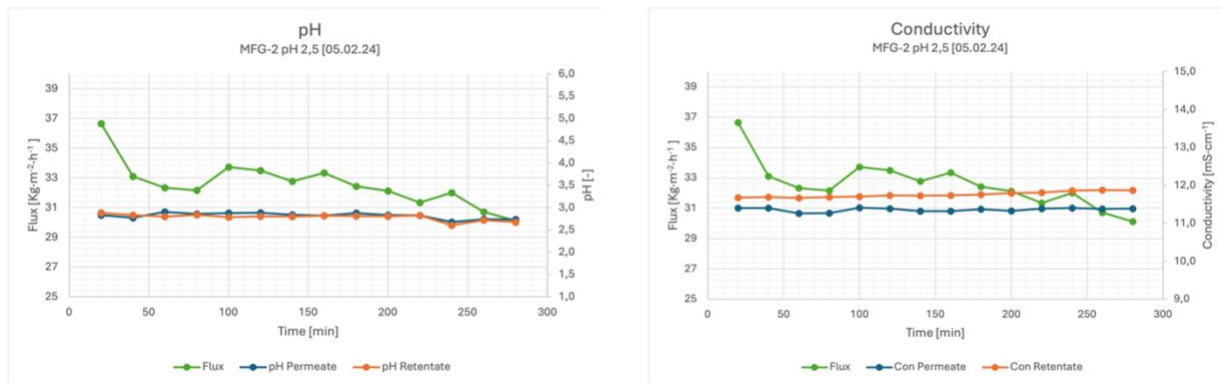


Figure 26 pH and Conductivity Measurement Points in MF Process Flow (Second Arrangement)

The Nanofiltration membrane (Alfa Laval NF) was utilized to separate Lactic Acid (LA) from the permeate stream produced by MFG-2. This experiment was conducted under the operating conditions of 30 bar and a temperature of 25°C, achieving an average flux of approximately $68.6 \text{ Kg}\cdot\text{m}^{-2}\cdot\text{h}^{-1}$.

As depicted in **Figure 27**, the concentration of sugar in the retentate was increased by 67.4%. Notably, the NF process resulted in minimal sugar loss in the permeate stream. Additionally, an increase of 74% in the permeate conductivity was observed as a consequence of the nanofiltration process.

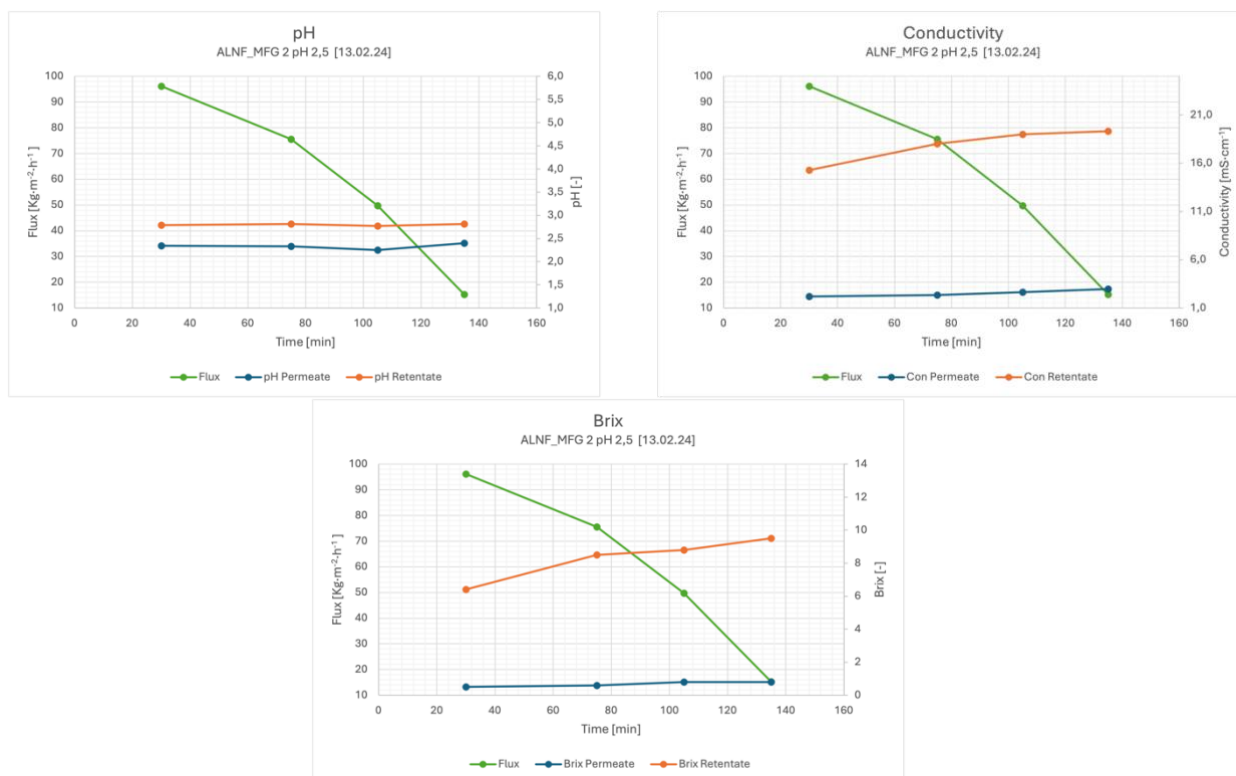


Figure 27 pH, Conductivity and Brix Measurement Points in NF Process Flow (Second Arrangement)

The permeate obtained from the nanofiltration process was further processed as described in the **4.1.1 First arrangement of the multistage process** with the same parameter again using a reverse osmosis membrane (RO98pHt) manufactured by Alfa Laval. The process was carried

out at a pressure of 40 bar and room temperature. The retentate stream was used to collect the concentrated lactic acid.

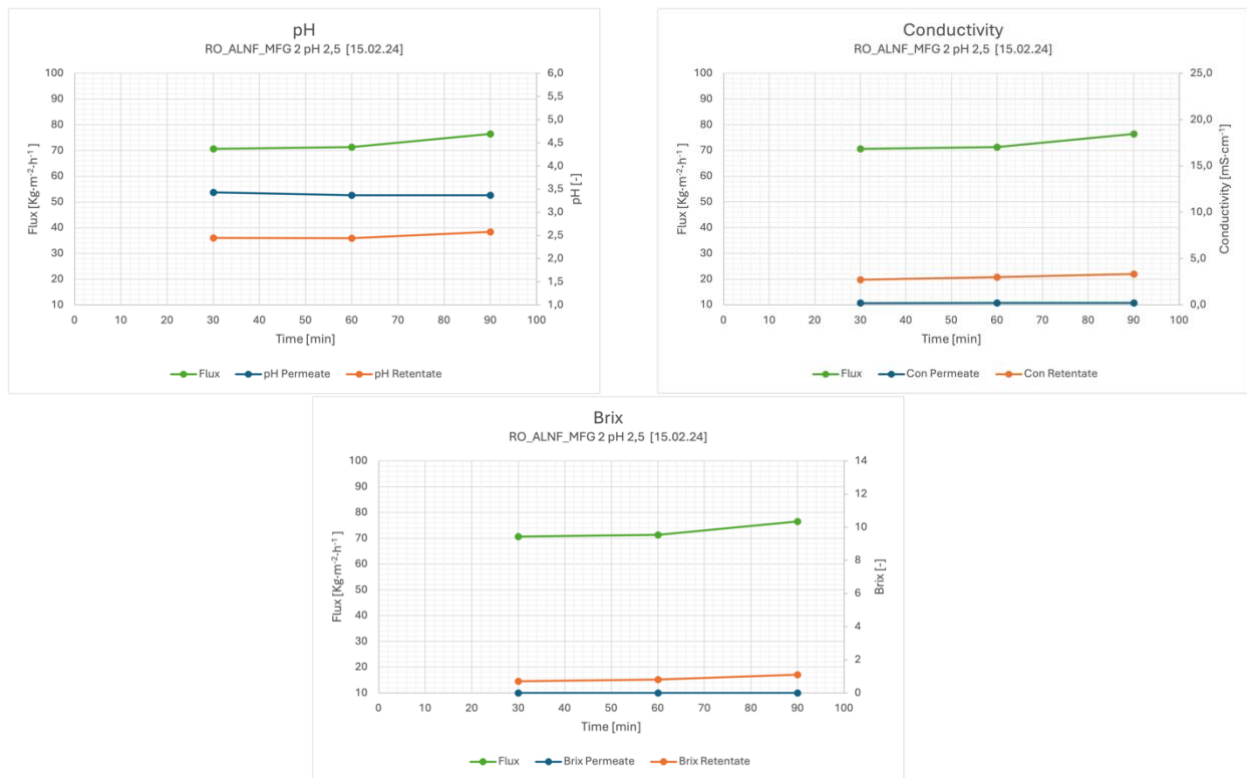


Figure 28 pH, Conductivity and Brix Measurement Points in RO Process Flow (First Arrangement)

Approximately 4.2% of lactic acid was lost during the Microfiltration process to the Retentate; the fractionation yield for lactic acid stood at 47.3%. For lactate anions with a larger radius, the charge center is farther from the surface. Consequently, the electrostatic interactions between lactate anions and the negatively charged membrane surface are weaker. Using a Reverse Osmosis (RO) membrane effectively concentrated the lactic acid, preserving it entirely in the retentate, which comprises our final product enriched with pure lactic acid.

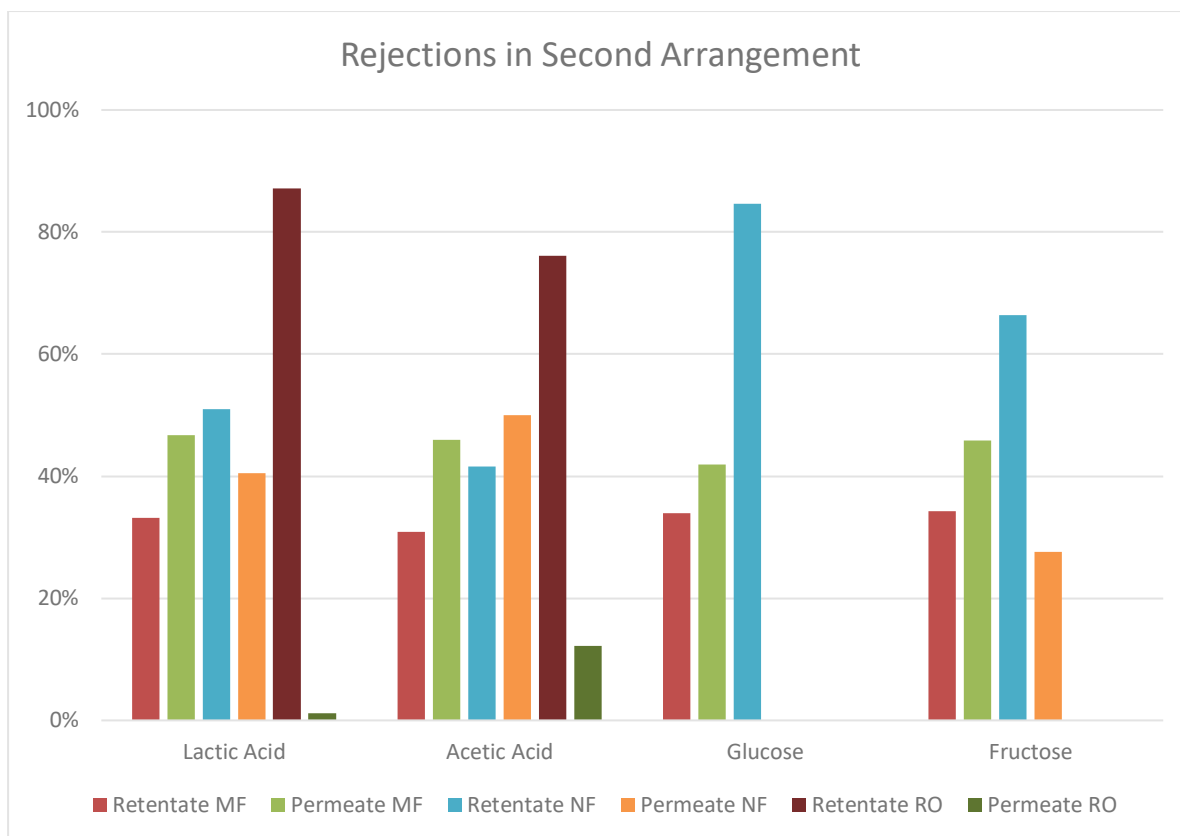


Figure 29 Rejection Profiles of Lactic Acid, Acetic Acid, Fructose, and Glucose Across through the Stages of the Second Arrangement

The MF membrane retained 3.0% of the acetic acid, while the nanofiltration process rejected 20.3% of acetic acid to the permeate. Conversely, the RO membrane was ineffectual in separating the acetic acid from the mixture, leading it instead toward the retentate. This behavior indicates again the potential need for an additional step to remove the acetic acid from our product.

Regarding glucose, the nanofiltration process achieved a 100% removal rate, with the glucose remaining in the retentate. The retention of glucose molecules in the nanofiltration process is determined by the size exclusion mechanism, which prevents molecules larger than a certain size from passing through the system. In other words, glucose molecules are too large to pass through the pores and are thus retained. On the other hand, electrostatic interactions between the polar glucose molecules and negatively charged NF membrane are insignificant and do not play a significant role in glucose retention.

4.1.3 Third arrangement of the multistage process

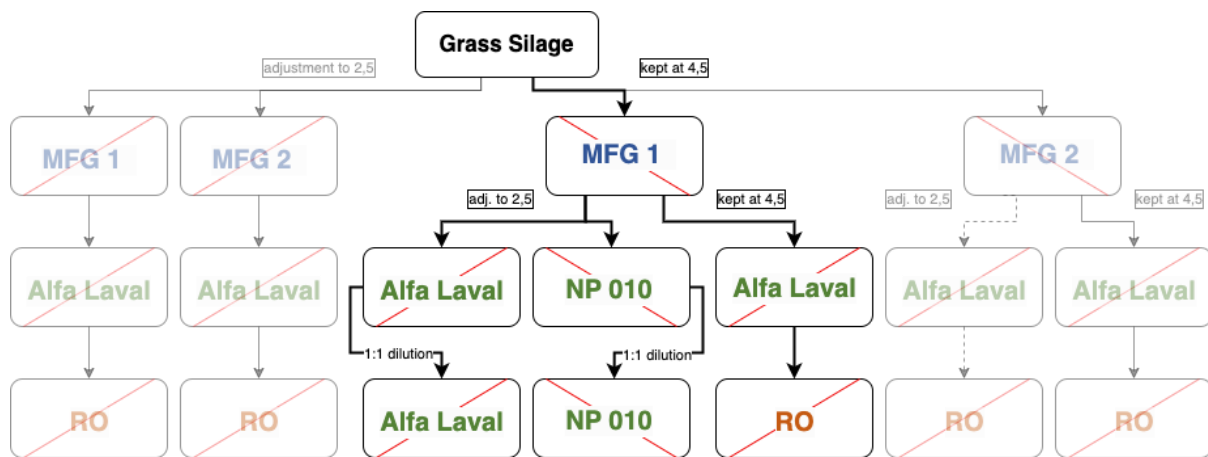


Figure 30 Experimental Design Flowchart: Third Arrangement

The pH of the grass silage was kept at 4.5. Next, the silage underwent filtration using the 0.1 μm MF membrane, MFG-1, manufactured by Alfa Laval. At the start of the filtration, the MFG-1 flux was $35 \text{ Kg}\cdot\text{m}^{-2}\cdot\text{h}^{-1}$. As the filtration process was completed, the recovery rate reached 70%, reducing flux to $32 \text{ Kg}\cdot\text{m}^{-2}\cdot\text{h}^{-1}$. During the filtration process, the MFG-1 flux experienced a decrease due to blocking some of the membrane porosity. Despite this, the Retentate and Permeate maintained a consistent Brix measurement throughout the entire filtration period. Specifically, the Brix measurement for the Permeate remained steady at 8.4° Brix, while the Retentate started at an 8.5° Brix and ended at an 8.6° Brix reading [Figure 32]. After conducting the MF process no significant difference in the conductivity levels of the retentate and permeate was observed. The retentate had a conductivity of $17.58 \text{ mS}\cdot\text{cm}^{-1}$ and permeate of $17.24 \text{ mS}\cdot\text{cm}^{-1}$ at the end of the filtration process [Figure 31]. The pH of both the Retentate and Permeate Stream was at 4.24 during the whole microfiltration process [Figure 31].

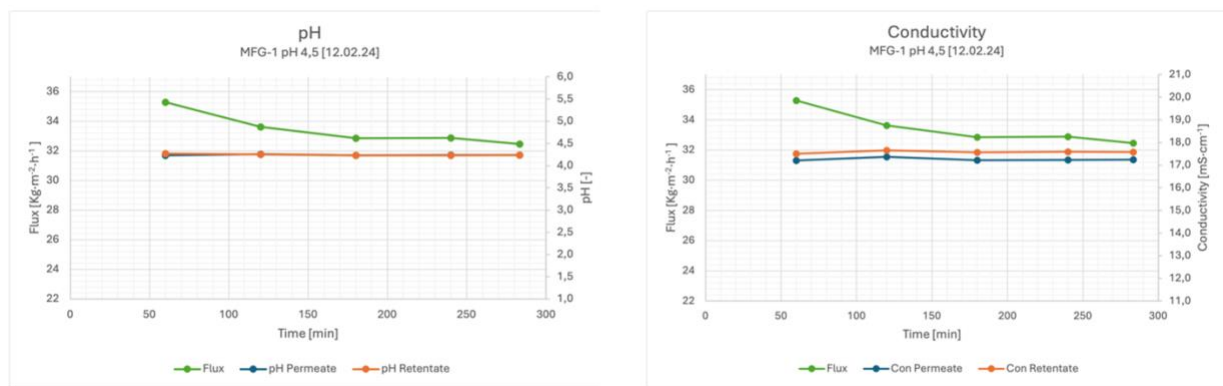


Figure 31 pH and Conductivity Measurement Points in MF Process Flow (Third Arrangement)

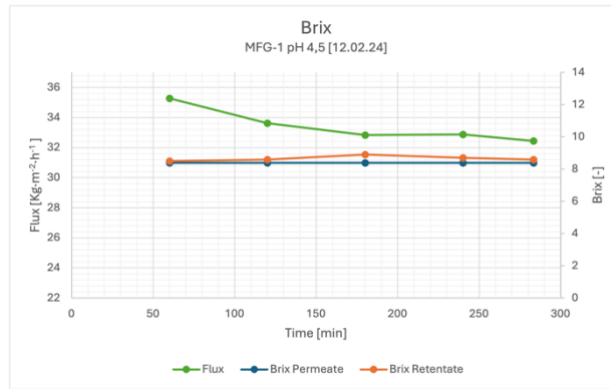


Figure 32 Brix concentration Permeate and Retentate over time during MF (Third Arrangement)

4.1.3.1 First Sub Arrangement

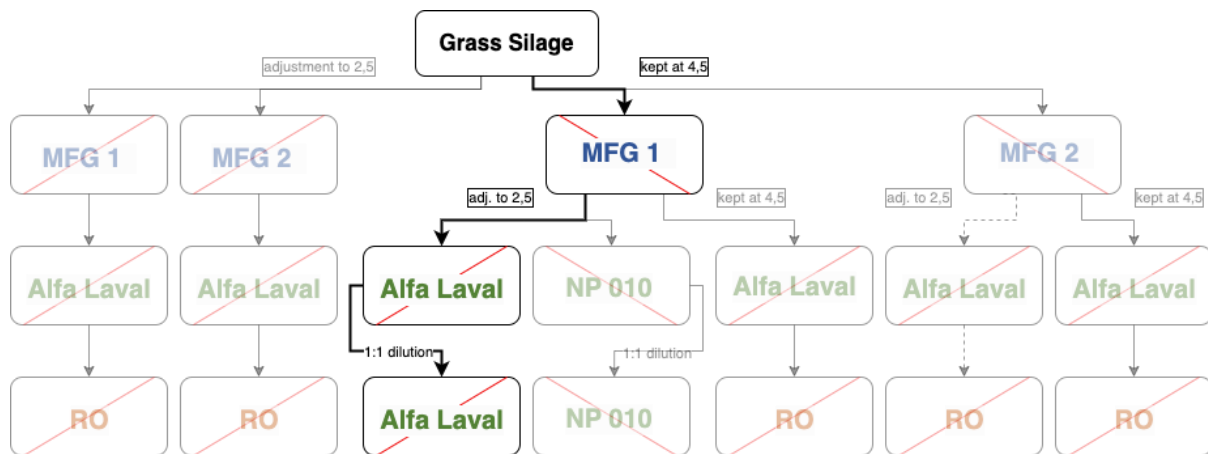


Figure 33 Experimental Design Flowchart: First Sub Arrangement of First Sub Arrangement

After the MF process, where the pH was maintained at 4.5, the grass silage was acidified to a pH of 2.5. This acidified feed underwent testing through a tight NF membrane provided by Alfa Laval, concluding the process after achieving a recovery rate of 25% over 4 hours. As depicted in **Figure 34**, there was a drastically drop in flux at the beginning of the experiment, plummeting from an initial $43.8 \text{ Kg}\cdot\text{m}^{-2}\cdot\text{h}^{-1}$ to an average of $9.9 \text{ Kg}\cdot\text{m}^{-2}\cdot\text{h}^{-1}$. The permeate flux started to decline quickly due to the build-up of a cake layer on the surface of the membrane caused by the current operating conditions [55]. As time went on, the cake layer became thicker, increasing the risk of long-term fouling of the membrane.

Throughout the experiment, the Brix, conductivity, and pH values remained stable for both the retentate and permeate.

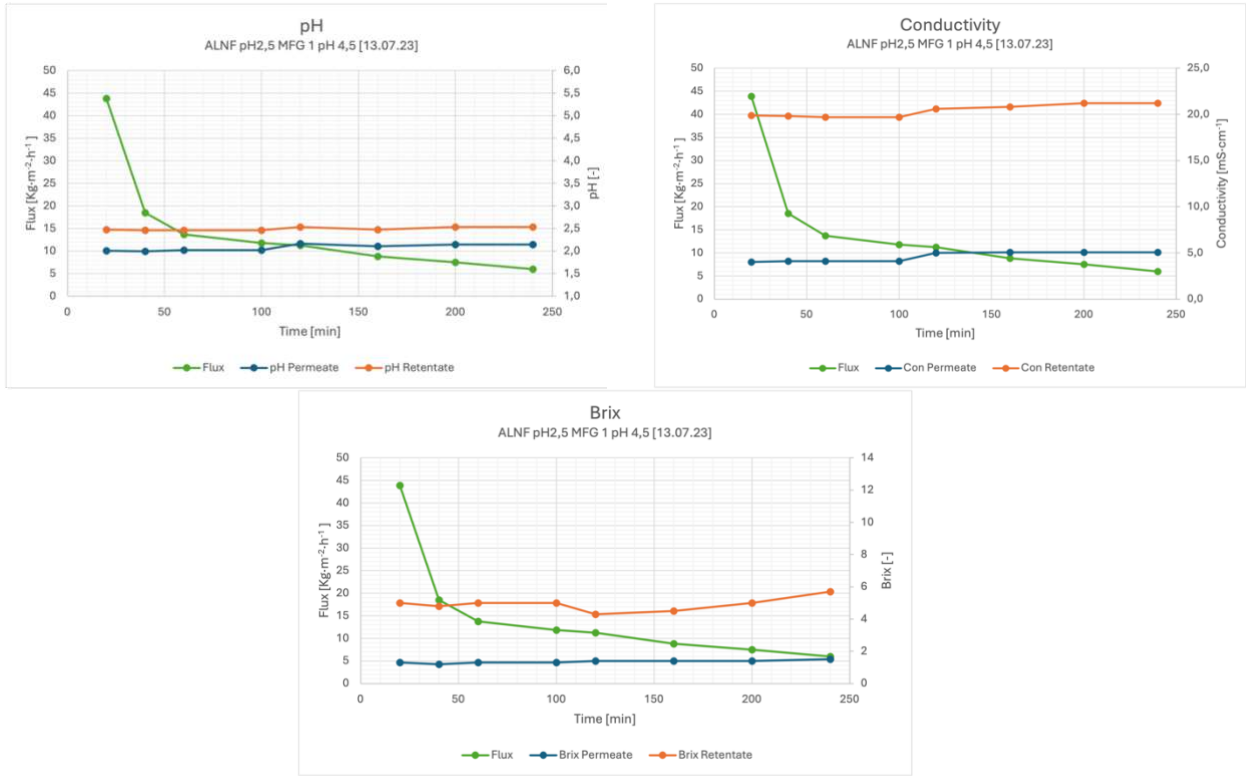


Figure 34 pH, Conductivity and Brix Measurement Points in NF Process Flow (First Sub Arrangement)

HPLC analysis of LA indicated an 85% rejection rate, leading to the decision against proceeding with RO due to the minimal presence of lactic acid on the permeate side.

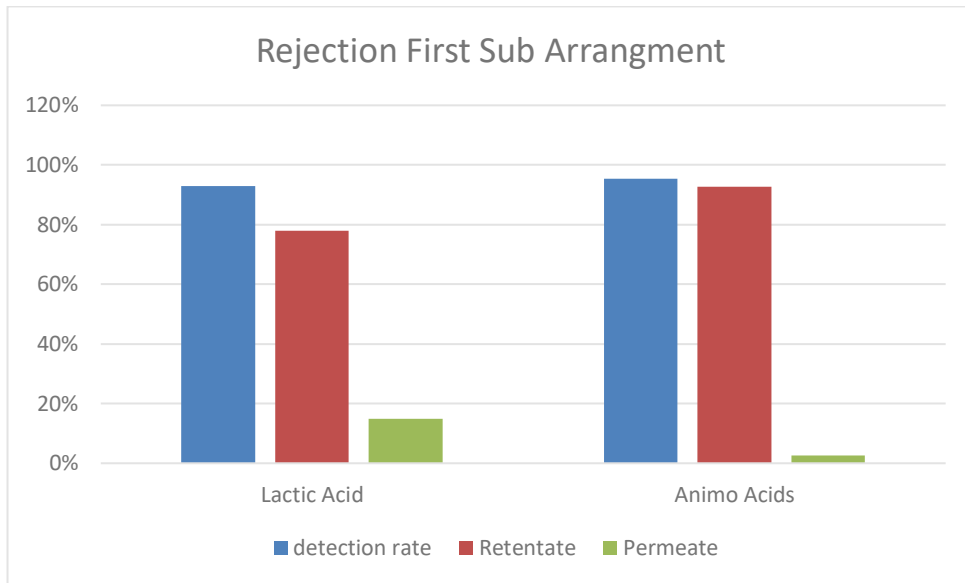


Figure 35 Rejection Profiles of Lactic Acid & Amino Acid through the NF Stage of the First Sub Arrangement

Diafiltration – Nanofiltration after 1:1 Dilution

A diafiltration approach improved the flux and LA separation from the MF permeate. The retentate from the initial filtration was diluted with water at a 1:1 ratio, aiming to achieve more efficient separation in the following filtration steps.

Following the replacement with a new membrane, which was not obstructed by clogging, there was a notable improvement in flux, reaching a value of $113.4 \text{ Kg}\cdot\text{m}^{-2}\cdot\text{h}^{-1}$. Since the previous membrane was removed due to the visible adsorption of suspended particulates to the membrane surface, conducting an HPLC analysis on the products was deemed unnecessary, as the membrane change significantly impacted the filtration efficiency.

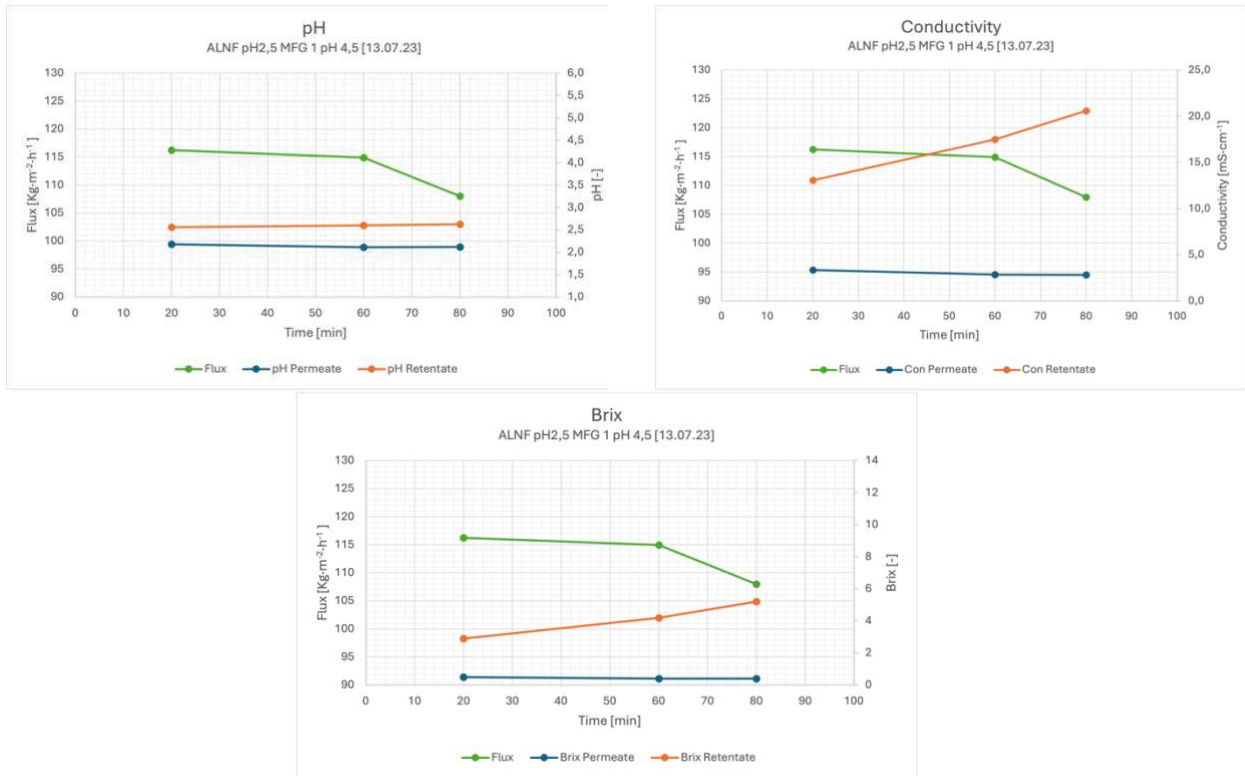


Figure 36 pH, Conductivity and Brix Measurement Points after Diafiltration (First Sub Arrangement)

4.1.3.2 Second Sub Arrangement

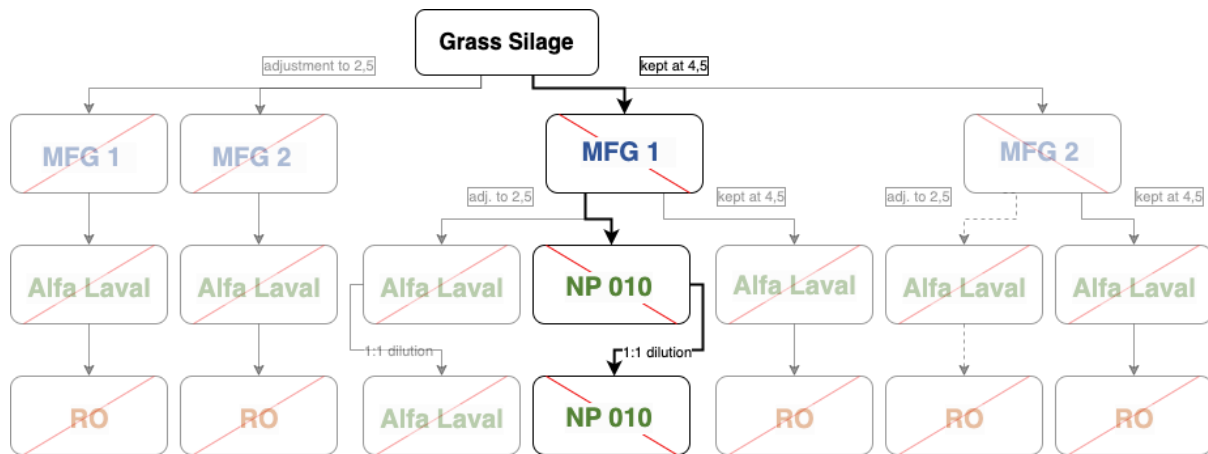


Figure 37 Experimental Design Flowchart: Second Sub Arrangement of Second Sub Arrangement

Observing the outcomes from the Alfa Laval setup, a second, loose NF membrane, the NP010 Nadir with a MWCO of 1000 Da, was tested for comparison. Like the Alfa Laval NF membrane, there was a significant initial drop in flux with the NP010 Nadir membrane, which stabilized to an average flux of $19 \text{ Kg}\cdot\text{m}^{-2}\cdot\text{h}^{-1}$. The process was terminated at a recovery rate of 25% after 3 hours.

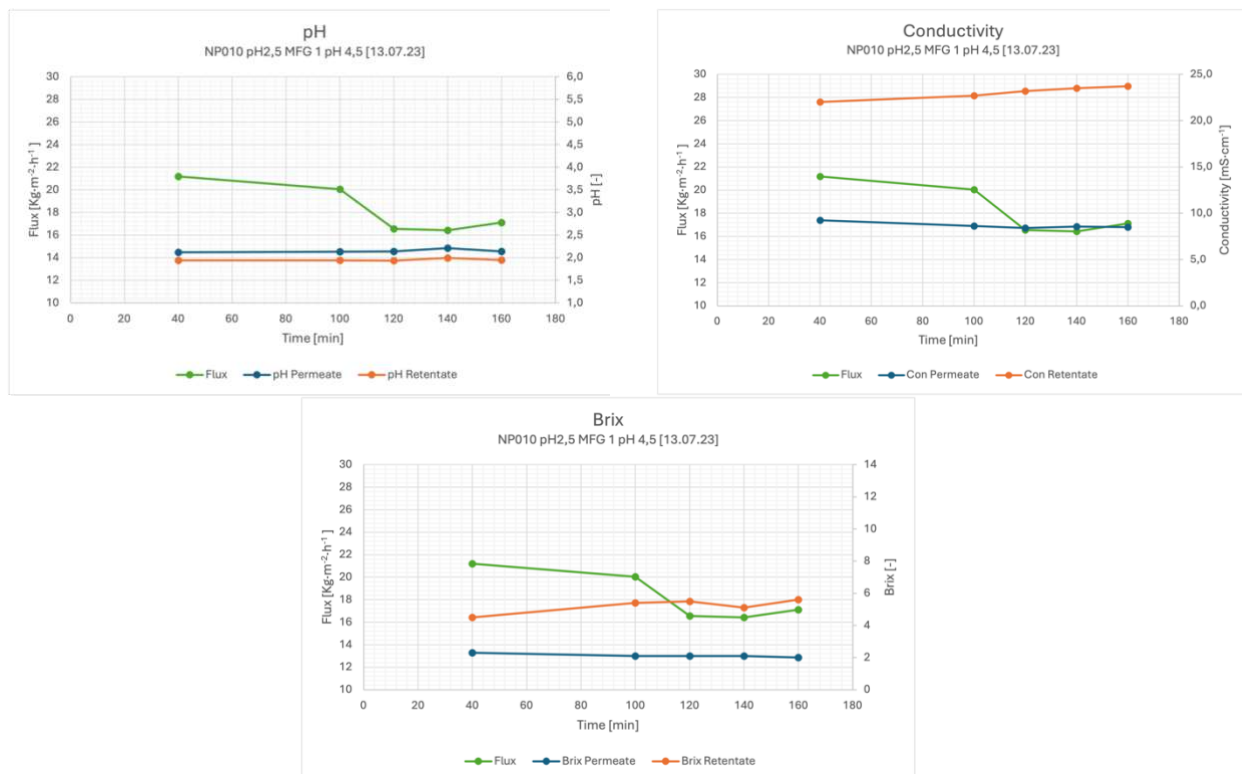


Figure 38 pH, Conductivity and Brix Measurement Points in NF Process Flow (Second Sub Arrangement)

Similarly to the Alfa Laval setup, the separation efficiency for lactic acid using the NP010 Nadir membrane was only 15%, rendering it not feasible as an optimal arrangement to achieve our goal. Despite this, diafiltration was tested as a contingency measure.

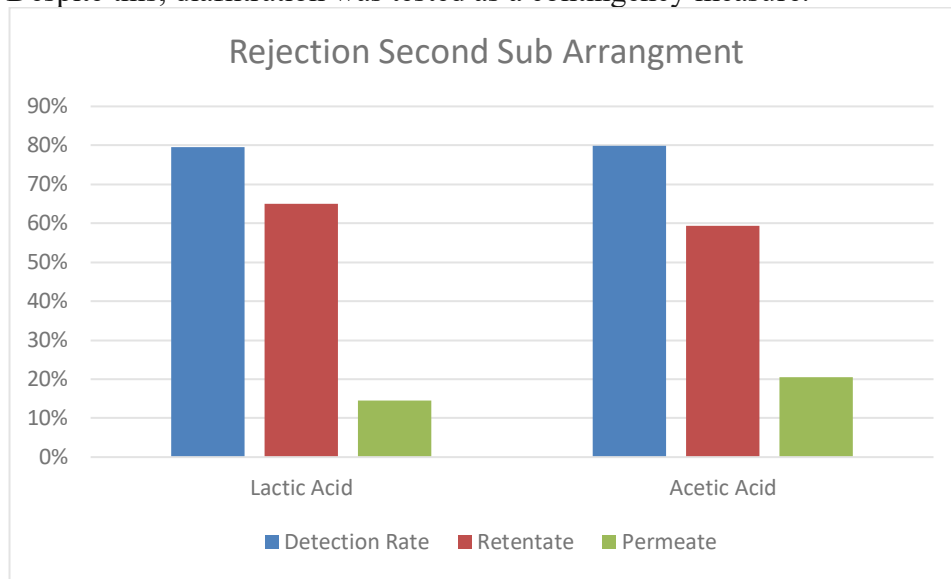


Figure 39 Rejection Profiles of Lactic Acid & Acetic Acid through the NF Stage of the Second Sub Arrangement

Diafiltration – Nanofiltration after 1:1 Dilution

After implementing diafiltration with a new membrane and losing the particulates attached to the membrane, we achieved a recovery rate of 50.2% and an average flux of $35.8 \text{ Kg}\cdot\text{m}^{-2}\cdot\text{h}^{-1}$.

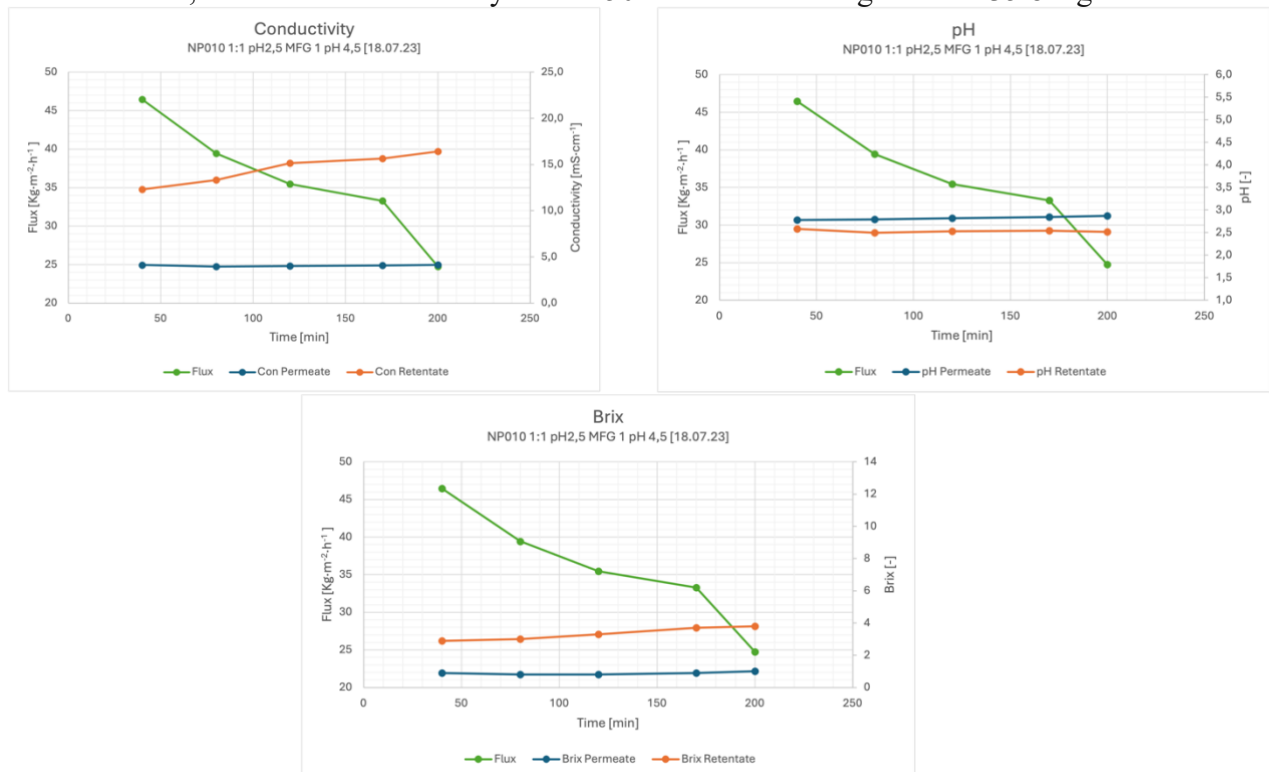


Figure 40 pH, Conductivity and Brix Measurement Points after Diafiltration (Second Sub Arrangement)

Following this process, an HPLC analysis revealed that a separation of 38% of lactic acid was obtained through dilution.

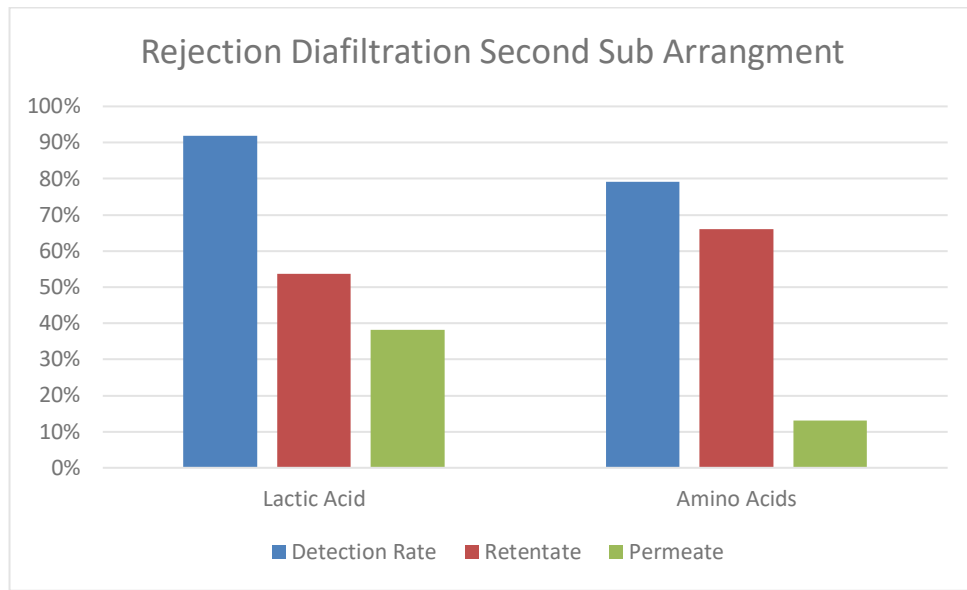


Figure 41 Rejection Profiles of Lactic Acid & Amino Acid after Diafiltration of the Second Sub Arrangement

4.1.3.3 Third Sub Arrangement

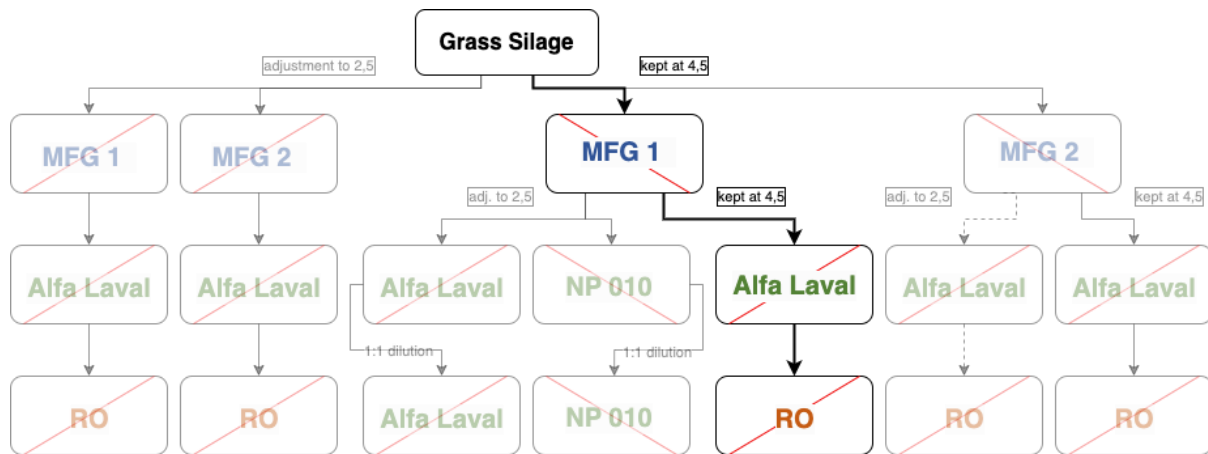


Figure 42 Experimental Design Flowchart: Third Sub Arrangement of Third Sub Arrangement

The MF Permeate stream underwent fractionation through a high-performance Nanofiltration membrane (Alfa Laval NF) at operating conditions 30 bar and 25°C, resulting in an average flux of approximately $30.6 \text{ Kg}\cdot\text{m}^{-2}\cdot\text{h}^{-1}$. The accompanying figure illustrates that the Retentate's Sugar concentration increased from 7.2 to 10.6 °Bx. It is worth noting that there was a 6% sugar loss on the permeate side during the process. The conductivity of the Permeate was increased from 1.51 to 2.22 $\text{mS}\cdot\text{cm}^{-1}$ due to the NF-Process, indicating an increase in mineral content.

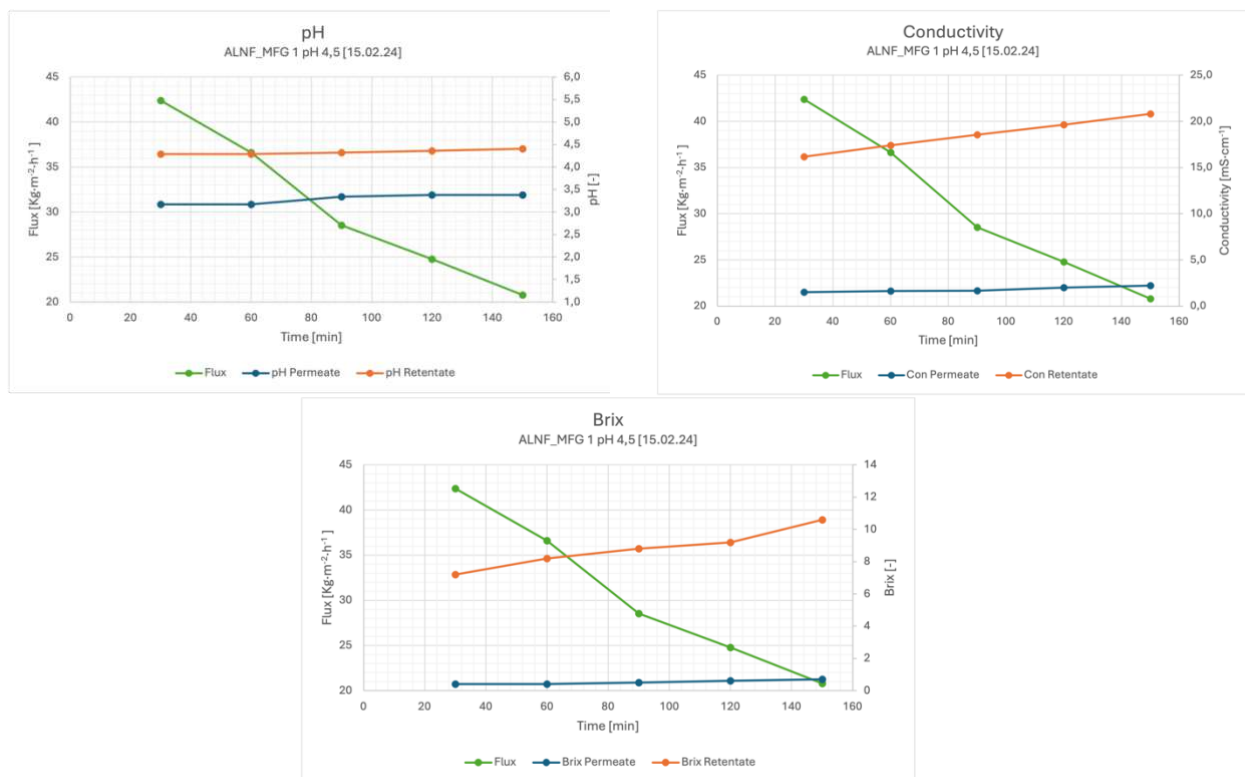


Figure 43 pH [left], Conductivity and Brix Measurement Points in MF Process Flow (Third Sub Arrangement)

The permeate obtained from the nanofiltration process was further processed using a reverse osmosis membrane (RO98pHt) manufactured by Alfa Laval. The process was carried out at a pressure of 30 bar and room temperature. The retentate stream was used to collect the concentrated lactic acid.

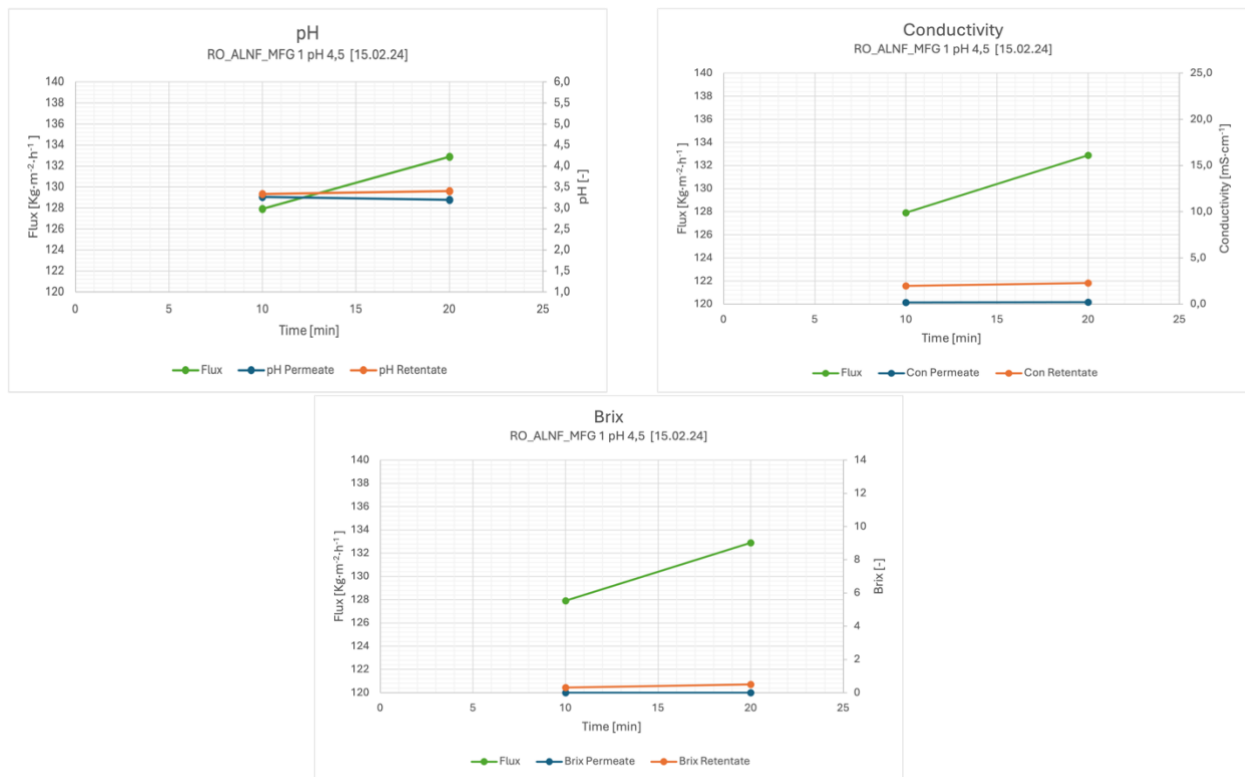


Figure 44 pH, Conductivity and Brix Measurement Points in NF Process Flow (Third Sub Arrangement)

The Microfiltration process resulted in a -27.2% loss of Lactic Acid, indicating that membrane rejection is influenced by the diffusion potential. The Molecular Weight for LA and Acetic Acid is approximately 90 & 60 g mol⁻¹, respectively, which is lower than the pore size of the MF membrane, facilitating the permeation of these smaller particles through the membrane. Consequently, the concentration of these acids on the permeate side is higher than on the feed side.

During the MF stage, Acetic Acid experienced a rejection rate of -30.6%. Nanofiltration demonstrated an AA rejection rate of -40.3% and LA rejection at 67.7%. Based on their Stokes radius and molecular weight, charged acid ions (acetate and lactate) have been found to differ in their retention by the membrane. Lactate, with the largest ions, was retained to a greater extent than acetate, which had the smallest ions. This suggests that retention of organic acids is influenced not only by the Donnan exclusion, but also by the sieve mechanism.

The Reverse Osmosis membrane achieved a 100% rejection rate for LA, effectively concentrating it on the retentate side. Also, no Glucose was detected in the feed.

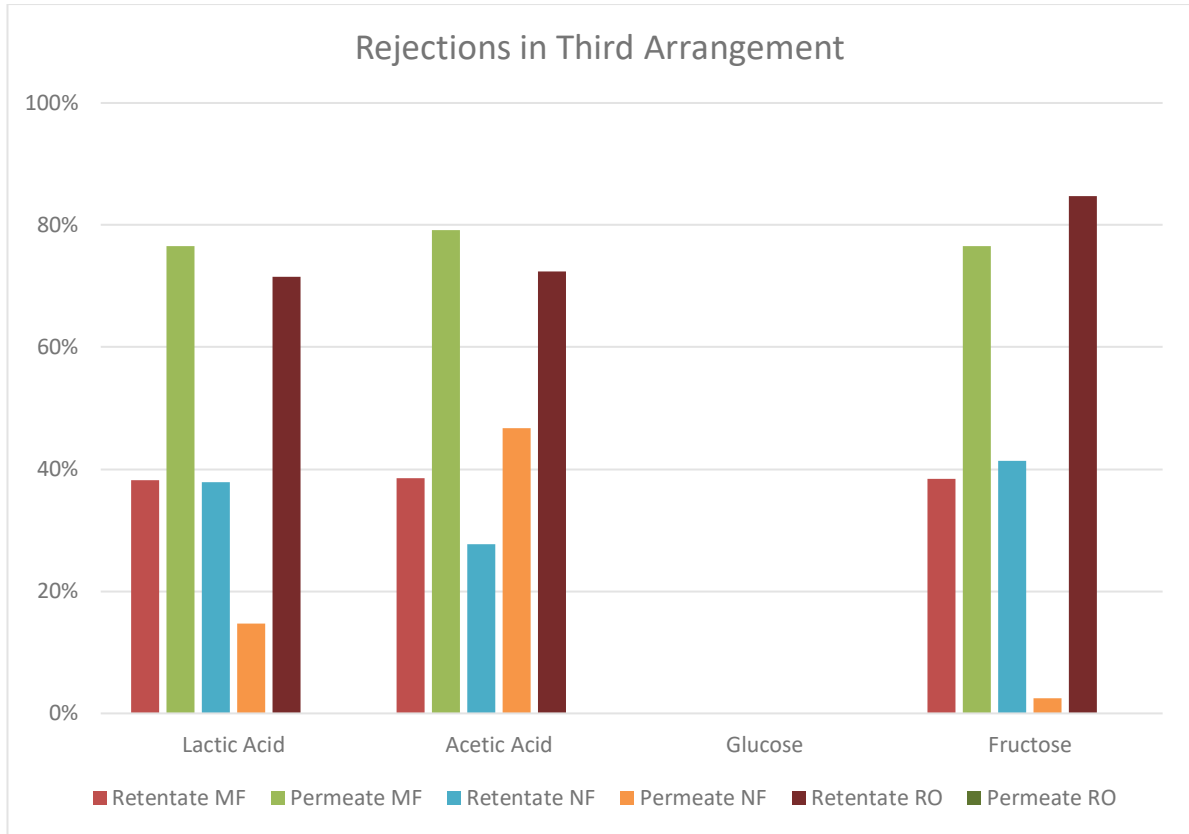


Figure 45 Rejection Profiles of Lactic Acid, Acetic Acid, Fructose, and Glucose Across through the Stages of the Third Arrangement

Upon comparing the data from various experiments, it's noted that introducing sulfuric acid into the mix results in decreased concentrations of organic acids, such as acetic and lactic acid, and a reduction in sugar levels, including glucose and fructose.

The absence of glucose in the feed that has not been acidified could be attributed to the effect of acidification on grass silage. Applying H_2SO_4 or similar acids breaks down the complex lignocellulosic structure found in grass, thereby making glucose and other sugars more readily available in the solution. In the absence of acidification, the lignocellulosic structure remains unaltered, which hinders the release of glucose into the solution. Acidic conditions facilitate the hydrolysis of bonds within cellulose and hemicellulose, converting them into simpler sugars, such as glucose. [12]

—

4.1.4 Fourth arrangement of the multistage process

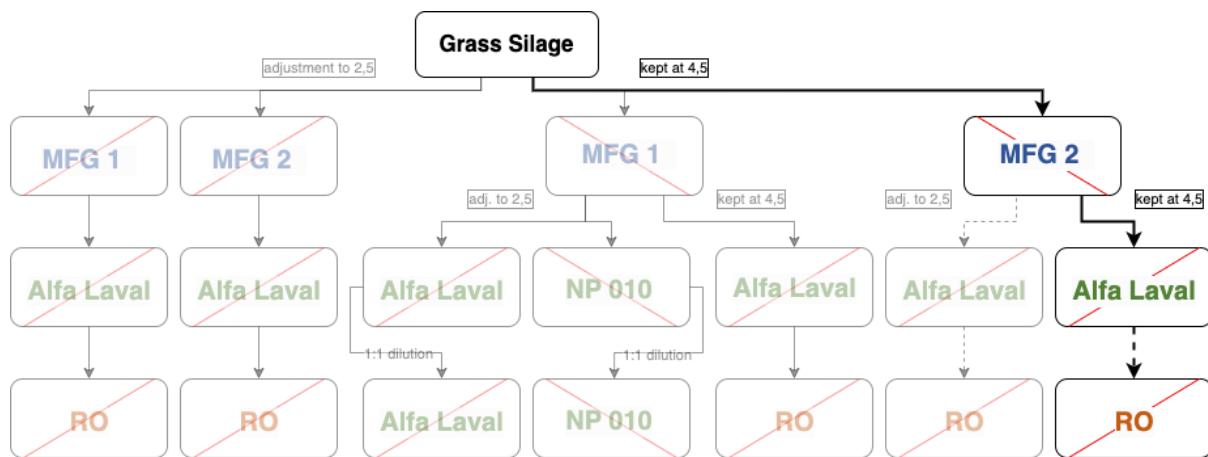
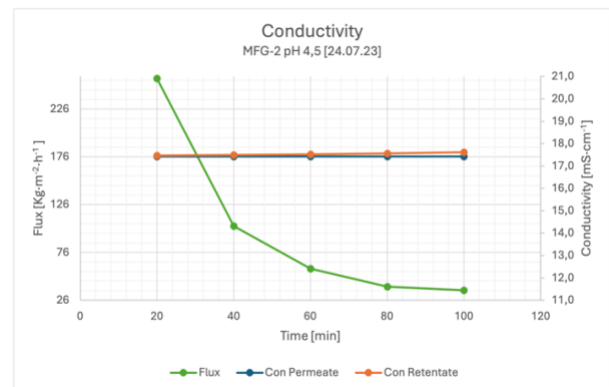
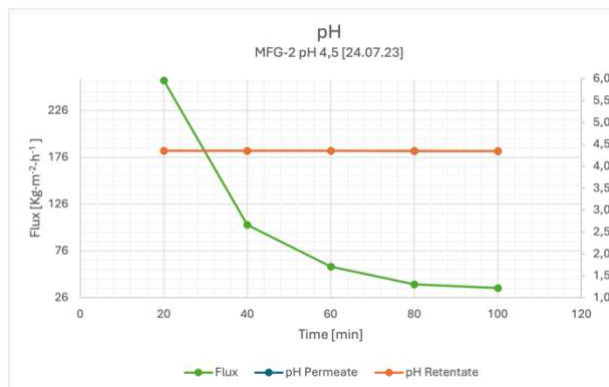


Figure 46 Experimental Design Flowchart: Fourth Arrangement

The pH of the grass silage was maintained at 4.5 before it was filtrated through a 0.2 μm Microfiltration membrane, MFG-2, produced by Alfa Laval.

The flux began at $258 \text{ Kg}\cdot\text{m}^{-2}\cdot\text{h}^{-1}$ and dropped to $36 \text{ Kg}\cdot\text{m}^{-2}\cdot\text{h}^{-1}$, with an average of $99.5 \text{ Kg}\cdot\text{m}^{-2}\cdot\text{h}^{-1}$ at a recovery rate of 70%. The Brix value concluded at 5.8° in the permeate and 6.1° in the retentate. Conductivity remained steady at $17.42 \text{ mS}\cdot\text{cm}^{-1}$ in the permeate and ended at $17.61 \text{ mS}\cdot\text{cm}^{-1}$ in the retentate, indicating consistent conductivity measurements throughout the filtration process.

Despite the apparent reduction in flux, which typically signifies an ongoing filtration process and the effective operation of the MF membrane, the constant values of Brix, conductivity, and pH might suggest an issue, such as a tear or some form of damage to the membrane or its housing. However, a comparison with data from three additional sets, each utilizing a new membrane, showed that these trends could be consistently reproduced, affirming the accuracy of the observed values.



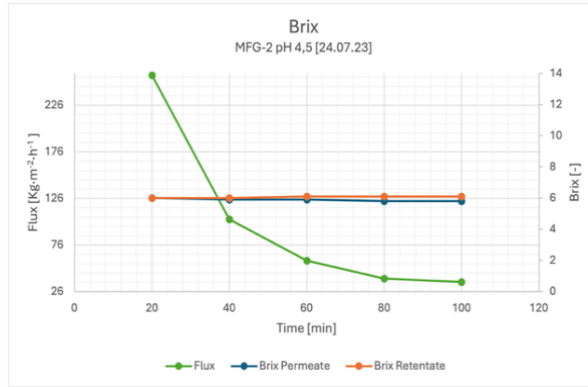


Figure 47 pH, Conductivity and Brix Measurement Points in MF Process Flow (Fourth Arrangement)

Following the Microfiltration process, with the pH maintained at 4.5, the solution was processed through a Nanofiltration membrane provided by Alfa Laval. This experiment phase was completed after reaching a recovery rate of 70.9% within 3 hours. The flux maintained an average of $52.23 \text{ Kg} \cdot \text{m}^{-2} \cdot \text{h}^{-1}$ throughout this process.

By the end of the NF process, the Brix value of the permeate was recorded at 1° , while the retentate Brix value reached 10.4° . The pH levels observed were 4.6 for the retentate and 3.8 for the permeate. Conductivity measurements indicated a final value of $5.32 \text{ mS} \cdot \text{cm}^{-1}$ for the permeate and $24.2 \text{ mS} \cdot \text{cm}^{-1}$ for the retentate. The rejection rates for lactic acid and acetic acid were 27% and 61%, respectively. Dissociation influences the rate of diffusion of a weak electrolyte in two important ways: Firstly, by increasing the number of free solute species, dissociation increases the chemical potential gradient that drives the solute through the solvent. Secondly, the movement of two separate ions experiences more frictional resistance than the transport of a single molecular species; dissociation tends to reduce the overall mobility of the weak electrolyte component. [56] Due to the lower amount of lactic acid in the permeate side, there is no meaning for further membrane process for the lactic acid concentration.

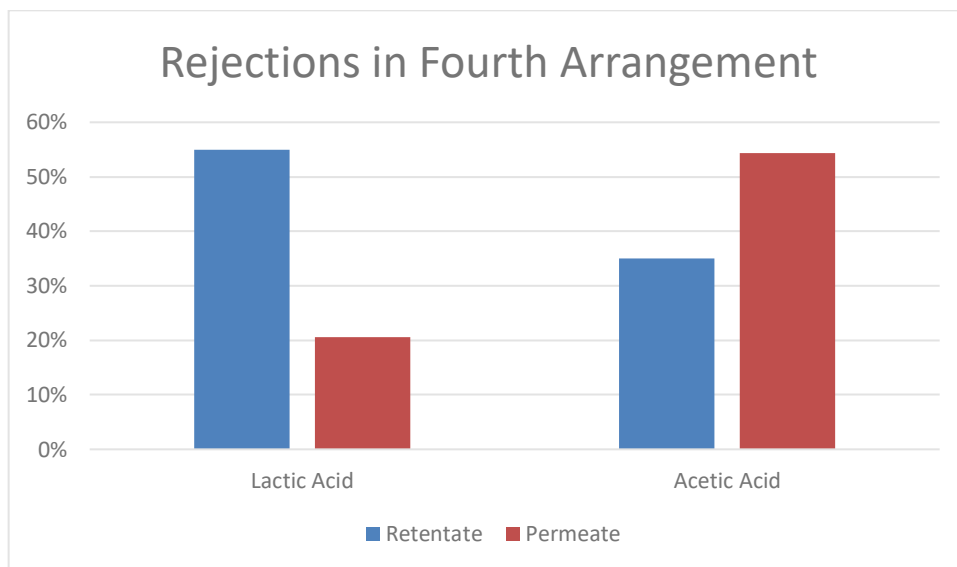


Figure 48 Rejection Profiles of Lactic Acid & Acetic Acid through the NF Stage of the Fourth Arrangement

4.2 PERFORMANCE OF NANOFILTRATION

The Nanofiltration Membrane from Alfa Laval, whose specifications are detailed in **Table 7**, underwent testing across various operational conditions and feed solution pH levels. The performance outcomes of this membrane are depicted in **Figure 49**. It was observed that the water permeability decreased to 60% of the initial water flux, signifying a substantial reduction in membrane porosity due to blockage.

Initially, water permeability was highest during the first few trials. By the time of the final trial, there was no discernible difference in water permeability before and after the experiment. Notably, the MFG-2 membrane achieved the highest permeate flux from the feed solution, recorded at $96 \text{ Kg}\cdot\text{m}^{-2}\cdot\text{h}^{-1}$, demonstrating its efficiency under the tested conditions.

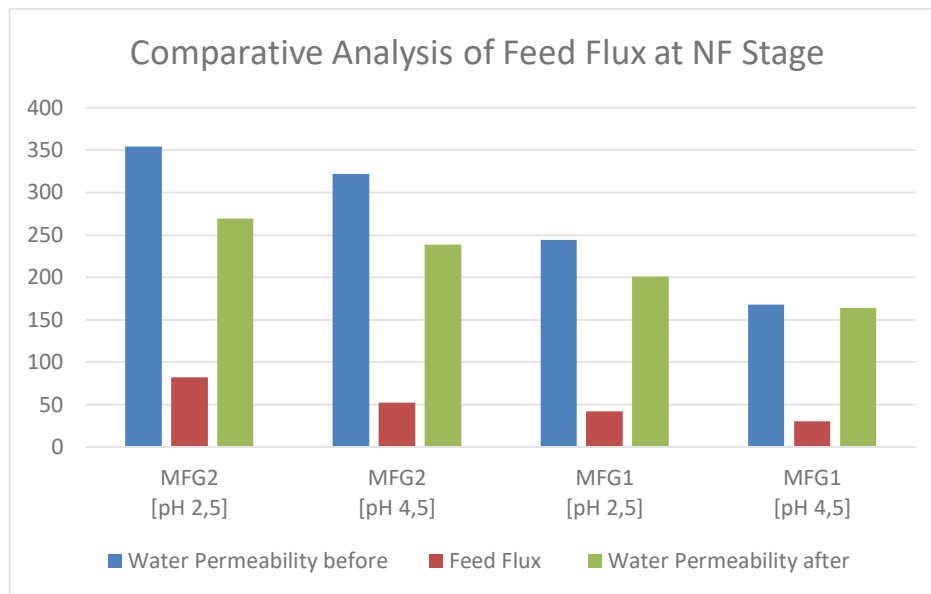


Figure 49 Comparative Analysis of Feed Flux and Water Permeability Before and After NF Processes

4.2.1 Rejection

Nanofiltration

Keeping the pH at 4.5 facilitates the separation of lactic acid from acetic acid. When the permeate of grass silage solution treated by Microfiltration is kept at pH 4.5, pure lactic acid can be concentrated in the retentate. Adding another NF step into the arrangement could allow lactic acid extraction. At this pH range, the separation efficiency is not dependent on the MWCO of the membranes, as both MF membranes yield similar results.

However, if the pH is adjusted to 2.5 before the MF, the MWCO becomes a significant factor. The MFG-2 membrane, optimal for achieving highly pure lactic acid, shows a reduced ability to separate acetic acid compared to the MFG-1 membrane, which has a smaller pore size and exhibits a greater capacity for acetic acid rejection.

Interestingly, acidifying the feed after the MF stage leads to a substantial rejection of both lactic acid and acetic acid, indicating the impact of post-treatment pH adjustments on the filtration process's effectiveness in separating these acids.

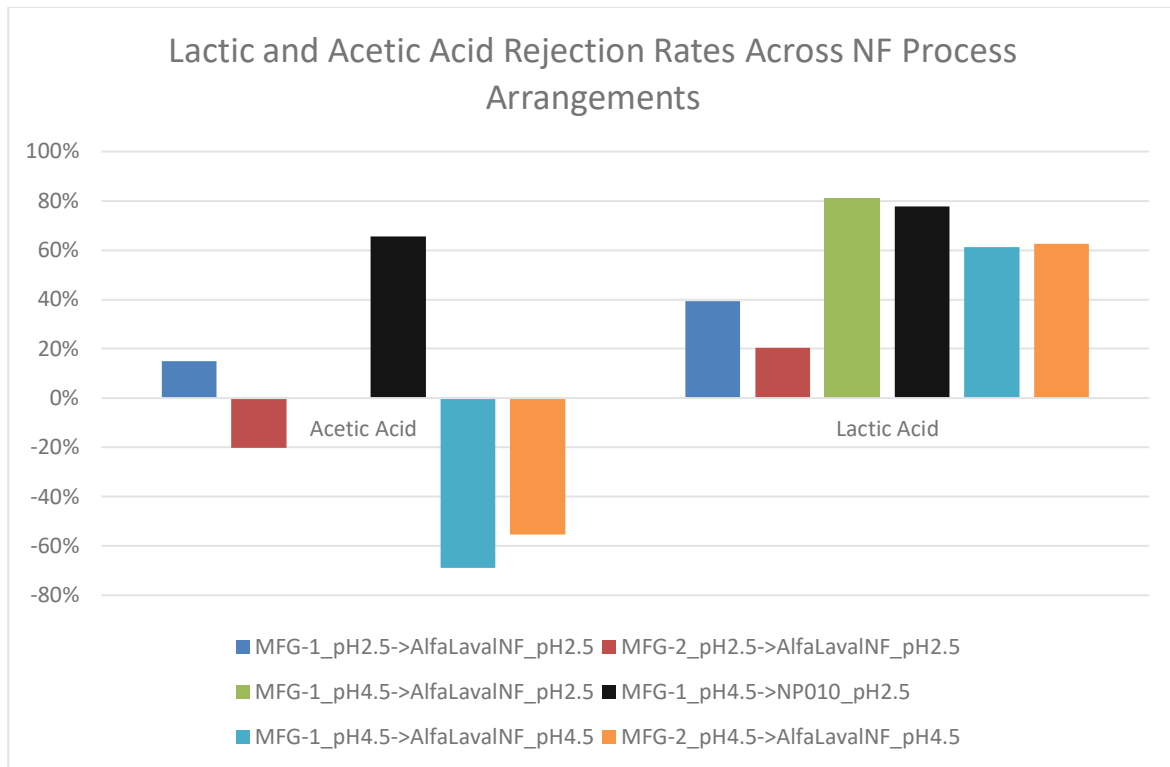


Figure 50 Efficacy of NF Stage in Rejecting Lactic and Acetic Acids: A Comparative View Across Different Arrangements

Reverse Osmosis

The data, as illustrated in **Figure 51**, demonstrates that pretreatment with the MFG-2 membrane at a pH of 2.5 enables the Reverse Osmosis membrane to recover nearly 100% from the filtration process. Additionally, it is observed that the flux does not decrease dramatically during filtration, unlike with other setups, suggesting its viability for long-term use.

In contrast, pretreatment with MF membranes having a lower Molecular Weight Cut-Off, specifically the MFG-1, exhibits a more significant difference in flux, particularly when comparing water permeability flux before and after filtration. This indicates a potential for irreversible membrane blockage.

When comparing the feed flux for feeds treated with MFG-1, it is evident that the feed adjusted to a pH of 2.5 experiences the most substantial drop in flux, highlighting the impact of pH adjustment on filtration efficiency.

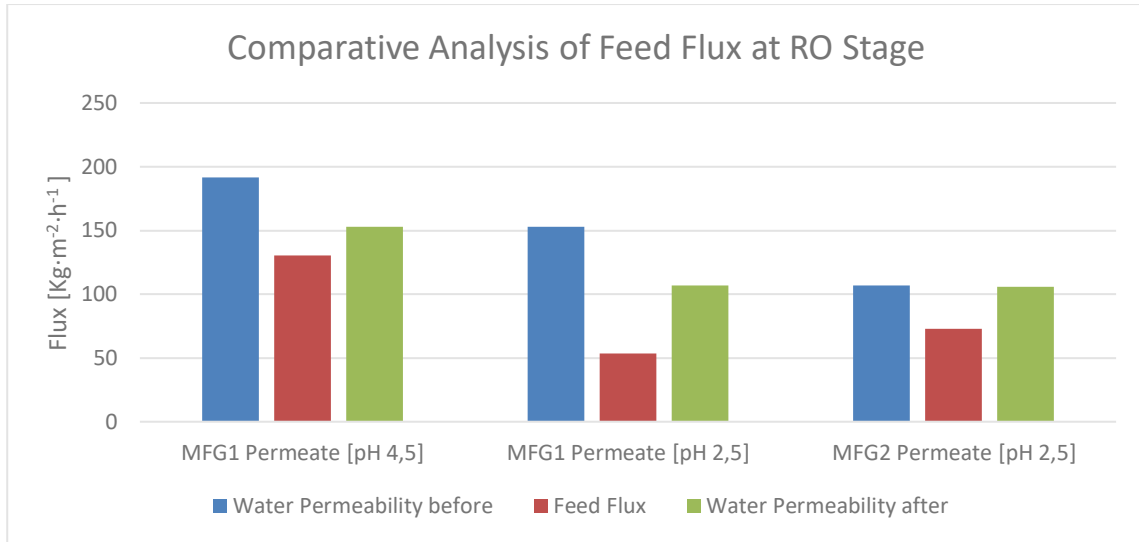


Figure 51 Comparative Analysis of Feed Flux and Water Permeability Before and After RO Processes

As illustrated in **Figure 52**, there appears to be no direct correlation between the rejection of lactic acid and the pH level. Conversely, the rejection rate of acetic acid is lower when the feed is pre-treated with the MFG-2 membrane. This pre-treatment enhances lactic acid and acetic acid separation efficiency, indicating that the choice of membrane and pre-treatment conditions significantly impact the separation process.

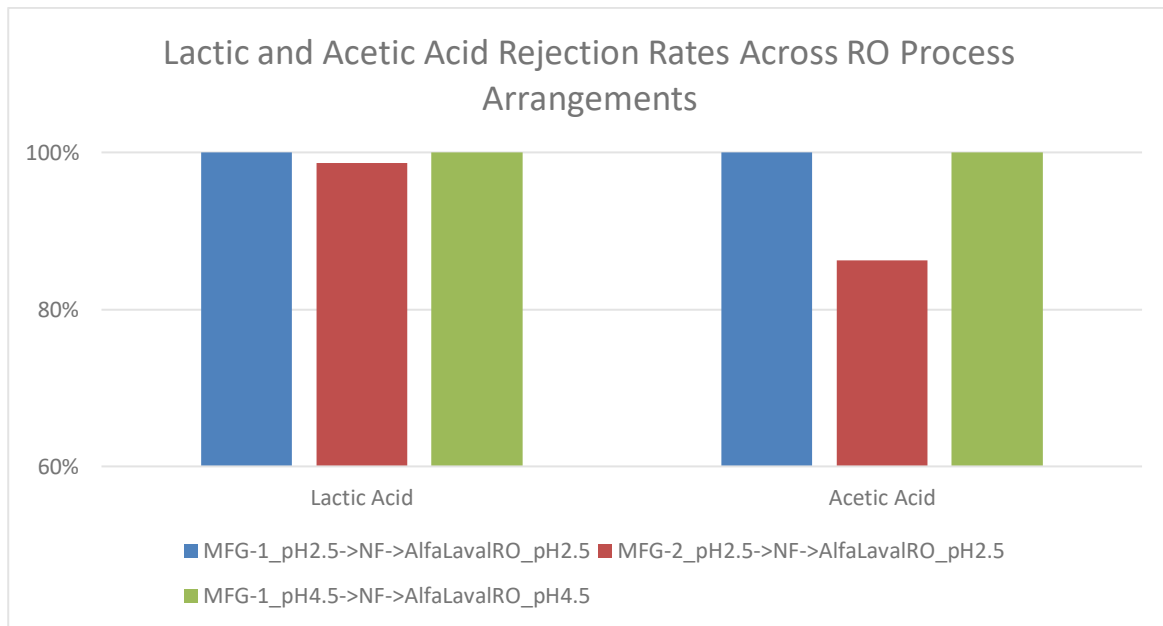


Figure 52 Efficacy of RO Stage in Rejecting Lactic and Acetic Acids: A Comparative View Across Different Arrangements

Chapter 5: Conclusion

This research explored the separation and concentration of lactic acid from grass silage using various configurations of multistage membrane processes, particularly focusing on microfiltration followed by nanofiltration and reverse osmosis (RO), within a biorefinery framework. All experiments were conducted at a laboratory scale using real grass silage, not synthetically produced test solutions.

The study underscores the critical role of pH adjustment for optimal lactic acid separation through membrane processes, especially during microfiltration. The application of H_2SO_4 or similar acids was found to break down the complex lignocellulosic structure in grass, making glucose and other sugars more accessible. Without acidification, the lignocellulosic structure remains intact, impeding the release of glucose. Acidic conditions are instrumental in hydrolyzing cellulose and hemicellulose into simpler sugars like glucose.

Additionally, acidification of the feed was identified as a crucial factor for the presence of fructose in the feed, as no fructose was detected in samples with a pH maintained at 4.5.

Adjusting the pH to 2.5 before microfiltration highlighted the importance of the pore size, with the MFG-2 (0.2 μm) membrane from Alfa Laval showing superior performance in terms of flux, lactic acid rejection, and lower permanent membrane blockage compared to the MFG-1 membrane at the same pH level.

In the nanofiltration stage, the NF-Alfa Laval membrane emerged as the optimal choice for separating lactic acid from the pretreated feed, especially when pre-treated with MFG-2 at a pH of 2.5. This setup achieved high flux, effective lactic and acetic acid separation, and showed minimal membrane blockage, suggesting prolonged membrane life.

Acidifying the feed post-MF stage significantly increased the rejection rates for both lactic and acetic acids, demonstrating the impact of pH adjustments after membrane filtration on the separation efficiency.

The highest recovery of lactic acid (100%) was obtained using RO with the Alfa Laval RO98pht membrane under specific operating conditions, following pH adjustment to 2.5 and subsequent MF and NF stages. This arrangement was unique in its ability to separate acetic acid from the retentate while maintaining high lactic acid rejection and showing promising results in terms of flux and membrane longevity.

The research concludes that acidification before the MF step is essential to prevent membrane blocking and enhance lactic acid purification. The study successfully demonstrates the capability of membrane technology in recovering and purifying lactic acid from grass silage, with the multistage setup of MF, NF, and RO proving that 2nd Arrangement is the optimal tested setup.

According to the results obtained through the process of Nanofiltration, it has been found that the separation of organic acids follows a particular rejection sequence. In this sequence, lactic acid is rejected more efficiently than acetic acid. The lactic acid and acetic acid rejection during

the nanofiltration process is based on the Donnan effect and sieve mechanism. It has been found that the retention of acids is determined by their charged ions' valency, Stokes radius, and molecular weight, and inversely proportional to the diffusion coefficient.

Chapter 6: Perspective

Future research should focus on the effects of pH adjustment on the GSJ – Feed solution. After the pH was adjusted to 2.5, the solution transitioned from a clear, amber-hued liquid reminiscent of soy sauce in colour and transparency to an opaque emulsion. This change raises questions about the underlying chemical dynamics that could be further explored. Overnight, a precipitate formed at the bottom of the storage container and running the solution through a filtration unit led to a reduction in flux, suggesting potential membrane blockage. A qualitative analysis of this precipitate would be important to ascertain its composition and understand its impact on the filtration process.

Considering the inefficacy of the tested membrane configurations in achieving a complete removal of acetic acid, future research should also explore alternative approaches. The integration of a distillation step following the reverse osmosis process might enhance the separation efficiency. Additionally, experimenting with different membrane configurations could potentially yield better outcomes. Based on the observations from using the third and fourth membrane arrangements, adjusting the pH to 4.5 post-reverse osmosis and subsequently implementing another nanofiltration setup followed by reverse osmosis appears to be a promising strategy. This approach merits thorough investigation to optimize the process and improve the yield and purity of the final product.

Bibliography

1. Lactic Acid Market Size, Trends, Growth, Report 2032 Available online: <https://www.precedenceresearch.com/lactic-acid-market> (accessed on 8 April 2024).
2. Komesu, A.; Oliveira, J.A.R. de; Martins, L.H. da S.; Wolf Maciel, M.R.; Maciel Filho, R. Lactic Acid Production to Purification: A Review. *Bioresources* **2017**, *12*, 4364–4383, doi:10.15376/biores.12.2.Komesu.
3. Ecker, J.; Schaffenberger, M.; Koschuh, W.; Mandl, M.; Böchzelt, H.G.; Schnitzer, H.; Harasek, M.; Steinmüller, H. Green Biorefinery Upper Austria – Pilot Plant Operation. *Sep Purif Technol* **2012**, *96*, 237–247, doi:10.1016/j.seppur.2012.05.027.
4. Kumar, A.; Thakur, A.; Panesar, P.S. Lactic Acid and Its Separation and Purification Techniques: A Review. *Rev Environ Sci Biotechnol* **2019**, *18*, 823–853, doi:10.1007/s11157-019-09517-w.
5. J.M. Wilkinson and B.A. Stark *Silage in Western Europe: A Survey of 17 Countries*; Chalcombe Publications: Marlow, 1992;
6. Kellogg, E.A. Evolutionary History of the Grasses. *Plant Physiol* **2001**, *125*, 1198–1205, doi:10.1104/pp.125.3.1198.
7. Kamm, B.; Schönicke, P.; Hille, Ch. Green Biorefinery – Industrial Implementation. *Food Chem* **2016**, *197*, 1341–1345, doi:10.1016/j.foodchem.2015.11.088.
8. 0 TH International Conference on Sustainable Energy and Environmental Protection Bioenergy and Biofuels.
9. Alonso, V.A.; Pereyra, C.M.; Keller, L.A.M.; Dalcero, A.M.; Rosa, C.A.R.; Chiacchiera, S.M.; Cavaglieri, L.R. Fungi and Mycotoxins in Silage: An Overview. *J Appl Microbiol* **2013**, *115*, 637–643, doi:10.1111/jam.12178.
10. Martin R. Adams; J.G. Anderson; C.G. Beddows; Michael A. Borowitzka; Jean-Louis Cordier; T.J. Elliott; Graham H. Fleet; Mark S. Fowler; Michael Ganzle; A. Godfrey; et al. *Microbiology of Fermented Foods*; Wood, B.J.B., Ed.; Springer US: Boston, MA, 1997; ISBN 978-1-4613-7990-4.
11. Rabaey, K.; Vervaeren, H.; Ronsse, F.; Carballa, M. Production of Lactic Acid and Derivatives from Grass Using Mixed Populations. **2017**, 199 pp.
12. Agbor, V.B.; Cicek, N.; Sparling, R.; Berlin, A.; Levin, D.B. Biomass Pretreatment: Fundamentals toward Application. *Biotechnol Adv* **2011**, *29*, 675–685, doi:10.1016/j.biotechadv.2011.05.005.
13. Ojo, A.O.; de Smidt, O. Lactic Acid: A Comprehensive Review of Production to Purification. *Processes* **2023**, *11*, 688, doi:10.3390/pr11030688.
14. Zabed, H.M.; Akter, S.; Dar, M.A.; Tuly, J.A.; Kumar Aswathi, M.; Yun, J.; Li, J.; Qi, X. Enhanced Fermentable Sugar Production in Lignocellulosic Biorefinery by Exploring a Novel Corn Stover and Configuring High-Solid Pretreatment Conditions. *Bioresour Technol* **2023**, *386*, 129498, doi:10.1016/j.biortech.2023.129498.
15. Takkellapati, S.; Li, T.; Gonzalez, M.A. An Overview of Biorefinery-Derived Platform Chemicals from a Cellulose and Hemicellulose Biorefinery. *Clean Technol Environ Policy* **2018**, *20*, 1615–1630, doi:10.1007/s10098-018-1568-5.
16. Budsberg, E.; Morales-Vera, R.; Crawford, J.T.; Bura, R.; Gustafson, R. Production Routes to Bio-Acetic Acid: Life Cycle Assessment. *Biotechnol Biofuels* **2020**, *13*, 154, doi:10.1186/s13068-020-01784-y.

17. Maiti, S.; Brar, S.K.; Verma, M.; Soccol, C.R.; Maiti, D.C. Butyric Acid. In *Platform Chemical Biorefinery*; Elsevier, 2016; pp. 119–132.
18. Li, S.-Y.; Ng, I.-S.; Chen, P.T.; Chiang, C.-J.; Chao, Y.-P. Biorefining of Protein Waste for Production of Sustainable Fuels and Chemicals. *Biotechnol Biofuels* **2018**, *11*, 256, doi:10.1186/s13068-018-1234-5.
19. Chen, X.; Song, S.; Li, H.; Gözaydın, G.; Yan, N. Expanding the Boundary of Biorefinery: Organonitrogen Chemicals from Biomass. *Acc Chem Res* **2021**, *54*, 1711–1722, doi:10.1021/acs.accounts.0c00842.
20. Ferguson, B.S.; Rogatzki, M.J.; Goodwin, M.L.; Kane, D.A.; Rightmire, Z.; Gladden, L.B. Lactate Metabolism: Historical Context, Prior Misinterpretations, and Current Understanding. *Eur J Appl Physiol* **2018**, *118*, 691–728, doi:10.1007/s00421-017-3795-6.
21. Jatindra Nath Mohanty, P.K.D.S.N.P.N. and P.P. Comparative Analysis of Crude and Pure Lactic Acid Produced by *Lactobacillus Fermentum* and Its Inhibitory Effects on Spoilage Bacteria. *Pharma Innov* **2015**, *3*, 38–42.
22. Lu, Z.; He, F.; Shi, Y.; Lu, M.; Yu, L. Fermentative Production of L(+)-Lactic Acid Using Hydrolyzed Acorn Starch, Persimmon Juice and Wheat Bran Hydrolysate as Nutrients. *Bioresour Technol* **2010**, *101*, 3642–3648, doi:10.1016/j.biortech.2009.12.119.
23. Castillo Martinez, F.A.; Balciunas, E.M.; Salgado, J.M.; Domínguez González, J.M.; Converti, A.; Oliveira, R.P. de S. Lactic Acid Properties, Applications and Production: A Review. *Trends Food Sci Technol* **2013**, *30*, 70–83, doi:10.1016/j.tifs.2012.11.007.
24. Alves de Oliveira, R.; Komesu, A.; Vaz Rossell, C.E.; Maciel Filho, R. Challenges and Opportunities in Lactic Acid Bioprocess Design—From Economic to Production Aspects. *Biochem Eng J* **2018**, *133*, 219–239, doi:10.1016/j.bej.2018.03.003.
25. Nagy Endre Front Matter. In *Basic Equations of Mass Transport through a Membrane Layer*; Elsevier, 2019; pp. 1–2 ISBN 9780128137222.
26. Selatile, M.K.; Ray, S.S.; Ojijo, V.; Sadiku, R. Recent Developments in Polymeric Electrospun Nanofibrous Membranes for Seawater Desalination. *RSC Adv* **2018**, *8*, 37915–37938, doi:10.1039/C8RA07489E.
27. Harasek.M Membrantechnik-VO-2023 2023.
28. Charcosset, C. *Membrane Processes in Biotechnology and Pharmaceutics*; Elsevier: Amsterdam ; Boston, 2012; ISBN 1283396300.
29. Carrère, H.; Blaszkow, F. Comparison of Operating Modes for Clarifying Lactic Acid Fermentation Broths by Batch Cross-Flow Microfiltration. *Process Biochemistry* **2001**, *36*, 751–756, doi:10.1016/S0032-9592(00)00271-5.
30. Roque, L.; Escudero, I.; Benito, J.M. Lactic Acid Recovery by Microfiltration Using Niosomes as Extraction Agents. *Sep Purif Technol* **2015**, *151*, 1–13, doi:10.1016/j.seppur.2015.07.018.
31. Papadopoulou, E.; González, M.C.; Reif, D.; Ahmed, A.; Tsapekos, P.; Angelidaki, I.; Harasek, M. Separation of Lactic Acid from Fermented Residual Resources Using Membrane Technology. *J Environ Chem Eng* **2023**, *11*, 110881, doi:10.1016/j.jece.2023.110881.
32. Carrère, H.; Blaszkow, F.; Balmann, H.R. de Modelling the Clarification of Lactic Acid Fermentation Broths by Cross-Flow Microfiltration. *J Memb Sci* **2001**, *186*, 219–230, doi:10.1016/S0376-7388(00)00677-3.
33. Wojtyniak, B.; Kołodziejczyk, J.; Szaniawska, D. Production of Lactic Acid by Ultrafiltration of Fermented Whey Obtained in Bioreactor Equipped with ZOSS Membrane. *Chemical Engineering Journal* **2016**, *305*, 28–36, doi:10.1016/j.cej.2016.01.048.

34. KOSCHUH, W.; THANG, V.; KRASTEVA, S.; NOVALIN, S.; KULBE, K. Flux and Retention Behaviour of Nanofiltration and Fine Ultrafiltration Membranes in Filtrating Juice from a Green Biorefinery: A Membrane Screening. *J Memb Sci* **2005**, *261*, 121–128, doi:10.1016/j.memsci.2005.01.049.
35. Ecker, J.; Raab, T.; Harasek, M. Nanofiltration as Key Technology for the Separation of LA and AA. *J Memb Sci* **2012**, *389*, 389–398, doi:10.1016/j.memsci.2011.11.004.
36. Sikder, J.; Chakraborty, S.; Pal, P.; Drioli, E.; Bhattacharjee, C. Purification of Lactic Acid from Microfiltrate Fermentation Broth by Cross-Flow Nanofiltration. *Biochem Eng J* **2012**, *69*, 130–137, doi:10.1016/j.bej.2012.09.003.
37. González, M.I.; Alvarez, S.; Riera, F.A.; Álvarez, R. Lactic Acid Recovery from Whey Ultrafiltrate Fermentation Broths and Artificial Solutions by Nanofiltration. *Desalination* **2008**, *228*, 84–96, doi:10.1016/j.desal.2007.08.009.
38. Liew, M.K.H.; Tanaka, S.; Morita, M. Separation and Purification of Lactic Acid: Fundamental Studies on the Reverse Osmosis down-Stream Process. *Desalination* **1995**, *101*, 269–277, doi:10.1016/0011-9164(95)00030-6.
39. Timmer, J.M.K.; van der Horst, H.C.; Robbertsen, T. Transport of Lactic Acid through Reverse Osmosis and Nanofiltration Membranes. *J Memb Sci* **1993**, *85*, 205–216, doi:10.1016/0376-7388(93)85169-W.
40. Arium® Pro Ultrapure Water Systems | Sartorius Available online: https://www.sartorius.com/en/products/water-purification/ultrapure-water-systems/arium-pro?utm_source=google&utm_medium=cpc&utm_campaign=na_ww_en_search_P-Max_ST-Always-On_Sartocheck5_plus&gad_source=1&gclid=CjwKCAiAi6uvBhADEiwAWiyRdvhUTGn7y0Kk4HwbQqs7LO4ceRH2W1xHdIbsJWA4BG469cxk6qilBoCah4QAvD_BwE (accessed on 8 April 2024).
41. Merck | Austria Available online: <https://www.sigmaaldrich.com/AT/de> (accessed on 15 April 2024).
42. Ecker, J.; Raab, T.; Harasek, M. Nanofiltration as Key Technology for the Separation of LA and AA. *J Memb Sci* **2012**, *389*, 389–398, doi:10.1016/j.memsci.2011.11.004.
43. Kölbel, F. Unsere “MemCell” - OSMO Membrane Systems Available online: <https://www.osmo-membrane.de/de/technology/pilotierung-verfahrenentwicklung/memcell.html> (accessed on 8 April 2024).
44. Cat Pumps Inc DATA SHEET 3 FRAME PLUNGER PUMPS Available online: https://www.catpumps.com/sites/default/files/2021-03/231_E.pdf (accessed on 8 April 2024).
45. Isotemp® Bath Circulators and Chillers Improve the Productivity of Your Laboratory with Accurate, Efficient Temperature Control Products from Fisher Scientific.
46. Alfa Laval Alfa Laval MF Flat Sheet Membranes Available online: https://www.alfalaval.com/globalassets/documents/products/separation/membranes/flat-sheet-membranes/mf-flat-sheet-membranes_200000059-en-gb.pdf (accessed on 8 April 2024).
47. Alfa Laval Alfa Laval NF and RO Flat Sheet Membranes Available online: <https://www.alfalaval.com/globalassets/documents/products/separation/membranes/flat-sheet-membranes/nf-and-ro-flat-sheet-membranes-200000076-3-en-gb.pdf> (accessed on 8 April 2024).
48. TRISEP® & NADIR® Membrane Products.
49. DR6000-T - Digital Refractometers with Peltier Temperature Control Available online: <https://www.kruess.com/en/produkte/refractometers/digital-refractometers/dr6000-t/> (accessed on 8 April 2024).

50. VWR ® MU 6100 H-Multi Meter Operating Manual. **2021**.
51. Configurator: COMPONENT Available online:
<https://www.thermofisher.com/store/instruments/configurators/hplc> (accessed on 8 April 2024).
52. Paul, C. The World Leader in Serving Science Revolutionising Chromatography with the Vanquish UHPLC Systems.
53. Alexandri, M.; Schneider, R.; Venus, J. Membrane Technologies for Lactic Acid Separation from Fermentation Broths Derived from Renewable Resources. *Membranes (Basel)* **2018**, *8*, 94, doi:10.3390/membranes8040094.
54. Cabrera-González, M.; Ahmed, A.; Maamo, K.; Salem, M.; Jordan, C.; Harasek, M. Evaluation of Nanofiltration Membranes for Pure Lactic Acid Permeability. *Membranes (Basel)* **2022**, *12*, 302, doi:10.3390/membranes12030302.
55. Li, Y.; Shahbazi, A.; Kadzere, C.T. Separation of Cells and Proteins from Fermentation Broth Using Ultrafiltration. *J Food Eng* **2006**, *75*, 574–580, doi:10.1016/j.jfoodeng.2005.04.045.
56. Ribeiro, A.C.F.; Lobo, V.M.M.; Leaist, D.G.; Natividade, J.J.S.; Veríssimo, L.P.; Barros, M.C.F.; Cabral, A.M.T.D.P. V. Binary Diffusion Coefficients for Aqueous Solutions of Lactic Acid. *J Solution Chem* **2005**, *34*, 1009–1016, doi:10.1007/s10953-005-6987-3.



Die approbierte gedruckte Originalversion dieser Diplomarbeit ist an der TU Wien Bibliothek verfügbar
The approved original version of this thesis is available in print at TU Wien Bibliothek.

